NASA TECHNICAL MEMORANDUM

NASA TM X-71726

NASA TM X-71726

AN APPLICATION OF MODERN CONTROL THEORY TO JET PROPULSION SYSTEMS

by Walter C. Merrill
Lewis Research Center
Cleveland, Ohio

May 1975

AN APPLICATION OF MODERN CONTROL THEORY TO JET PROPULSION SYSTEMS

by

Walter C. Merrill

Submitted in partial fulfillment

of the requirements of the

Doctor of Philosophy Degree

University of Toledo

June 1975

Certified by: _____

Advisor and Chairman of Systems Committee

Accepted by: _____

Dean, Graduate School

This research has been supported by the Graduate Research Program in Aeronautics at the National Aeronautics and Space Administration - Lewis Research Center under NASA Grant NGR-36-010-024.

ABSTRACT

The control of an airbreathing turbojet engine by an on-board digital computer is studied. The approach taken is to model the turbojet engine as a linear, multivariable system whose parameters vary with engine operating environment. From this model adaptive closed-loop or feedback control laws are designed and applied to the acceleration of the turbojet engine.

A linear state variable model of turbojet engine dynamics is identified by a technique that determines first the model structure then the model parameters. Models are identified at several operating conditions to completely describe the entire engine operating range. Only inputs and noise corrupted outputs realizable at an actual engine are considered.

Adaptive feedback controls are designed using sampled-data control theory. The necessary optimality conditions for the optimal sampled-data output regulator are derived. These necessary conditions and a variable sampling rate to reduce computer processing time (adaptive sampling) are combined to form an adaptive digital control scheme. This scheme generates constant proportional feedback laws that are functionally dependent on the control system sampling rate and that require process outputs rather than states for control purposes. This adaptive digital control scheme is applied to the previously identified engine models to control a turbojet engine. Several engine acceleration transients are simulated to study the effectiveness of the result-

ant adaptive control and the relative improvements in computer processing time. Additionally, the incorporation of certain physical engine constraints into the overall control problem is considered.

ACKNOWLEDGMENTS

This research has been sponsored by the National Aeronautics and Space Administration's Graduate Research Program in Aeronautics and the Lewis Research Center.

I would like to thank the members of the Dynamics and Controls Branch of the Lewis Research Center for their time, encouragement, and excellent technical assistance. In particular, I would like to thank Mr. Jack Zeller for his support of this research and Dr. F. K. B. Lehtinen for his technical advice and editing.

Finally, I would like to thank Dr. Gary Leininger for his direction of this dissertation and my wife, Lillie, for her encouragement and understanding.

TABLE OF CONTENTS

LIST OF FIGURES

CHAPTER I

INTRODUCTION AND BACKGROUND

The purpose of this dissertation is to develop techniques for the application of modern control theory to turbojet engine control system design. The approach taken is to consider the turbojet engine as a linear, multivariable, dynamically varying system and design adaptive feedback controls that meet engine operation and performance requirements. Specific techniques used in the design process include stochastic system identification, discrete output regulator theory, and adaptive sampling. Before proceeding with the development and application of the adaptive control design, the history and significance of turbojet engine control are discussed.

1.1 Engine Control Problem

Initially turbojet engine configurations were simple combinations of a compressor, combustor, turbine, and exhaust nozzle. As Sobey and Suggs (1963) indicate, the first control systems for these engines were hydromechanical and used the principle of the flyball governor extensively for fuel-rotor speed control. As performance demands on turbojet engines increased, so did engine and control system complexity. The addition of a second compressor, driven by its own turbine, enabled greater flexibility of compressor performance at high discharge to intake pressure ratios. However, this "twin spool" arrangement put greater demands on the control system since the rotational speed of two mechanically independent turboshafts were now to be controlled. The

addition of thrust augmentation schemes such as afterburning and variable exhaust nozzle areas added auxiliary control tasks to the basic fuel-speed control. With increased performance demands physical engine constraints such as maximum allowable turbine temperature and stable compressor operation became important engine control system design considerations. Still another major factor in the evolution of engine control systems was the application of engines to advanced aircraft propulsion. An example would be the application of the variable cycle engine to supersonic or short takeoff and landing (STOL) aircraft (Beattie, 1974). Since a variable cycle engine incorporates variable compressor and turbine geometries on both spools and two variable area exhaust nozzles, it requires more control functions than current engines and therefore will require a correspondingly complex control.

Thus from a control viewpoint a modern engine can be considered as a nonlinear multivariable (multi-input multi-output) system with several different control tasks to be accomplished simultaneously. In spite of this complexity, however, each control system can be considered as consisting of a basic fuel-speed control and a variety of other auxiliary control functions. The basic requirements of such a fuel-speed control are (1) to accelerate the engine without violation of physical constraints and (2) to control steady-state fuel flow. Although many schemes have been developed to accomplish these basic objectives, they all contain the basic structure shown in Figure 1.1.

The computational device is given as input information the commanded throttle setting, the environmental conditions of the engine (e.g., altitude and flight speed), and some physical engine variables (rotor speeds, temperatures, pressures, etc.). From this information

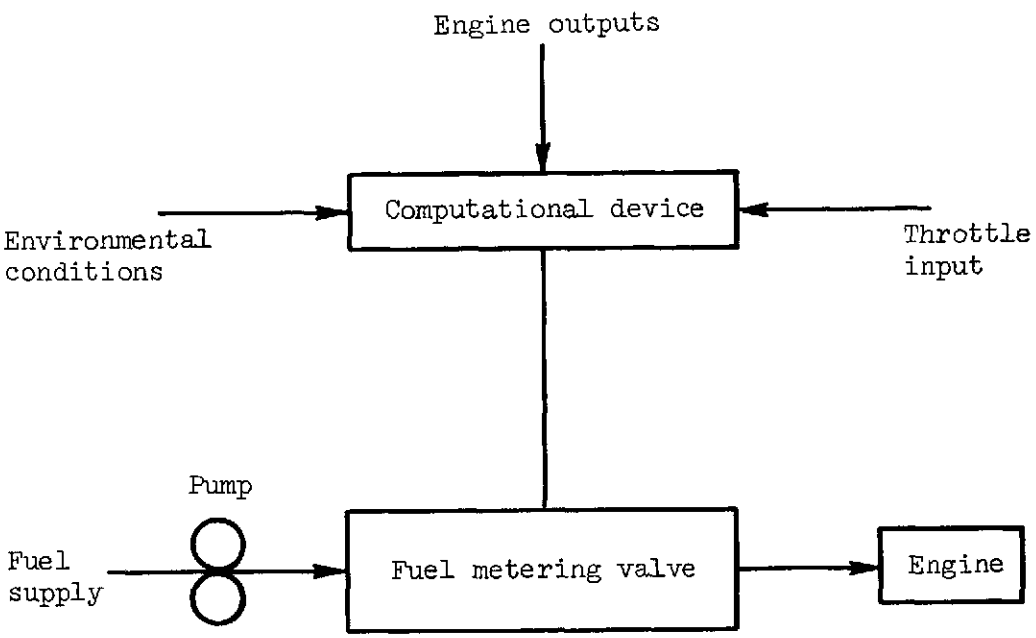

Figure 1-1. - Basic fuel-speed control system.

the computational device generates the required fuel metering valve position and consequently the appropriate engine fuel flow. The computational device is generally mechanized as either a hydromechanical or an electrical system, or a combination of both.

Hydromechanical controls are the oldest and most popular of the available mechanizations. As Leeson (1974) points out hydromechanical controls are essentially devices that maintain a schedule of desired engine temperature or acceleration. The scheduling and resultant multiplication can be accomplished in a variety of ways using cams, linkages, nozzles, springs, and valves. On the other hand steady-state fuel control is normally accomplished by simple flyball type governors that mechanically sense rotor speed and directly move the metering valve.

Electronic fuel controls are thought of as a modern innovation. However, one of the first serious applications was developed in the late 1940's (Leeson, 1974). Electronic controls can be divided into two categories, analog and digital. The vast majority of electronic engine control systems are analog. Typically an analog control would perform the same control functions as its hydromechanical counterpart but with electromagnetic pickups for sensing rotor speed, thermocouples for sensing temperature, differential transformers for position indication, a two-stage servo valve to perform the necessary work for metering valve position, and various electronic amplifiers. An example of an analog engine control is given in detail by Prue (1974) and Loft (1969).

Although most controls are either hydromechanical or analog, most of the current research interest and emphasis is in digital electronic engine control because of its future promise. Digital engine control

requires the use of a digital computer with either supervisory control over a basic hydromechanical fuel control system (Griffiths and Powell, 1974) or full authority control over all aspects of engine control functions (Bentz, 1974). Actual applications of digitally controlled jet engines have been reported by Cwynar and Batterton (1975), Batterton et al. (1974), Waters (1974), Arpasi et al. (1972), Frazzini (1970), Eccles and Shutler (1970), Bayati and Frazzini (1968); and Lewis and Munns (1968). The next section discusses how engine control systems, both hydromechanical and electronic, have been designed in the past and possible future design techniques.

1.2 Engine Control Design Methods

For a complex engine configuration much of the control development is based on good steady-state turbomachinery operation and acceleration response with respect to throttle changes while maintaining various physical engine constraints. Traditionally the control requirements were met by scheduling engine inputs as functions of flight conditions, pilot throttle demand, and one engine output, rotor speed. Recently, however, control systems have been designed that use additional measured engine output variables to yield better steady-state and transient definitions of the engine operating constraints. The vast majority of these systems have been designed using classical frequency response techniques.

Classical frequency response techniques are restricted to single-input single-output time-invariant systems. Consequently for a multivariable engine the control function for each input is designed independently. When these independently designed control functions are combined into a complete engine control, input interaction may signifi-

cantly degrade engine performance. This problem can be overcome by adjusting appropriate control function bandwidths or by designing decoupling paths between interacting engine inputs. However, bandwidth adjustments degrade system response, and decoupling, a nonsystematic procedure, may require many attempts to find an acceptable solution. In addition to these traditional control problems increased engine complexity and performance requirements (e.g., better integration of all engine control functions, optimization of fuel consumption, etc.) have placed demands on the development of control systems that cannot be met by traditional design methods. Modern Control Theory (MCT) offers possible solutions to these design problems.

MCT is a general title that includes several different control concepts. Some of these concepts are the state space representation of systems, optimal control theory, estimation and identification theory, Pontryagin's maximum principle, and several vector frequency response tehcniques. In general MCT design techniques are computer oriented and thus can systematically handle more complex multivariable problems. MCT has therefore become an increasingly important tool to many industrial and research concerns in the design and analysis of jet engine controls.

In particular, some preliminary engine control design using vector frequency response techniques has been done by MacFarlane, et al. (1971) and McMorran (1970). Chen (1972), Ahlbeck (1966), and Mueller (1971) have applied frequency response techniques to find the transfer-function matrix of known dimension of a gas turbine system. Also, Michael and Farrar (1973) have applied continuous-time linear optimal state regulator theory (Kwakernaak and Sivan, 1972) to engine control

design. This work assumed the availability of each state to implement the control law. Michael and Farrar (1973) have used a least squares curve fitting technique to fit an assumed model to engine simulation data. Recently, Michael and Farrar (1975) combined their least squares identification with a dynamic nonlinear filter to identify gas turbine dynamics from stochastic input-output data. In each of the identification papers a priori assumptions were made about system order and structure. Sevich and Beattie (1975) have used nonlinear programming to develop optimal engine variable trajectories.

Much of the potential of MCT has not been fully realized. The principal objective of this dissertation is to develop design techniques that further exploit the capabilities of MCT when applied to jet engine control. In the next section research areas of significance are identified, problem objectives defined, and the proposed solutions outlined.

1.3 Problem Statement

One of the basic assumptions of this research is the presence of an on-board digital computer for full authority engine control. Since there exists a finite limit to the time available for control update purposes, the efficiency with which the computer functions is of the utmost importance. Efficient computer utilization would allow (1) the time-sharing of several control tasks by a single computer or (2) the use of small, less expensive, specialized computers.

At first, complex continuous-time control systems were approximated on the digital computer (as in Michael and Farrar, 1973). Such approximation techniques often are computationally inefficient and require large, fast, expensive machines to achieve a satisfactory ap-

proximation. Alternately, since a computer accepts data in discrete form, a control designed by sampled-data theory could be used.

When a digital computer is introduced into the control loop, the resultant system can be handled by sampled-data control theory (Kuo, 1970). Sampled-data theory allows the control designer to implement a discrete equivalent of the continuous solution rather than an approximation of the continuous solution with a digital computer. A control system designed by sampled-data theory would allow (1) the use of smaller, less expensive computers and (2) the utilization of computer time-sharing capabilities (Levis, et al., 1971) and would therefore provide for efficient use of the computational facilities. To further increase the efficiency of the control computer, adaptive sampling (Dorf, et al., 1962) can be introduced into the control algorithm.

Adaptive sampling varies the frequency with which the computer samples the continuous signal for digital processing. The frequency is varied as a function of some continuous system parameter. The overall effect of such a scheme is to increase the control activity of the computer during high information periods (engine transients, for example) and reduce the activity during periods of low information. Thus the first objective of this dissertation is to develop a sampled-data (discrete) engine control algorithm that incorporates adaptive sampling for efficient on-board computer utilization.

In addition to efficient computer operation there is a need for a systematic design procedure that yields a practical and implementable control law and eliminates the problem of input interaction in a complex engine. Michael and Farrar (1973) have shown that an adaptive control designed by continuous-time state regulator theory can fulfill

this requirement. In general regulator theory can be used not only to systematically design controls that take advantage of input interaction, but also to easily evaluate control effectiveness. Also, the linear feedback law of optimal regulator theory is both practical and implementable.

One drawback of the control formulation of Michael and Farrar is the assumption of full state availability for control purposes. The resultant control is inflexible in that state variables must be physically present in either a sensed or estimated form. One alternative to this is the linear output regulator formulation of Levine and Athans (1970). This output regulator formulation retains the benefits of state regulator theory but no longer requires full state availability. Different combinations and numbers of output variables can be used as feedback variables and the resultant control laws readily designed. Thus, the second objective of this dissertation is to design a practical adaptive engine control using an output regulator formulation.

Implicit in the second objective is the need for a usable dynamic engine model. Such a model must be of reasonably low order while accurately predicting turbojet engine dynamics. As previously mentioned some work in this area has already been accomplished. However, no attention has been given to the important considerations of state variable selection, model order, and model structure. The usual procedure is to select a priori the order, structure, and states, identify a model, and verify the model. If the verification test fails another selection of order, structure, and states may be made and the process repreated until a satisfactory result is obtained (assuming a satisfactory result is possible using the given data and the verification

test). Even if the model verification is satisfactory, questions about the validity of the state variable selection can remain. The process is one of trial and error and it may be time consuming. In response to this need the third objective of this research is the identification of a low order model of turbojet engine dynamics by a technique that requires a minimum of a priori assumptions about system order and structure.

In summary the three objectives of this dissertation are

(1) To develop a sampled-data (discrete) engine control algorithm that incorporates adaptive sampling for efficient on-board computer utilization

(2) To design a practical adaptive engine control using an output regulator formulation

(3) To identify a low-order model of turbojet engine dynamics by a technique that requires a minimum of a priori assumptions about model structure and order

To solve the problems associated with these objectives the remaining chapters are organized in the following manner. Chapter II discusses the physics, basic control principles, and the computer simulation of a single-spool turbojet engine. The topic of Chapter III is the third research objective. In particular a technique by Tse and Weinert (1973) is applied to the identification of turbojet engine dynamics. The technique requires a minimum of a priori assumptions and can handle stochastic output data. A model is determined for the turbojet engine described in Chapter II using realistically simulated data. In Chapter IV a digital adaptive control scheme is developed to jointly satisfy the first and second objectives delineated above.

First, the optimal discrete output regulator problem is posed and solved using Lagrangian techniques for the time-invariant case. Next, an adaptive sampling law is developed. Finally, the optimal discrete output regulator and the adaptive sampling law are combined to form the adaptive digital control law. The adaptive digital control law is applied to a linearized fifth order model of a twin spool engine and the results simulated on a computer to evaluate its control effectiveness. In Chapter V the adaptive digital control scheme is applied to the turbojet engine simulation of Chapter II using the model developed in Chapter III. Results are simulated for various engine accelerations using different feedback control arrangements. Finally, this dissertation is concluded with a summary of results and recommendations for future research.

CHAPTER II

TURBOJET ENGINES

Turbojet engines are a common element in today's modern commercial and military aircraft. Therefore, the operation and control of these engines is of great practical importance. This chapter discusses the physical characteristics computer simulation, and some of the control concepts and requirements of turbojet engines.

2.1 Physical Characteristics

The purpose of a turbojet engine is to develop thrust by imparting momentum to a propellant fluid. In a turbojet this is accomplished by continuously extracting, compressing, heating, and expanding air from the atmosphere. In addition to acting as the propellant fluid, the air also acts as the working fluid in a thermodynamic process.

An ideal turbojet engine can be represented thermodynamically as a Brayton cycle on a classical temperature-entropy diagram (see Fig. 2.1). The individual processes that comprise this cycle are

1-2 Reversible, adiabatic (isentropic) compression between minimum and maximum pressures

2-3 Heat addition at constant maximum pressure

3-4 Reversible, adiabatic (isentropic) expansion between maximum and minimum pressures

4-1 Heat rejection at constant minimum pressure

In the turbojet air drawn from the atmosphere is compressed, heated,

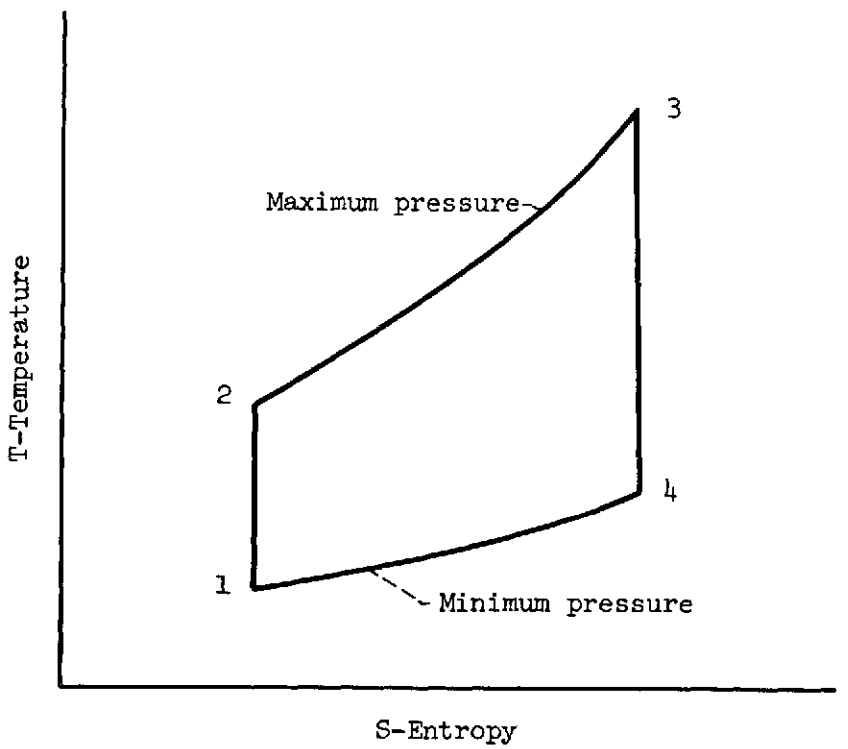

Figure 2.1. - Ideal turbojet cycle.

expanded, and discharged to the atmosphere by the internal engine components forming the continuous cycle. The internal component arrangement of a single-spool turbojet engine is shown schematically in Figure 2.2. In flowing through these components the air undergoes several processes. The air is

a-1 Brought, from far upstream of the engine, to the inlet with some acceleration or deceleration. Normally, this is an isentropic process.

1-2 Decreased in velocity by the inlet diffuser

2-3 Compressed in a dynamic mechanical compressor

3-4 Heated in the conbustor by mixing and burning fuel in the air

4-5 Expanded through a turbine to obtain power to drive the compressor

5-6 Accelerated and exhausted through the exhaust nozzle

These processes are represented on the temperature-entropy diagram of Figure 2.3. In this diagram the increase in entropy due to irreversibilities are considered for each process. The effectiveness with which a turbojet generates thrust by these processes is highly dependent on individual component performance, the physical matching of the compressor and turbine, and the engine operating environment.

The engine operating environment for a single spool turbojet engine (with fixed geometry) is determined by the engine fuel flow rate and the pressure, temperature, and velocity of the incoming airstream. The airstream velocity can be given by its Mach number (ratio of fluid velocity to velocity of sound in that fluid) and the airstream temperature and pressure are determined by the engine operating

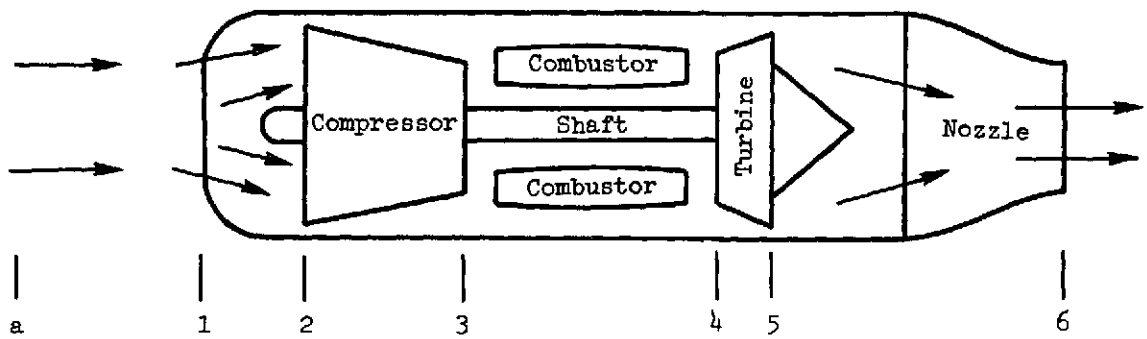

Figure 2.2. - Schematic diagram of single spool turbojet engine.

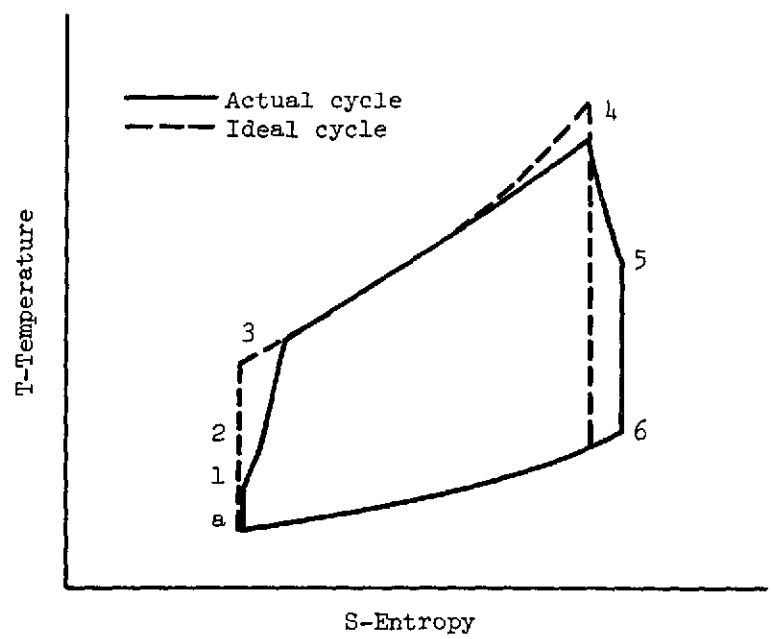

Figure 2.3. - Typical turbojet cycle.

altitude. Thus, a complete, but not unique, set of independent variables that specify engine performance are Mach number, altitude, and fuel flow rate. Other examples of complete sets of independent variables could be obtained by replacing engine fuel flow rate with engine rotational speed or the mass flow rate of air. In each case, however, the independent variables define an engine operating or steady-state point.

Component performance characteristics are normally presented graphically as "maps" in terms of component pressure ratio, a rotational speed parameter, adiabatic component efficiency, and a mass flow rate parameter. Examples of compressor and turbine maps are given in Figure 2.4. The curve, denoted as "surge line" in Figure 2.4, represents the boundary of stable compressor operation. Operation below this stability boundary is essential for satisfactory engine performance.

The matching of compressor and turbine performance is a straightforward problem. The turbine mass flow must equal combustor fuel flow and compressor airflow, and the power supplied by the turbine must equal that demanded by the compressor. Normally, the compressor operates near its peak efficiency throughout its operating range when a desirable match is achieved. The locus of steady-state matching conditions, called an operating line, intersects the centers of the constant compressor efficiency contours and is shown schematically in Figure 2.5. In Figure 2.5 lines of constant temperature ratio, T_R (turbine inlet to compressor inlet) have been plotted to aid in the future discussion of the important problem of turbojet acceleration. A more complete discussion of jet engine turbomachinery is given by Hill and

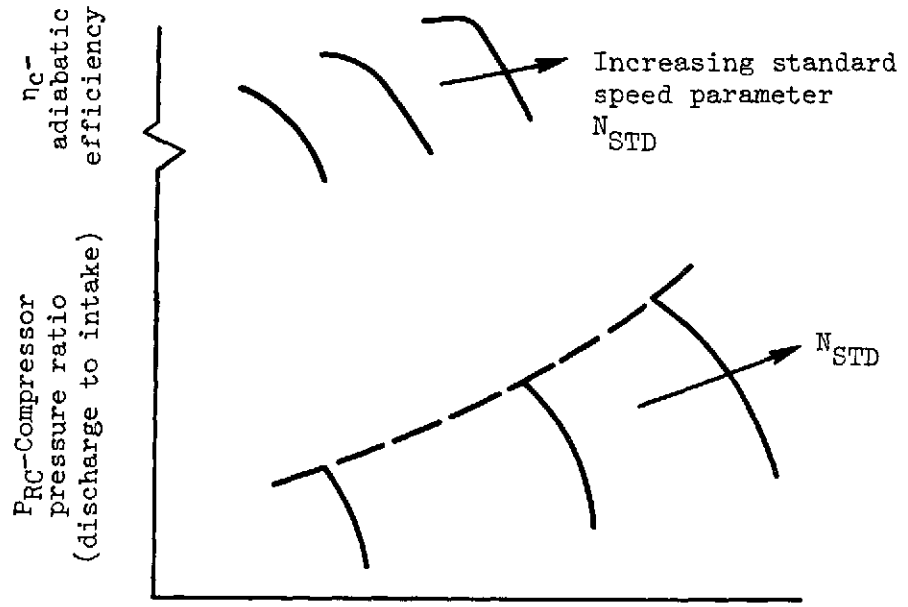

(a) Compressor

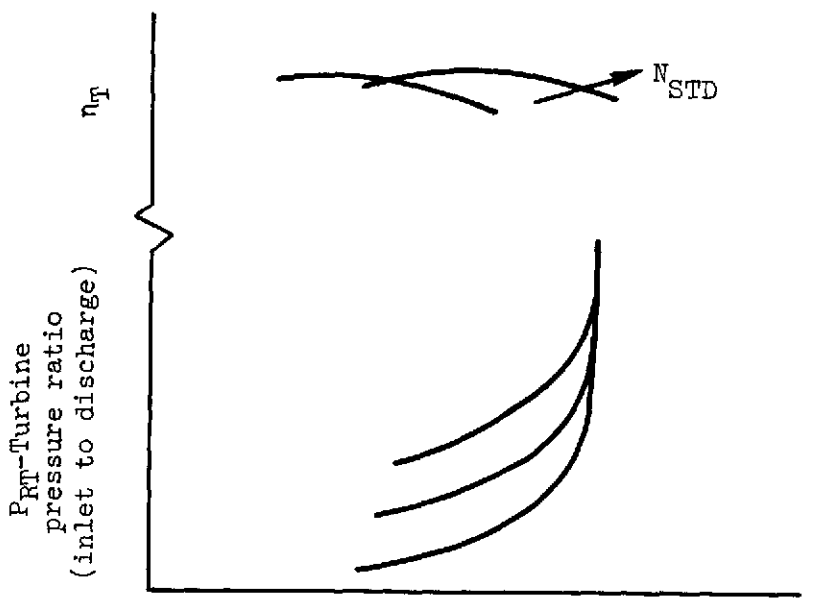

(b) Turbine.

Figure 2.4. - Typical compressor and turbine performance maps.

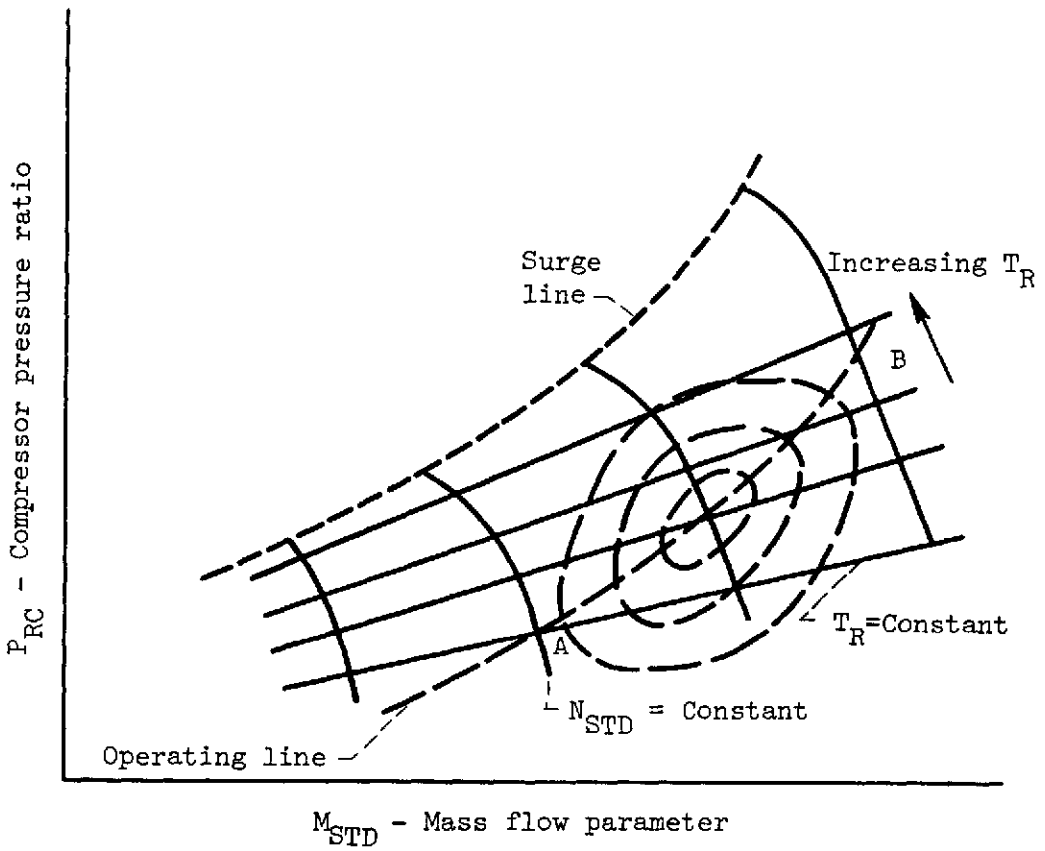

Figure 2.5. - Operating line on a compressor map.

Peterson (1970).

2.2 Computer Simulation

Mathematical simulation techniques for turbojet steady-state and dynamic behavior are very useful since they enable engine dynamics and controls problems to be studied without endangering a valuable engine. Techniques for simulating an engine on analog, digital, and hybrid computers are fairly common and have been reported by several authors, e.g., Saravanamuttoo and Fawke (1970), Seldner et al. (1971), Sellers and Teren (1974), and Szuch (1974).

The digital simulation of a single spool turbojet used as the data source for the research of this dissertation was converted to a digital simulation from an analog simulation developed by Seldner et al. (1972). This simulation incorporates experimentally determined compressor stage data, experimentally determined lumped turbine data, and a real gas combustion model. The dynamics are represented by formal one-dimensional inviscid continuity, momentum, and energy approximations to unsteady intra-compressor stage, combustor, and exhaust nozzle conditions.

2.3 Control Requirements

In general the basic control requirement of a turbojet engine is the determination of engine fuel flow such that (1) the engine is accelerated without violating physical engine constraints from one operating point to another, or (2) the steady-state operating point is maintained in the face of external disturbances. Maintaining a steady-state fuel flow schedule presents no major control problems. Engine acceleration, on the other hand, is a more difficult control problem.

Suppose, for example, the engine is to be accelerated from operating point A to B shown in Figure 2.5. A sudden increase in fuel flow causes a sudden rise in T_R (the ratio of turbine inlet to compressor inlet temperature) before the turbomachinery has a chance to accelerate. Thus, the operating point moves up a constant speed line toward the surge line. The compressor, therefore, is moving closer to a region of unstable operation and possible physical damage. Additionally, a high turbine inlet temperature may be physically damaging to the turbine rotor blades. Still another physical engine constraint is the maximum engine rotational speed. Each of these control problems requires that fuel flow be carefully limited during accelerations.

A basic fuel control for a single-spool turbojet is given in Figure 2.6. This control generates a fuel flow as a function of throttle setting that maintains engine constraints during accelerations and establishes a steady-state fuel flow schedule. Several basic control techniques are used that are common to most fuel-speed engine controls. In this particular example, the throttle setting determines both a steady-state and an acceleration limit fuel flow. A compensated fuel flow error term is added to the steady-state fuel flow and this sum is compared to the acceleration fuel flow limit. The smaller of these values is compared to a lower limit (minimum fuel flow) and an upper limit (maximum feedback fuel flow). If either limit is exceeded, that limit value is selected as the engine fuel flow input. If neither limit is exceeded, the fuel flow selected in the first comparison is the engine fuel flow input. The resultant engine speed output is used to generate both the fuel flow error and the maximum

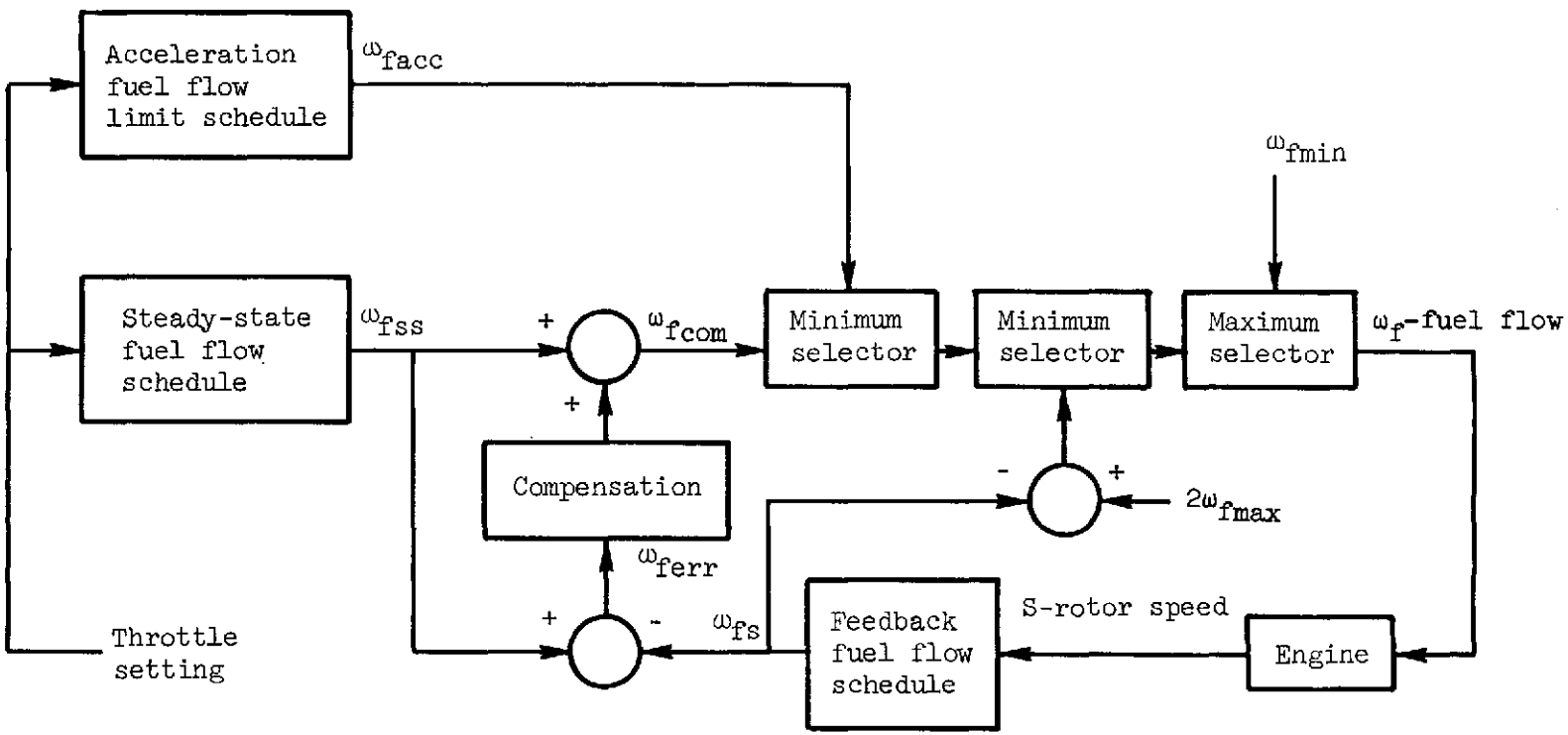

Figure 2.6. - Basic turbojet control.

feedback fuel flow terms.

The acceleration fuel flow limit schedule is designed to assure that turbine temperature and compressor stability constraints are not violated. The steady-state schedule and the speed error feedback term assure low steady-state speed errors. The limiter is used to insure that the fuel flow never exceeds an overspeed fuel flow limit or falls below a minimum fuel flow limit.

Certain sophistications are added to this basic control to improve engine performance. One is the addition of flight conditions, such as ambient temperature and flight speed as inputs to the fuel control. Now steady-state, feedback, and acceleration fuel flow schedules become multivariate functions of flight conditions and their respective inputs. This additional input information yields a better definition of engine constraints and, therefore, better engine performance. Another sophistication is the use of compressor discharge pressure as a control input to reduce the sensitivity of the control to surge producing disturbances. By normalizing or correcting fuel flow by a desired compressor discharge pressure, surge producing disturbances in the actual discharge pressure cause reductions in the engine fuel flow and a return to stable compressor operation.

Figure 2.7 shows a possible engine rotor velocity trajectory and the resultant control modes when the basic fuel control of Figure 2.6 is applied to a turbojet engine. The same trajectory and control modes are shown on a compressor map in Figure 2.8. For the trajectory the engine is initially at minimum rotor speed when a throttle setting change occurs that commands an engine acceleration. The dia-

gram shows the engine rotor acceleration, overshoot, and steady-state plateau.

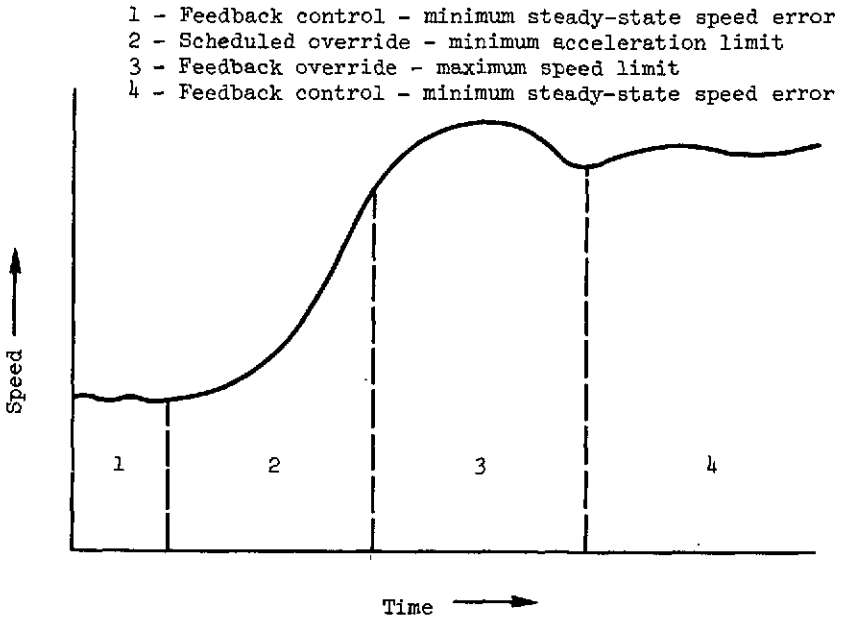

Figure 2.7. - Engine speed trajectory

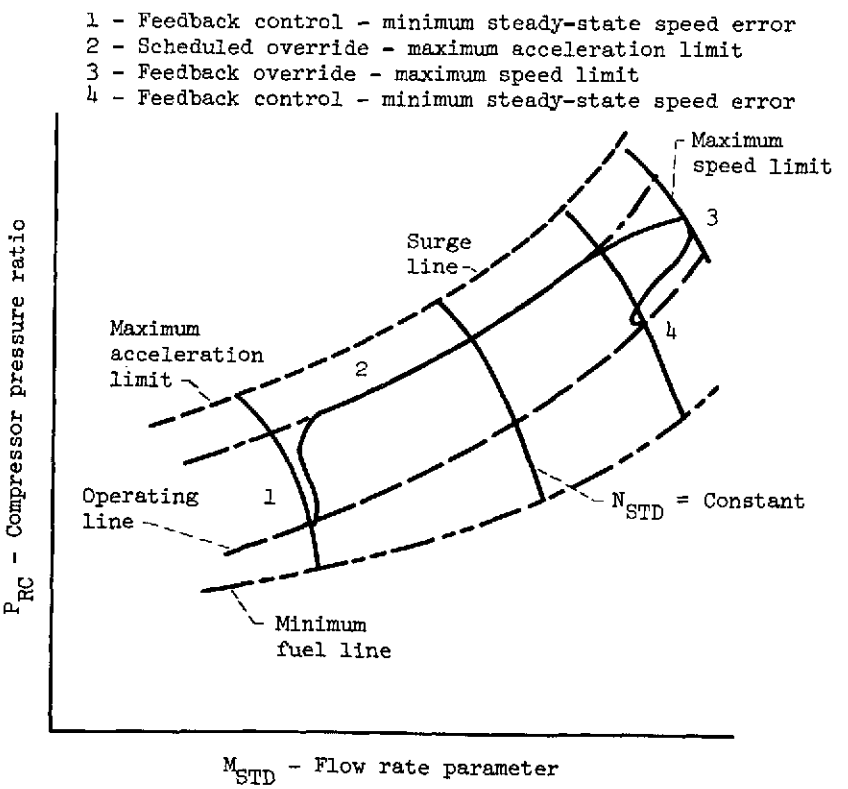

Figure 2.8. - Engine speed trajectory

CHAPTER III

ENGINE MODEL IDENTIFICATION

During the past two decades significant theoretical developments in the area of automatic control (optimal regulator control theory, Pontryagin's maximum principle, Bellman's dynamic programming, etc.) have been made. The practical utilization of these theories requires the identification of system models from observed data to predict system response. Thus, much work in the identification field has been reported. Sage and Melsa (1971) and Eykhoff (1974) summarize most of these results.

One goal of the research reported in this dissertation is to identify a usable dynamic model for a gas turbine engine. This model will be used in the application of modern control theory to turbine engine control. Work in identifying gas turbine engine models has been done by Otto and Taylor (1951), Crooks and Willshire (1956), Ahlbeck (1966), Chen (1972), Michael and Farrar (1973), and Mueller (1971). These techniques assume a model order and linearize the nonlinear dynamics about an operating point to obtain linear operating point models. The parameters in the models of Ahlbeck, Mueller, and Chen were determined from transfer function analysis. Michael and Farrar used a least squares curve fitting technique to find the system parameter values. These examples show that, for control purposes, linearized operating point models can adequately represent the nonlinear response of turbine engines.

In the previously mentioned papers on engine identification the model order and the model structure were assumed. Then the parameters were determined from available system data for this assumed structure. If these initial model assumptions are incorrect, the result may be a model that is too complex or too simplistic for design and control purposes. One of the contributions of this dissertation is to apply an identification technique that will not only identify the parameters of a suitable linear operating point model of a turbojet engine, but also determine the appropriate model order from accessible engine data. Such a technique eliminates the need for initial model order and structure assumptions and has been developed by Tse and Weinert (1973) for autonomous linear discrete systems.

The remainder of this chapter describes the Tse and Weinert identification technique and its application to the identification of autonomous linear operating point models of the single-spool turbojet described in Chapter III. To complete the model, parameters relating system control variables to engine response are identified by gradient search. Finally, the engine response as predicted by the completed model is compared with the actual response of the simulation.

3.1 Tse and Weinert Identification Technique

Tse and Weinert have developed a method that identifies from output data a constant, multivariable, stochastic, linear system which has unknown dimension, system, matrices, and noise covariances. A general stochastic model is not identifiable from steady-state output data since the output data determine an equivalence class of systems (Tse and Weinert, 1973). The systems in this equivalence class have steady-state Kalman filters with the same impulse response and inno-

vations covariance (Tse and Anton, 1972; Tse and Weinert, 1973). If the system matrices are chosen in a certain unique canonical form (Weinert and Anton, 1972), it is possible to obtain consistent estimates of the Kalman filter parameters. The procedure for consistently estimating the Kalman filter parameters, transition, observation, gain, and noise covariance matrices, and noniteratively estimating system order is described below.

Problem statement. Consider the linear discrete system represented by

$$\begin{aligned} x(k+1) &= Ax(k) + w(k) \\ y(k) &= Cx(k) + v(k) \end{aligned} \tag{3.1.1}$$

where $x \epsilon R^n$, $y \epsilon R^m$, and $w(k)$ and $v(k)$ are zero-mean Gaussian noises with covariances

$$\begin{aligned} E\{w(k)w'(j)\} &= W\delta_{kj} \\ E\{v(k)v'(j)\} &= V\delta_{kj} \\ E\{w(k)v'(j)\} &= D\delta_{kj} \end{aligned} \tag{3.1.2}$$

The unknown vector of parameters is

$$\theta = \{x_0, A, C, W, V, D\} \tag{3.1.3}$$

The object is to identify θ using the observed output data $Y^N = \{y(1), y(2), \ldots, y(N)\}$.

Tse and Anton (1972) have shown that using the observation data Y^N the appropriate parameter vector to identify is $\theta_1 = \{A, C, B, Q\}$ where the steady-state Kalman filter associated with (3.1.1) is

$$\hat{x}(k + 1/k) = A\hat{x}(k/k - 1) + B\mu(k)$$
$$\mu(k) = y(k) - C\hat{x}(k/k - 1) \tag{3.1.3}$$

and

$$E\{\mu(k)\mu'(j)\} = Q\delta_{kj} \tag{3.1.4}$$

The variable $\mu(k)$ is the innovation process (Kailath, 1970) and B is the steady-state Kalman filter gain given by

$$B = (APC' + D)Q^{-1} \tag{3.1.5}$$

$$P = APA' + W - BQB' \tag{3.1.6}$$

$$Q = CPC' + W \tag{3.1.7}$$

P is the steady-state one-step prediction error covariance. The assumptions on θ_1 are

(1) A is stable.

(2) (A,C) is an observable pair.

(3) (A,B) is a controllable pair.

(4) (A - BC) is stable.

(5) The system dimension n is finite and unknown.

(6) The effect of any initial condition on the system has died out (i.e., the system is in steady-state).

System canonical form. A canonical structure for (A,C) derived in Weinert and Anton (1972) is summarized as follows. Let c_i' be the i^{th} row of C. Consider the rows of the observability matrix in this order:

$$
\begin{aligned}
&c_1', c_1'A, \ldots; \\
&c_2', c_2'A, \ldots; \\
&\cdot \\
&\cdot \qquad\qquad (3.1.8) \\
&\cdot \\
&c_m', c_m'A, \ldots;
\end{aligned}
$$

Let p_i be the smallest non-negative integer such that $c_1'A^{p_i}$ is linearly dependent on the vectors in all the preceding rows of (3.1.8). Then

$$\sum_{i=1}^{m} p_i = n \qquad (3.1.9)$$

By the definition of $\{p_i\}_{i=1}^{m}$ there is a unique set for $i = 1,2, \ldots,m$ such that

$$c_i'A^{p_i} = \sum_{j=1}^{i} \sum_{k=0}^{p_i-1} \beta_{ijk} c_j'A^k \qquad \text{if } p_i > 0 \qquad (3.1.10)$$

$$c_i' = \sum_{j=1}^{i-1} \sum_{k=0}^{p_i-1} \beta_{ijk} c_j'A^k \qquad \text{if } p_i = 0 \qquad (3.1.11)$$

Given the set $\{p_i,\beta_{ijk}\}$, a canonical form for (A,C) is uniquely specified by

$$A = \begin{bmatrix} A_{11} & & \\ \cdot & \cdot & \\ \cdot & \cdot & 0 \\ \cdot & & \cdot \\ A_{m1}, & \ldots, & A_{mm} \end{bmatrix} \qquad (3.1.12)$$

$$\underset{(p_i \times p_i)}{A_{ii}} = \left[\begin{array}{c|c} 0 & I \\ \hline \beta_{ii0}, \beta_{ii1}, \ldots, \beta_{ii,p_i-1} & \end{array}\right] \tag{3.1.13}$$

$$\underset{\substack{(p_i \times p_j) \\ i > j}}{A_{ij}} = \left[\begin{array}{c} 0 \\ \hline \beta_{ij0}, \beta_{ij1}, \ldots, \beta_{ij,p_j-1} \end{array}\right] \tag{3.1.14}$$

and

$$c_i' = [0, \ldots, 0, 1, 0, \ldots, 0] \qquad p_i > 0 \tag{3.1.15}$$

where the 1 in c_i is in column $1 + p_1 + p_2 + \ldots + p_{i-1}$, and if $p_i = 0$

$$c_i' = [\beta_{i10}, \ldots, \beta_{i1,p_1-1}, \beta_{i20}, \ldots, \beta_{i2,p_2-1}, \ldots, \beta_{i,i-1,p_{i-1}-1}, 0, \ldots, 0] \tag{3.1.16}$$

The matrix B has no special form but its entries and $\{p_i, \beta_{ijk}\}$ are uniquely determined by Y^N (Weinert, 1973). Therefore to identify the system dimension n, the system transition matrix A, and the observation matrix C, it is sufficient to estimate $\{p_i, \beta_{ijk}\}$. Tse and Weinert estimate these parameters using time series analysis.

Time series analysis. As stated above the estimation of $\{p_i, \beta_{ijk}\}$ is sufficient for the identification of n, A, and C. Time series analysis is used to accomplish this estimation. Consider the system

$$\begin{aligned} z(k+1) &= Az(k) + B\mu(k) \\ y(k) &= Cz(k) + \mu(k) \end{aligned} \tag{3.1.17}$$

which is equivalent to (3.1.3) when

$$E\{\mu(k)\mu'(j)\} = Q\delta_{kj} \tag{3.1.18}$$

Now, let

$$R(\sigma) = E\{y(k + \sigma)y'(k)\} \qquad \sigma = 0,1,2, \ldots \tag{3.1.19}$$

In Appendix A it is shown that the set $\{p_i,\beta_{ijk}\}$ can be determined from the elements of $R(\sigma)$. This is accomplished as follows. Let $r_{ij}(\sigma)$ be the i,j^{th} element of $R(\sigma)$.

$$R(\sigma) = [r_{ij}(\sigma)] \tag{3.1.20}$$

Define

$$L_k = \sum_{i=1}^{k} p_i \tag{3.1.21}$$

Note that $L_m = n$, where n is the system dimension. Also define the following vectors

$$r_i^j = [r_{ij}(p_i + 1), r_{ij}(p_i + 2), \ldots, r_{ij}(p_i + L_i)]' \tag{3.1.22}$$

and

$$\beta_i' = [z_1 \mid z_2 \mid \ldots \mid z_i] \tag{3.1.23}$$

$$z_\ell = [\beta_{i\ell 0}, \beta_{i\ell 1}, \ldots, \beta_{i\ell,p_\ell - 1}] \tag{3.1.24}$$

Also, define the identifiability matrix as

$$\Phi_{i+1}^{j}(k) = \left[\begin{array}{c|c} \Phi_i^j(p_i) & \begin{array}{l} r_{i+1,j}(1), r_{i+1,j}(2), \ldots, r_{i+1,j}(k) \\ r_{i+1,j}(2), r_{i+1,j}(3), \ldots, r_{i+1,j}(k+1) \\ \vdots \\ r_{i+1,j}(L_i + k), \ldots, r_{i+1,j}(L_i + 2k - 1) \end{array} \\ \hline Z_1 \mid Z_2 \mid \ldots \mid Z_i & \end{array}\right] \tag{3.1.25}$$

where

$$\Phi_1^j(k) = \begin{bmatrix} r_{1j}(1), r_{1j}(2), \ldots, r_{1j}(k) \\ r_{1j}(2), r_{1j}(3), \ldots, r_{1j}(k+1) \\ \vdots \\ r_{1j}(k), r_{1j}(k+1), \ldots, r_{1j}(2k-1) \end{bmatrix} \tag{3.1.26}$$

$i = 1,2, \ldots, m$ and

$$Z_\ell = \begin{bmatrix} r_{\ell j}(L_i + 1), \ldots, r_{\ell j}(L_i + p_\ell) \\ r_{\ell j}(L_i + 2), \ldots, r_{\ell j}(L_i + p_\ell + 1) \\ \vdots \\ r_{\ell j}(L_i + k), \ldots, r_{\ell j}(L_i + p_\ell + k - 1) \end{bmatrix} \tag{3.1.27}$$

The index j may take any integer value between 1 and m in equations (3.1.22) to (3.1.27).

Tse and Weinert (1973) show that (see Appendix A)

$$r_i^j = \Phi_i^j(p_i)\beta_i \tag{3.1.28}$$

Defining

$$d_i^j(k) = \text{Determinant } \Phi_i^j(k) \tag{3.1.29}$$

The values for $\{p_i\}$ are found by testing $d_i^j(k)$, $k = 1,2, \ldots$ until $d_i^j(q) = 0$, in which case $p_i = q - 1$. The parameter β_i is then found by solving (3.1.28).

Since only Y^N is available, $R(\sigma)$ will not be known exactly. It can be estimated, however, as follows:

$$\hat{R}(\sigma) = \frac{1}{N}\sum_{k=1}^{n-\sigma} y(k + \sigma)y'(k) \tag{3.1.30}$$

Using estimated values in (3.1.22) to (3.1.29) $\hat{p}_i$ is obtained by selecting some threshold ε and testing $\hat{d}_i^j(k)$, $k = 1,2, \ldots$ until $|\hat{d}_i^j(\ell)| < \varepsilon$. Now $\hat{p}_i = \ell - 1$. The parameter $\hat{\beta}_i$ is the solution to

$$\hat{r}_i^j = \hat{\Phi}_i^j(\hat{p}_i)\hat{\beta}_i \tag{3.1.31}$$

From (3.1.19), (3.1.30) and Parzen (1967), it can be shown that $\hat{r}_{ij}(\sigma)$ is an asymptotically ($N \to \infty$) unbiased, normal, and consistent estimate of $r_{ij}(\sigma)$. Results in Mehra (1971) can be used to show that $\hat{\beta}_i$ is an asymptotically unbiased, normal, and consistent estimate of β_i, given that $\hat{p}_i = p_i$.

3.2 Application to Engine Simulation

This section discusses the development of linearized operating point models of engine dynamics, and the application of Tse and

Weinert's method to the identification of these operating point models. The digital simulation of the turbojet engine described in Chapter III is the data source for this dissertation. Linear operating point models are determined from this simulation using only inputs and outputs realizable at an actual engine.

Linearized operating points. It is assumed that the dynamical input-output-state relations for the ordinance engine are given by the nonlinear, vector differential and algebraic equations

$$\begin{aligned} \dot{x} &= f(x,u) + \zeta \\ y &= y(x,u) + \gamma \end{aligned} \tag{3.2.1}$$

The vector $x \varepsilon R^n$ represents the state of the system, the vector $u \varepsilon R^q$ is the system input, and the vector $y \varepsilon R^m$ is the system output. The vectors ζ and γ are Gaussian white noise vectors with unknown statistics. The functions $f(.\ ,\ .)$ and $g(.\ ,\ .)$ are assumed continuous and twice differentiable in their arguments. The vectors x, u, ζ, and γ are functions of time.

Expanding the functions $f(.\ ,\ .)$ and $g(.\ ,\ .)$ in a Taylor series about the steady-state operating point (x_{ss},u_{ss}) results in the following system equations where $f(x_{ss},u_{ss}) = 0$.

$$\dot{x}_{ss} + \dot{\delta}_x = f(x_{ss},u_{ss}) + \left.\frac{\partial f(x,u)}{\partial x}\right|_{\substack{x=x_{ss} \\ u=u_{ss}}} \delta\dot{x} + \left.\frac{\partial f(x,u)}{\partial u}\right|_{\substack{x=x_{ss} \\ u=u_{ss}}} \delta u + \text{H.O.T.} + \zeta \tag{3.2.2}$$

$$y_{ss} + \delta y = g(x_{ss},u_{ss}) + \left.\frac{\partial g(x,u)}{\partial x}\right|_{\substack{x=x_{ss}\\u=u_{ss}}} \delta x + \left.\frac{\partial g(x,u)}{\partial u}\right|_{\substack{x=x_{ss}\\u=u_{ss}}} \delta u + \text{H.O.T.} + \gamma \tag{3.2.3}$$

Dropping the higher order terms (H.O.T.) and defining

$$F = \left.\frac{\partial f(x,u)}{\partial x}\right|_{\substack{x=x_{ss}\\u=u_{ss}}}$$

$$G = \left.\frac{\partial f(x,u)}{\partial u}\right|_{\substack{x=x_{ss}\\u=u_{ss}}} \tag{3.2.4}$$

$$H = \left.\frac{\partial g(x,u)}{\partial x}\right|_{\substack{x=x_{ss}\\u=u_{ss}}}$$

$$E = \left.\frac{\partial g(x,u)}{\partial u}\right|_{\substack{x=x_{ss}\\u=u_{ss}}}$$

and simplifying equations (3.2.3) gives the first order or linearized approximations to equation (3.2.1)

$$\dot{\delta x} = F\delta x + G\delta u + \zeta$$

$$\delta y = H\delta x + E\delta u + \gamma \tag{3.2.5}$$

Mathematically (3.2.5) constitutes a set of linear, constant coefficient, multivariable, stochastic differential and algebraic equations. If this linearization procedure is accomplished over a sufficiently large number of steady-state operating points, engine

dynamics can be approximated over the entire operating range of the engine.

For the single-spool turbojet described in Chapter III, an operating point is uniquely specified by engine rotor speed, flight Mach number, and flight altitude. In this dissertation the engine is assumed to operate at a sea level static condition. This standard test condition specifies the Mach number and the flight altitude. Therefore, the engine operating point, and consequently the operating point models, vary only with engine rotor speed.

The linear, time-invariant, operating point models identified in this chapter are used to construct a composite engine model and to generate output feedback gains. The composite engine model will be used to verify the identification results of this chapter by comparing composite model and simulation dynamics. The feedback gains will be generated from individual operating point models and combined into the adaptive digital control described in a subsequent chapter.

Application of Tse and Weinert's method. The model equations, as determined in the previous section, for an operating point are

$$\begin{aligned} \dot{\delta x} &= F\delta x + G\delta u + \zeta \\ \delta y &= H\delta x + E\delta u + \gamma \end{aligned} \tag{3.2.5}$$

Because Tse and Weinert's method requires a discrete model, a discrete version of equation (3.2.5) is required. Following the procedure of Appendix D a discrete version of (3.2.5) is

$$\delta x(k+1) = A\delta x(k) + B\delta u(k) + \zeta_1(k)$$

$$\delta y(k) = C\delta x(k) + D\delta u(k) + \gamma_1(k) \tag{3.2.6}$$

if $\delta u(t)$ is assumed constant over the sampling period, T, and

$$A = e^{FT} \tag{3.2.7}$$

$$B = \int_0^T e^{Ft}\, dt \tag{3.2.8}$$

$$C = H \tag{3.2.9}$$

$$D = E \tag{3.2.10}$$

Also, it is assumed that $\zeta_1(k)$ and $\gamma_1(k)$ are discrete Gaussian white noise vectors with zero mean and unknown covariances.

$$E\{\zeta_1(k)\} = 0$$

$$E\{\gamma_1(k)\} = 0 \tag{3.2.11}$$

The digital turbojet simulation used in this dissertation does not include possible engine noise sources such as random variations in the compressor inlet conditions or the combustion process. To further simulate a real engine and to facilitate identification, zero mean white noise was introduced into the simulation. This was accomplished simply by adding a Gaussian random number to the value of rotor speed at each iteration of the simulation.

Eight outputs (m = 8) were selected for the identification procedure. They are

$$y' = [S, T_C, P_C, T_Z, P_Z, T_T, P_T, F_Z] \tag{3.2.12}$$

where the variables are defined as follows

S rotor speed

T_C compressor discharge temperature

P_C compressor discharge pressure

T_Z nozzle inlet temperature

P_Z nozzle inlet pressure

T_T turbine inlet temperature

P_T turbine inlet pressure

F_Z engine thrust

The first five variables are all readily measurable.

Initially a sample transient was simulated to determine approximate dynamics. Since the Tse and Weinert procedure requires data that is representative of the system as $t \to \infty$, some estimate of system time constants is needed to insure that the interval of data taking is sufficiently long. For a step change in engine fuel flow, w_f, the respective change in rotor speed, S, is shown in Figure 3.1. The rotor speed time constant (typically the engine's largest time constant) is approximately 1 second. Thus data taken over a 10 to 15 second interval will adequately approximate data taken over an infinite interval. The maximum frequency of interest is assumed to be 5 hertz. Thus, the data sampling period is $T = 0.1$ second as determined by the sampling theorem (Shannon, 1949).

The identification algorithm requires the vector $\delta y(k)$. Defining $y(k)$ as

$$y(k) = y_{NOM} + \delta y(k) \tag{3.2.13}$$

where y_{NOM} is some constant nominal vector and $y(k)$ is available

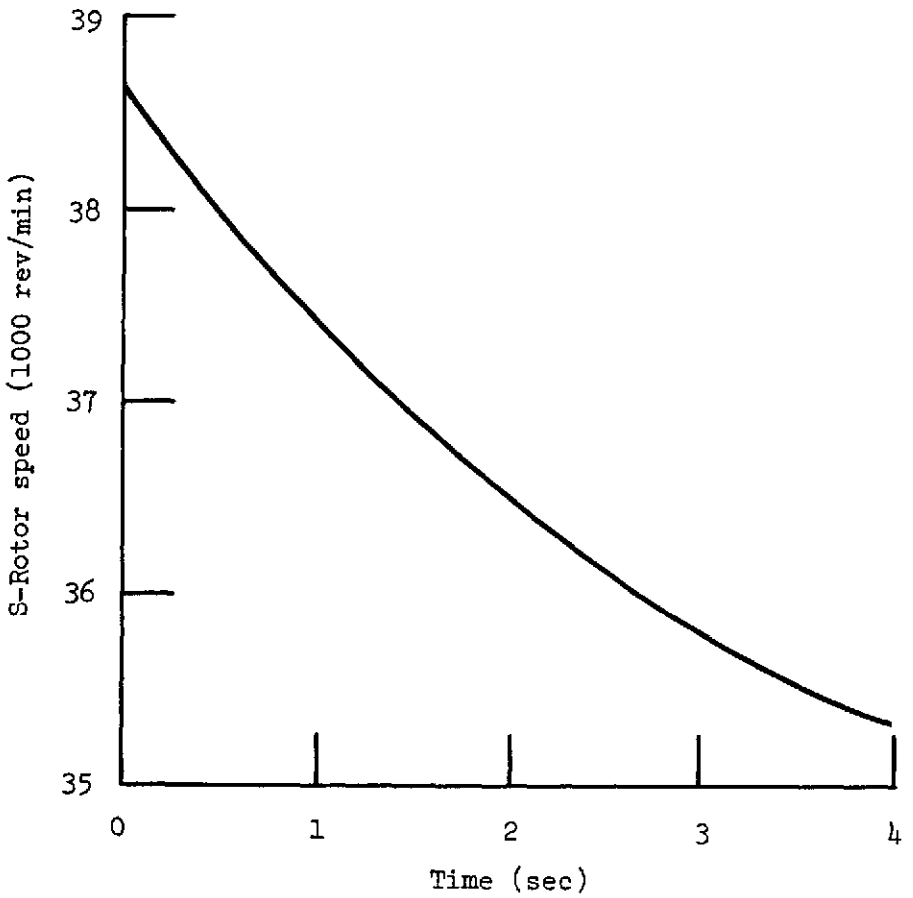

Figure 3.1. - Response of rotor speed to a step change in fuel flow.

from the simulation. Also, the identification algorithm does not allow for a deterministic input. Thus the input vector $u(t)$ will be held constant which implies that

$$\delta u(k) = 0 \tag{3.2.14}$$

Then

$$\begin{aligned} \delta x(k+1) &= Ax(k) + \zeta_1(k) \\ \delta y(k) &= Cx(k) + \gamma_1(k) \end{aligned} \tag{3.2.15}$$

Since steady-state is assumed, the effect of $x(0)$ has been eliminated. Then since

$$\delta x(k) = A^k \overset{0}{\delta x(0)} + \sum_{i=1}^{k} A^{i-1}\zeta_1(i) \tag{3.2.16}$$

and

$$E\{\delta x(k)\} = E\left\{\sum_{i=1}^{k} A^{i-1}\zeta_1(i)\right\} = 0 \tag{3.2.17}$$

then

$$E\{\delta y(k)\} = E\{C\delta x(k) + \gamma_1(k)\} = 0 \tag{3.2.18}$$

From (3.2.18) and (3.2.13)

$$E\{y(k)\} = E\{y_{NOM}\} = y_{NOM} \tag{3.2.19}$$

Since the data interval is finite, the vector y_{NOM} will be estimated as

$$y_{NOM} = \frac{1}{N} \sum_{i=1}^{N} y(i) \tag{3.2.20}$$

where N is the number of data points. Then

$$\delta y(k) = y(k) - \frac{1}{N} \sum_{i=1}^{N} y(i)$$

The time histories $\{\delta y(k)\}_1^N$ are the data required by the Tse and Weinert algorithm. These time histories were simulated at four different operating points. Figure 3.2 shows typical trajectories for two components of the output vector defined in equation (3.2.12) when the simulation is disturbed by noise.

The first step in the algorithm is the determination of the model structure. The model structure is defined by the parameters $\{p_i\}_1^m$. The parameters are estimated as outlined previously by determining when the determinant of the identification matrix (3.1.25) falls below a certain threshold value or exhibits a sharp decline in value.

From the definition of the observation matrix C it can be seen that at least one output variable can be made a state variable of the identified system. Since much of the control work to follow will be centered around rotor speed, and since the operating point is a function of rotor speed, rotor speed was the output variable initially selected as that state variable.

To determine the structure parameter p_1 the correlation matrix estimate $[\hat{R}(\sigma)]$ was calculated from the observed data for the four chosen operating points. Then the identification matrix $\Phi_{i+1}^j(k)$ was formed from the elements of $\hat{R}(\sigma)$. The determinant of $\Phi_i^j(k)$, $i = 1$

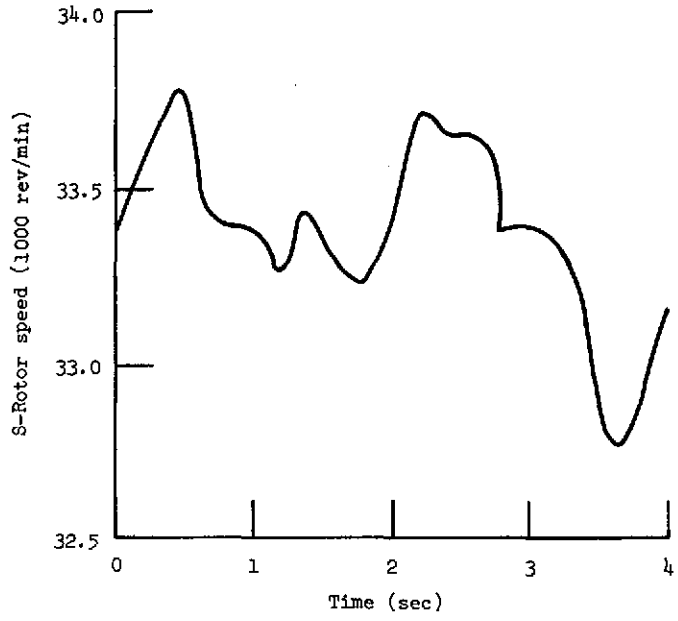

(a) Rotor speed.

Figure 3.2. - Typical output trajectories for a Gaussian disturbance.

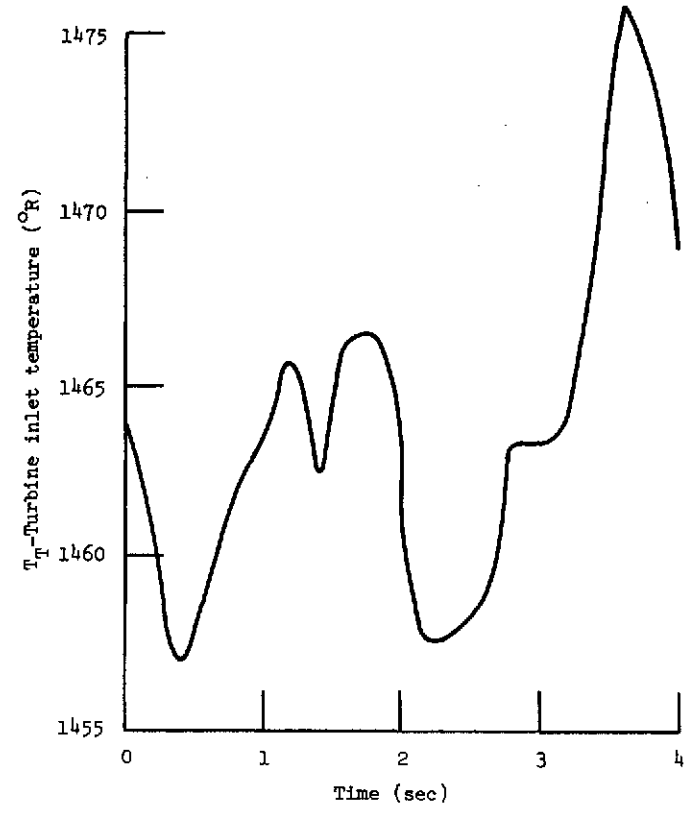

(b) Turbine inlet temperature.

Figure 3.2. - Concluded. Typical output trajectories for a Gaussian disturbance.

for various values of k and j is given in Figure 3.3. Typical plots for other j values give similar results. From the plots and the criteria mentioned above it appears that a first order system would adequately model the dynamics of the rotor speed output variable. However, a second order model was chosen to give greater control design flexibility and more accurate prediction of system response.

Next the matrices $\Phi_i^j(k)$, i = 2, . . .,8 were calculated for various values of j and k. For each of these matrices the respective estimate of the structure parameter, $\hat{p}_i$, was equal to zero. This indicates that each corresponding output is a linear combination of the state variables.

The structure of the model now becomes using equations (3.1.12) to (3.1.14)

$$A = \begin{pmatrix} 0 & 1 \\ \beta_{110} & \beta_{111} \end{pmatrix} \tag{3.2.22}$$

since $\hat{p}_1 = 2$. From equation (3.1.16)

$$C = \begin{bmatrix} 1 & 0 \\ \beta_{210} & \beta_{211} \\ \beta_{310} & \beta_{311} \\ \beta_{410} & \beta_{411} \\ \beta_{510} & \beta_{511} \\ \beta_{610} & \beta_{611} \\ \beta_{710} & \beta_{711} \\ \beta_{810} & \beta_{811} \end{bmatrix} \tag{3.2.23}$$

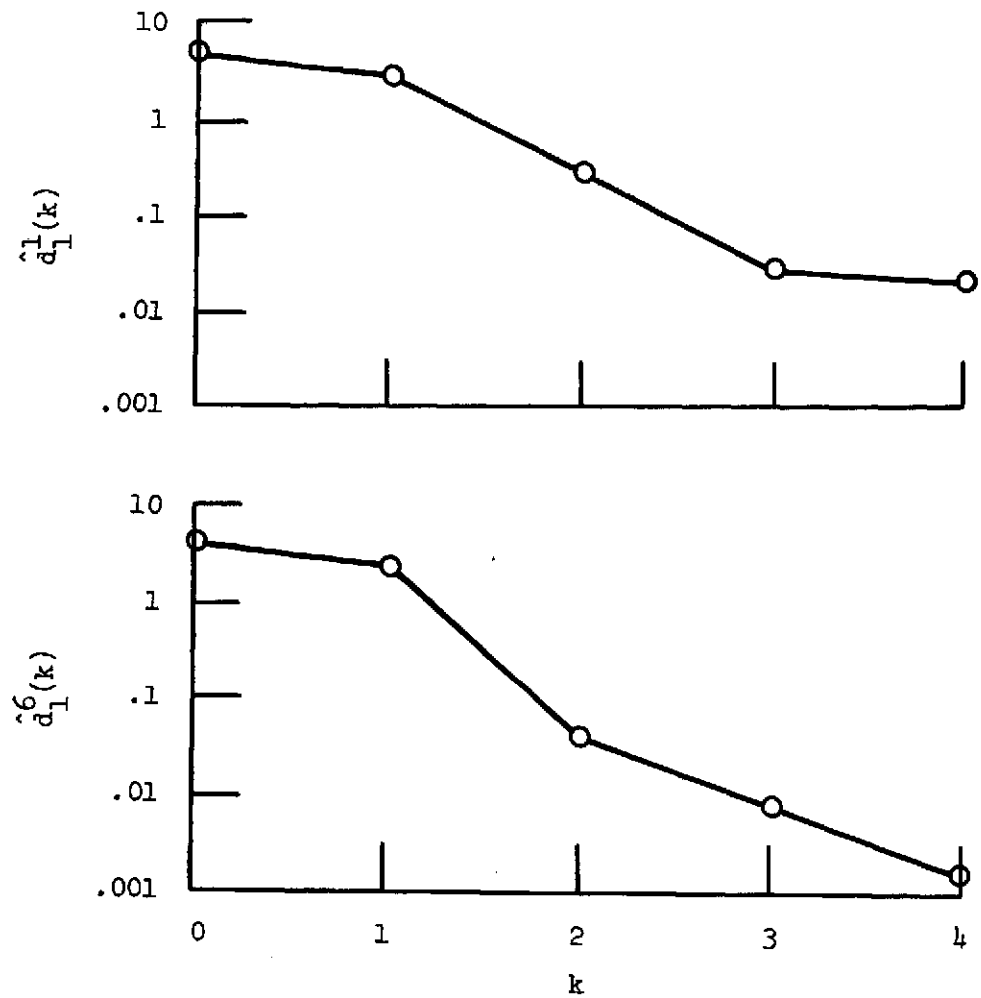

Figure 3.3. - DET $\hat{\Phi}_i^j(k) = \hat{d}_i^j(k)$ vs k for $i = 1$ and $j = 1,6$.

since $p_i = 0$, $i = 2,3, \ldots,m$; $m = 8$. Once the model has been parameterized, the next step is to estimate the values of these parameters. These estimated parameter values are determined by equation (3.1.31) at each operating point.

Four operating points were selected to approximate the engine's operating range. Designating the design speed of 36 960 rev/sec as 100 percent rotor speed, the four operating points selected correspond to 80, 90, 100, and 104.5 percent rotor speed. This set of operating points represents the endpoints (80 and 104.5%), the design point (100%), and an intermediate point (90%) of the operating range. The identified discrete system matrices, A and C, for each operating point are given in Figure 3.4. Since the continuous system matrices will be required in a subsequent chapter, F and H are calculated from their discrete counterparts, A and C, using the concept of a logarithm of a matrix (Gantmacher, 1959) and listed in Figure 3.5. Appendix B shows the procedure followed to transform the discrete system to a continuous one.

3.3 The Control Matrices

The discrete model for the system is given as

$$\delta x(k+1) = A\delta x(k) + B\delta u(k) + \zeta_1(k)$$
$$\delta y(k) = C\delta x(k) + D\delta u(k) + \gamma_1(k) \qquad (3.2.6)$$

Tse and Weinert's algorithm was used to determine A and C in a specified canonical form. For this canonical form the control matrix B and the direct link matrix D will have no special form. Thus B has $n \times q$ elements and d has $m \times q$ elements that must be identified.

% Speed	Matrix	Matrix elements						
80	A	0 -.354	1 1.233					
	C'	1 0	.0127 -.00046	.0019 -.00009	-.0338 .00418	.00029 -.00002	-.028 .0035	.0016 -.00011	.018 -.0012
90	A	0 -.340	1 1.183			.00038		
	C'	1 0	.0144 -.00069	.0023 -.00017	-.0264 .00380	.00089 -.00004	-.023 .0037	.0021 -.00017	.023 -.0023
100	A	0 -.258	1 1.060					
	C'	1 0	.0153 -.00064	.0025 -.00020	-.0200 .00366	.00051 -.00006	-.017 .0038	.0023 -.00023	.026 -.0034
104.5	A	0 -.318	1 1.119					
	C	1 0	.0163 -.0013	.0027 -.00049	-.018 .0047	.00053 -.00008	-.016 .0036	.0025 -.00034	.028 -.0044

Figure 3.4. - Identified values of A and C vs. % speed-discrete model.

% Speed	Matrix	Matrix elements
80	F	-15.4258 16.6030 -5.8816 5.0482
	H'	Same as C' in Figure 3.4
90	F	-15.4915 17.0706 -5.8021 4.7002
	H'	Same as C' in Figure 3.4
100	F	-17.0582 19.4081 -5.0076 3.5108
	H'	Same as C' in Figure 3.4
104.5	F	-15.6751 17.7771 -5.6552 4.2211
	H	Same as C in Figure 3.4

Figure 3.5. - Identified values of F and H vs. % speed-continuous model.

The order of the system has been determined, $n = 2$. The control variable of the simulation is fuel flow, thus $q = 1$ and the B matrix has two unknown elements. Since the number of output variables is 8, the number of unknown elements in the D matrix is 8.

These ten elements were determined at each operating point by a simple gradient search procedure. First a control input was selected as

$$\delta u(k) = \delta w_f(k) = \Lambda[\sin(0.1\ wkT + \psi_1) + \sin(wkT + \psi_2) + \sin(10\ wkT + \psi_3)] \qquad (3.3.1)$$

where $\Lambda = 0.00667$, $w = 2$, $\psi_1 = 0.1$, $\psi_2 = 0$, and $\psi_3 = 1$. This control input was applied to the nonlinear simulation and $y(t)$, the output vector, was calculated for a 5-second interval. Then an initial guess, B_i and D_i, for the matrices B and D was chosen and the equations of (3.2.6) simulated to give $y_i(k)$ using $B = B_i$ and $D = D_i$. The trajectory $y(t)$ was compared at the appropriate sampling points to the output estimate

$$\hat{y}(k) = y_N + \delta y_i(k) \qquad (3.3.2)$$

The squares of the errors were summed to form a cost function J_i.

$$J_i = \frac{1}{N} \sum_{k=1}^{N} [y(k) - \hat{y}_i(k)]'[y(k) - \hat{y}_i(k)] \qquad (3.3.3)$$

Another guess for B and D, called B_{i+1} and D_{i+1}, was determined by perturbing one element of the B_i or D_i matrix by a small amount b_{ERR}. The estimated trajectory $\delta y_{i+1}(k)$ again was simulated and com-

pared to $y(t)$. The cost function J_{i+1} was calculated according to (3.3.2). The gradient of the cost function with respect to one element of the matrix B or D is estimated by

$$\frac{\partial J_i}{\partial b_i} \simeq \frac{J_{i+1} - J_i}{b_{ERR}} \tag{3.3.4}$$

where b_i is one of the elements of the B or D matrix. A new choice for b_{i+2} can then be found according to

$$b_{i+2} = b_i + K \frac{\partial J_i}{\partial b_i} \tag{3.3.5}$$

This procedure is followed successively for the first and second elements of B and the eight elements of D until the gradient for each element becomes small. The values for B and D determined by this gradient search procedure are listed in Figure 3.6.

The continuous counterpart, G, to the B matrix can be found from

$$B = \int_0^T e^{Ft} G \, dt \tag{3.3.6}$$

by integrating and solving for G.

$$G = (A - I)^{-1} FB \tag{3.3.7}$$

The G matrices for the four operating points are also listed in Figure 3.6. The continuous matrix E is equal to the discrete matrix D and is listed in Figure 3.7.

% Speed	Matrix	Matrix elements
80	B	48004.7 27815.9
	G	635422.31 356737.52
90	B	43653.5 24165.8
	G	582468.85 318733.54
100	B	45947.6 19977.63
	G	687484.82 291423.03
104.5	B	40617.6 19662.8
	G	565445.20 278306.55

Figure 3.6. - Identified values of B and G vs. % speed.

% Speed	Matrix	Matrix elements							
80	E'	-12227.78	-15.25	12.47	3508.81	2.598	3991.66	13.96	-11703.98
90	E'	-10573.77	-33.38	4.550	2920.59	2.970	3427.02	9.0856	114.41
100	E'	-18929.90	-223.59	-26.322	2535.71	-.9140	2870.89	-23.632	-117.678
104.5	E'	-14468.60	-203.73	-19.96	2299.11	.5885	2632.15	-20.069	-43.53

Figure 3.7. - Identified values of D and E vs. % speed.

3.4 Model Verification

From the operating point models obtained at four engine rotor speeds, a continuous function of speed was calculated by linear interpolation for each model parameter. The model equations become

$$y(t) = y_{NOM}(t) + \delta y(t)$$

$$\delta\dot{x}(t) = F(S)\delta x(t) + G(S)\delta w_f(t) \qquad (3.4.1)$$

$$\delta y(t) = H(S)\delta x(t) + E(S)\delta w_f(t)$$

where the vector $y(t)$ is as defined in equation (3.1.12) and S is rotor speed.

The composite model was simulated on a digital computer. A block diagram of the composite model is given in Figure 3.8. Note that the nominal fuel flow, w_{fNOM}, is found by time averaging the engine fuel flow, w_f. Since steady-state fuel flow determines an operating point, the nominal output vector, $y_{NOM}(t)$, can be defined as the steady-state engine output if a constant fuel flow, w_{fNOM}, is supplied to the engine. Thus, the nominal output vector can be scheduled as a function of nominal fuel flow.

A test input was selected as a combination of three basic control inputs, the step, ramp, and parabola. This test input, shown in Figure 3.9 was applied to the engine simulation and to the composite model. The engine simulation output, the composite model output, and their difference (error) are plotted in Figure 3.10. Also a listing of the average error and error variance for each output is given in Figure 3.11. The normalized average error for each output was less

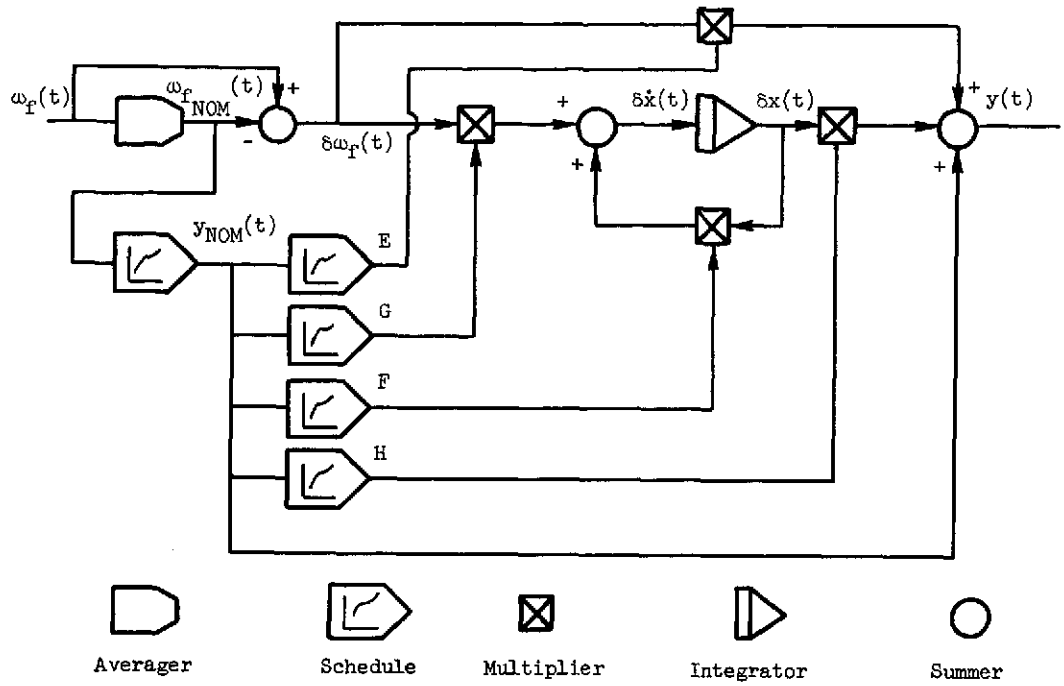

Figure 3.8. - Composite engine model block diagram.

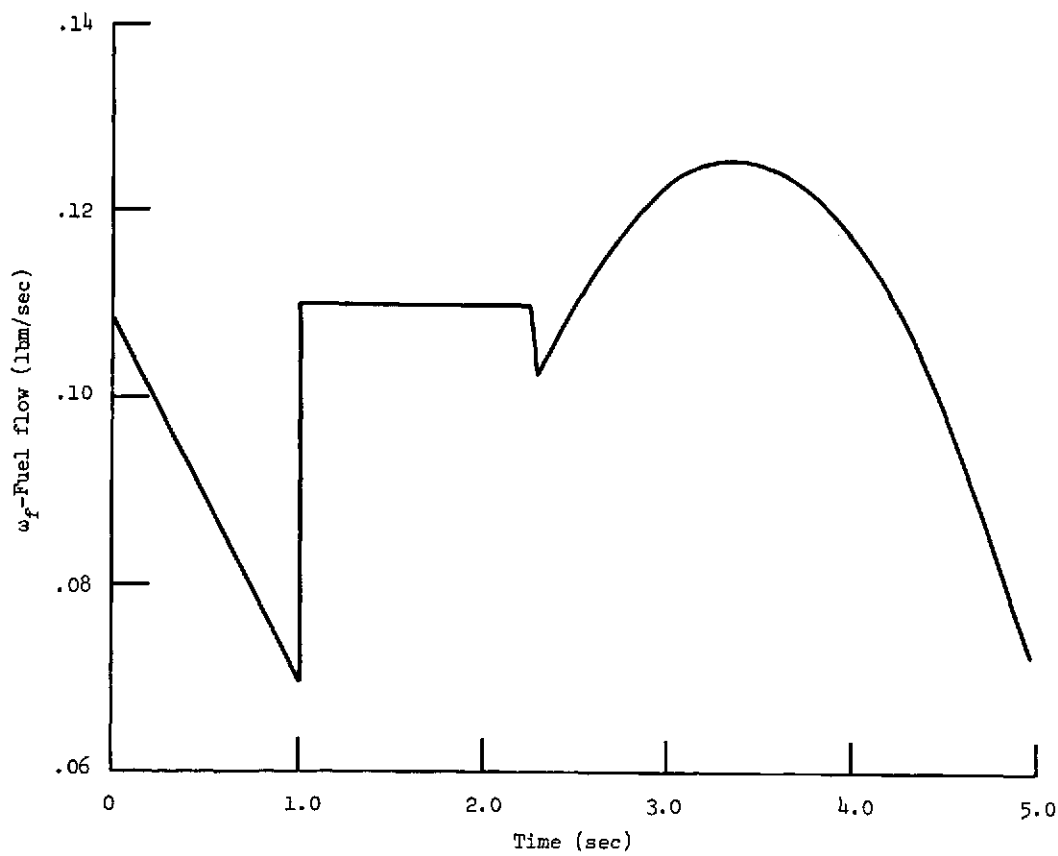

Figure 3.9. - The test input.

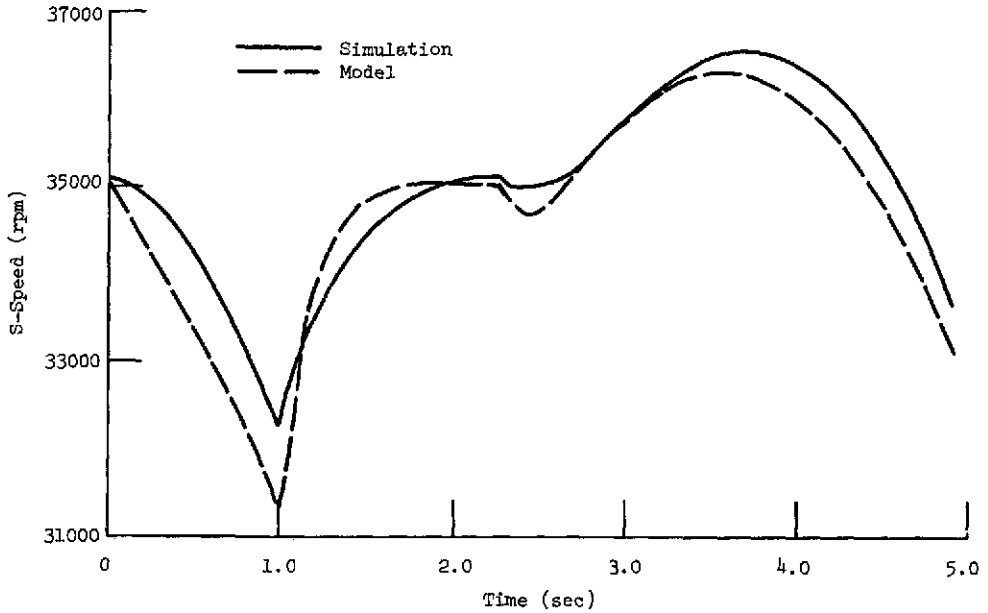

(a) Rotor speed.

Figure 3.10. - Simulation and composite model trajectories.

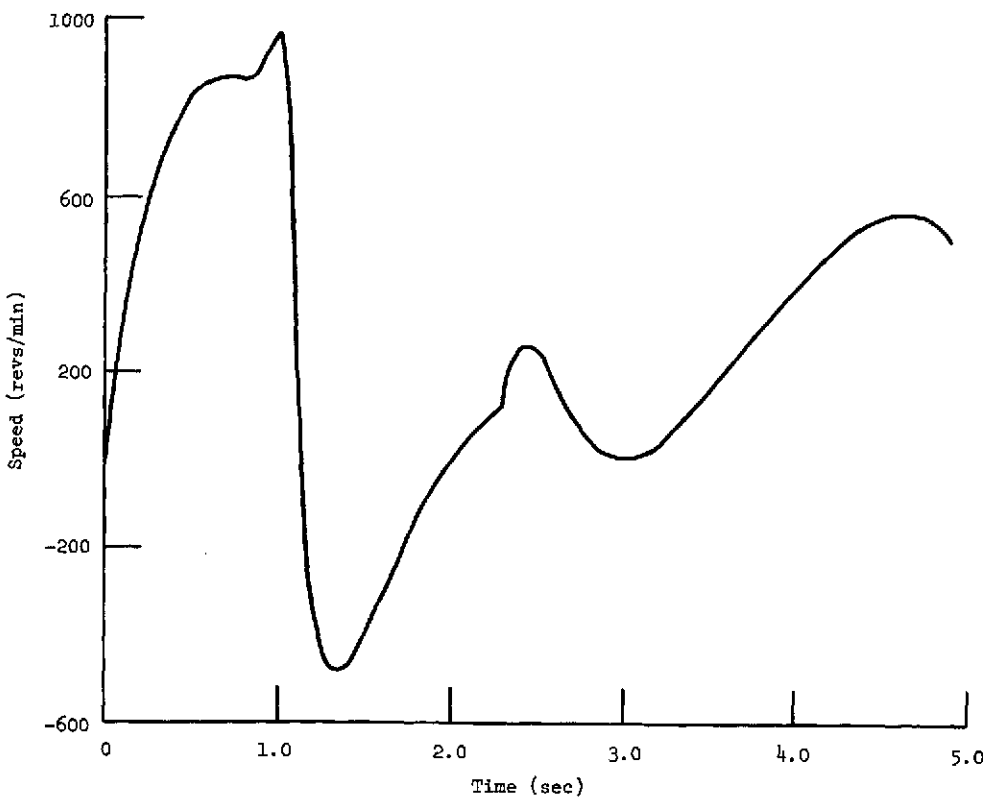

(aa) Rotor speed error.

Figure 3.10. - Simulation and composite model trajectories.

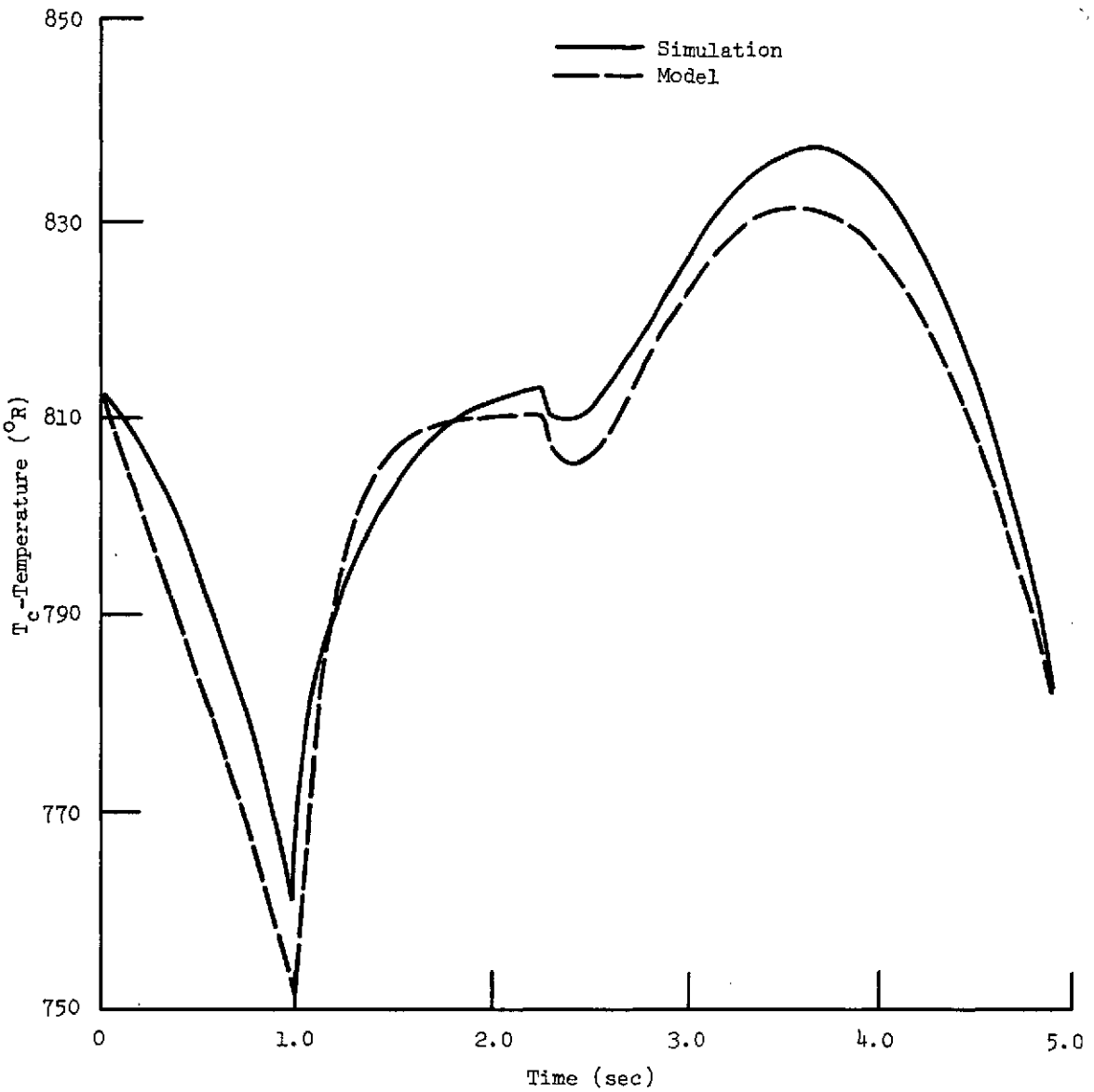

(b) Compressor discharge temperature.

Figure 3.10. - Simulation and composite model trajectories.

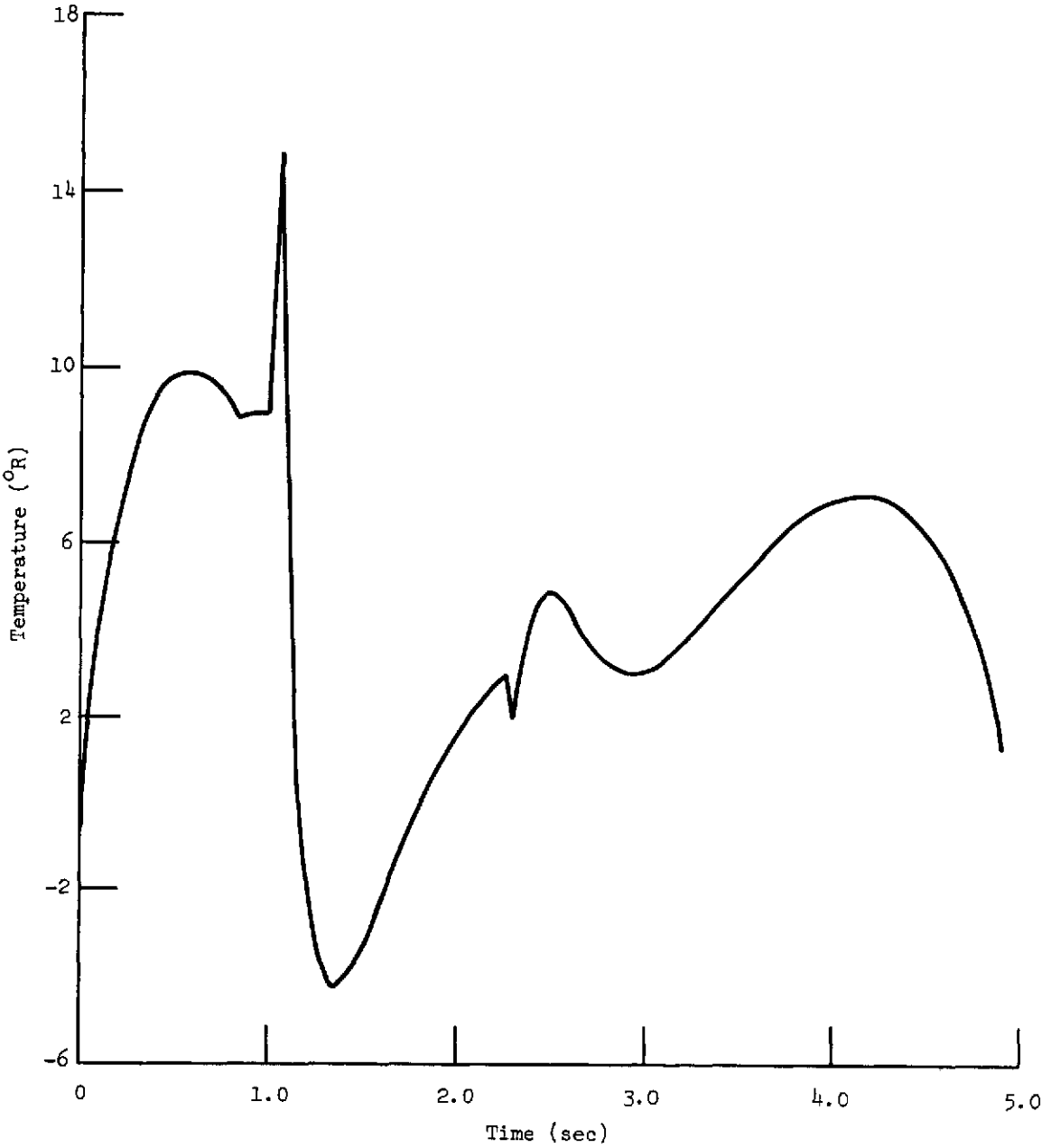

(bb) Compressor discharge temperature error.

Figure 3.10. - Simulation and composite model trajectories.

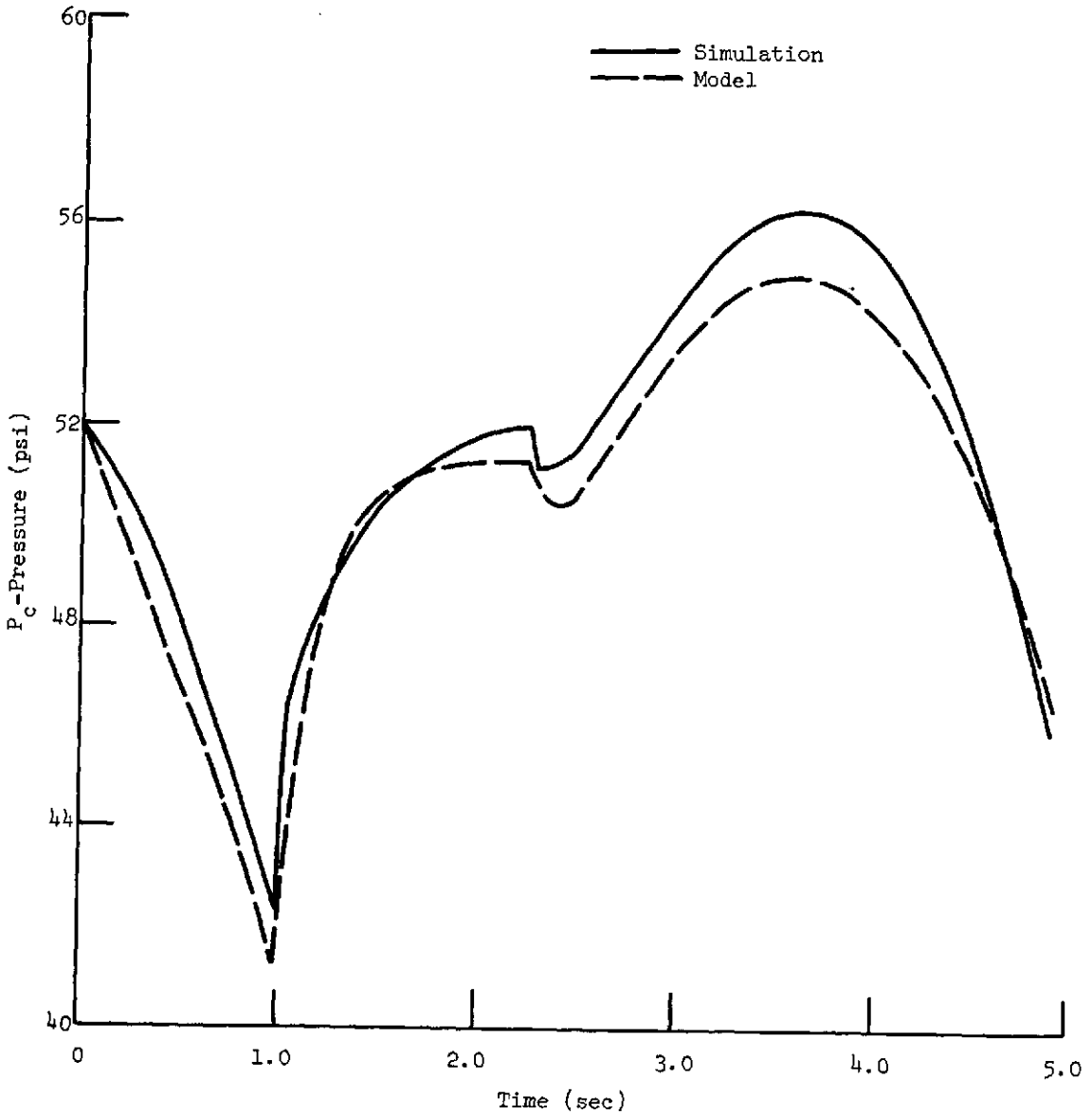

(c) Compressor discharge pressure.

Figure 3.10. - Simulation and composite model trajectories.

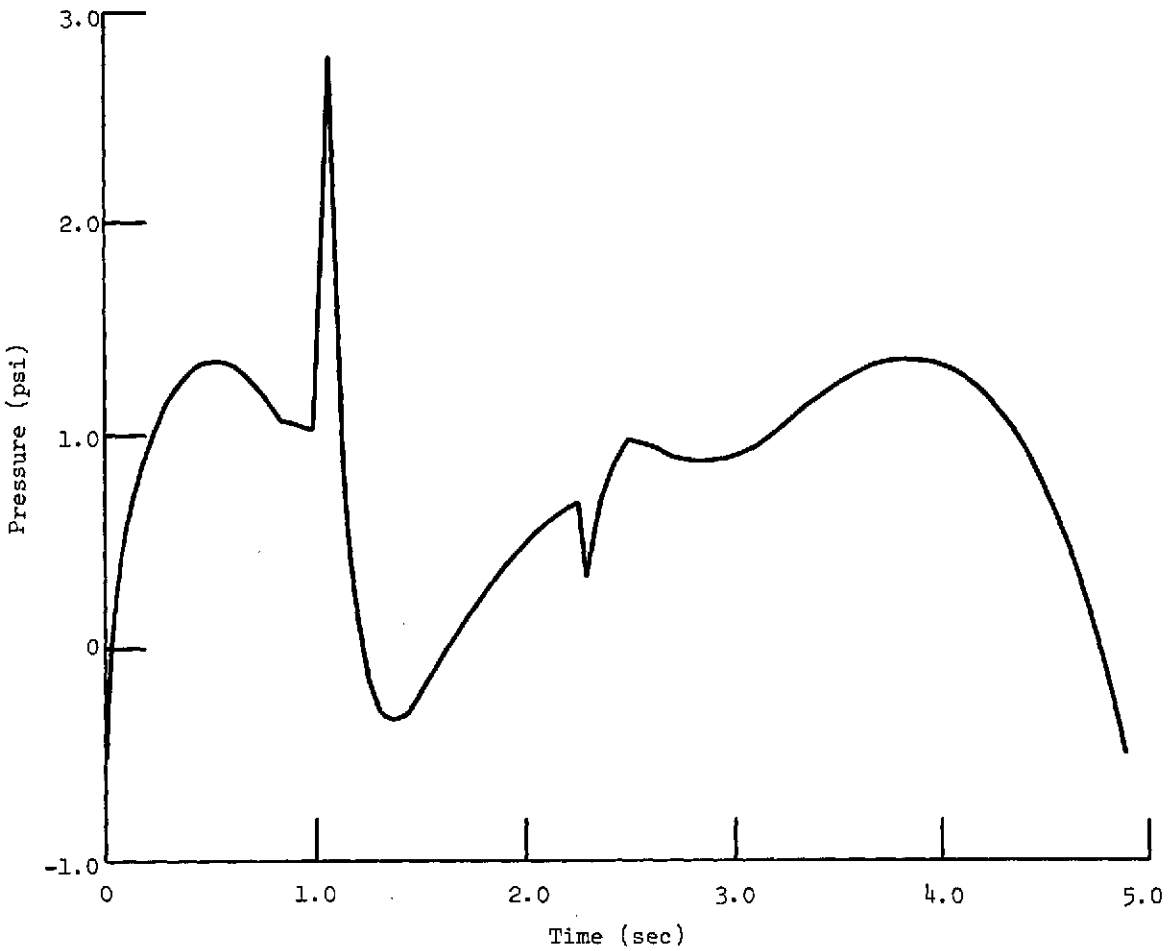

(cc) Compressor discharge pressure error.

Figure 3.10. - Simulation and composite model trajectories.

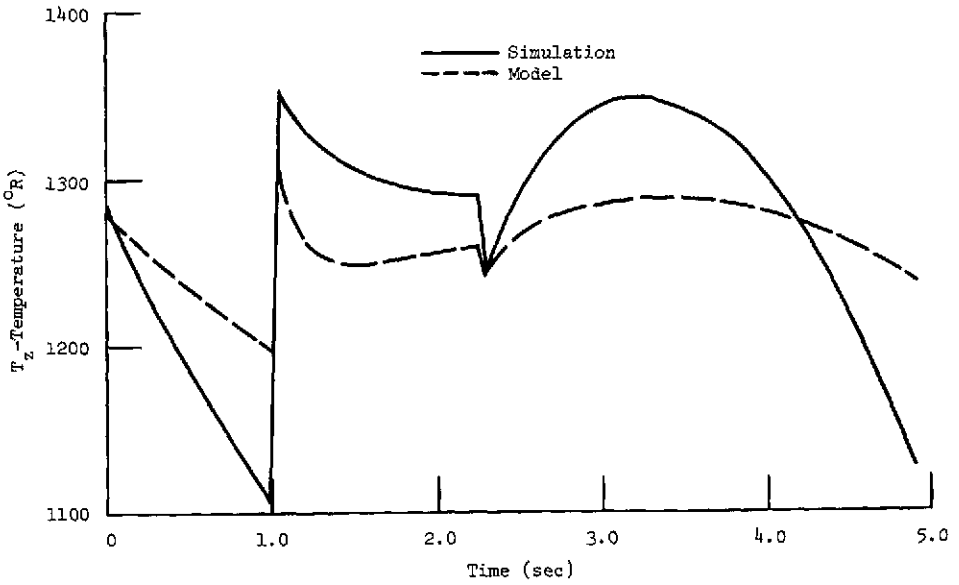

(d) Nozzle inlet temperature.

Figure 3.10. - Simulation and composite model trajectories.

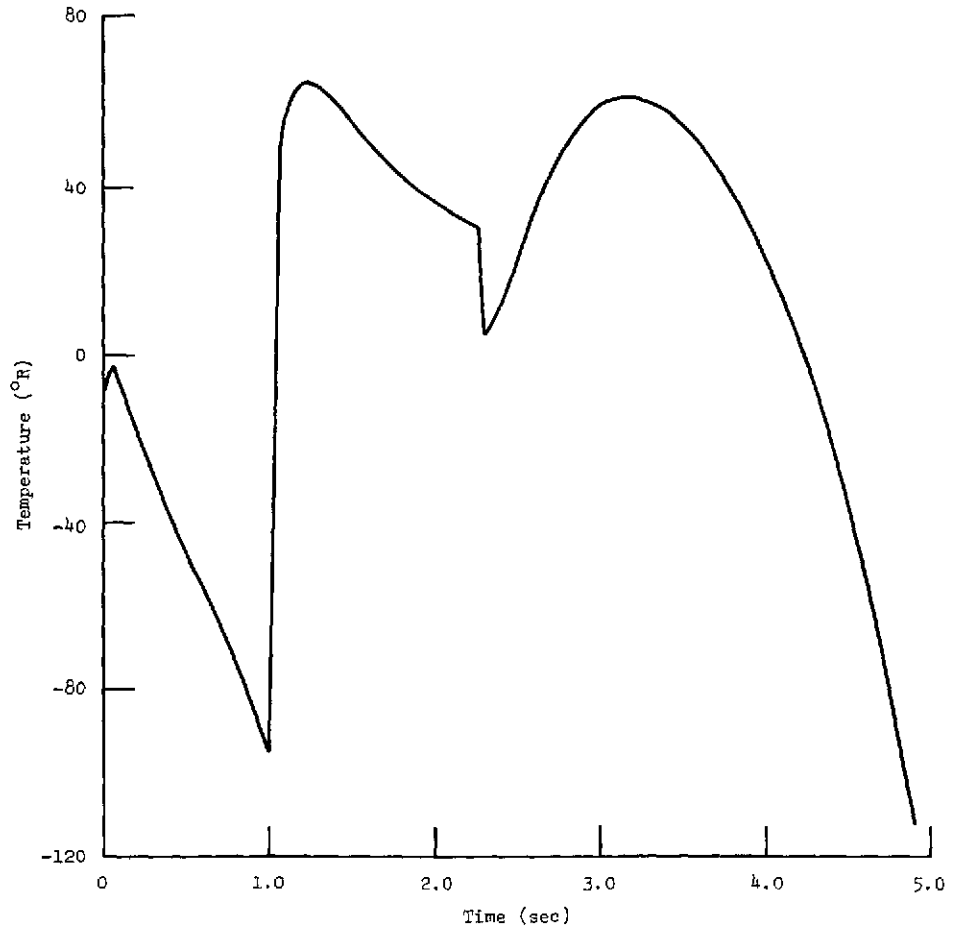

(dd) Nozzle inlet temperature error.

Figure 3.10. - Simulation and composite model trajectories.

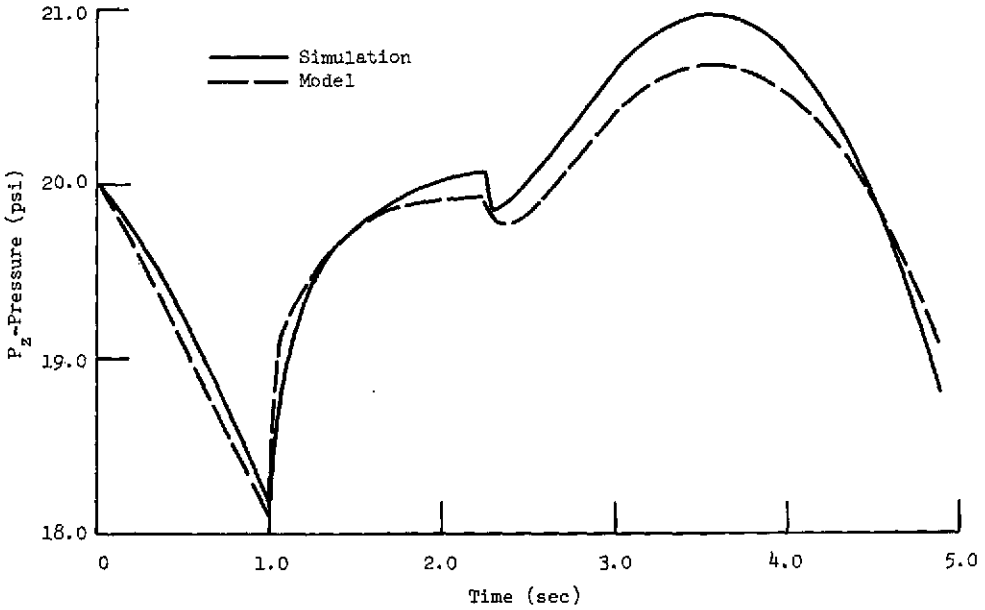

(e) Nozzle inlet pressure.

Figure 3.10. - Simulation and composite model trajectories.

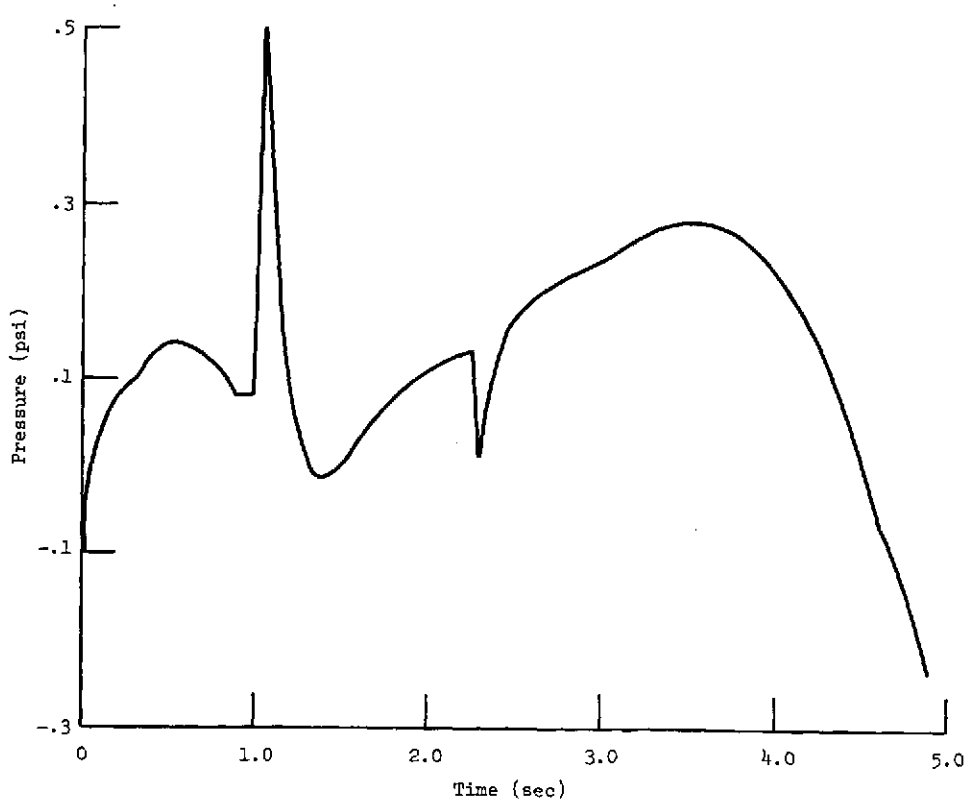

(ee) Nozzle inlet pressure error.

Figure 3.10. - Simulation and composite model trajectories.

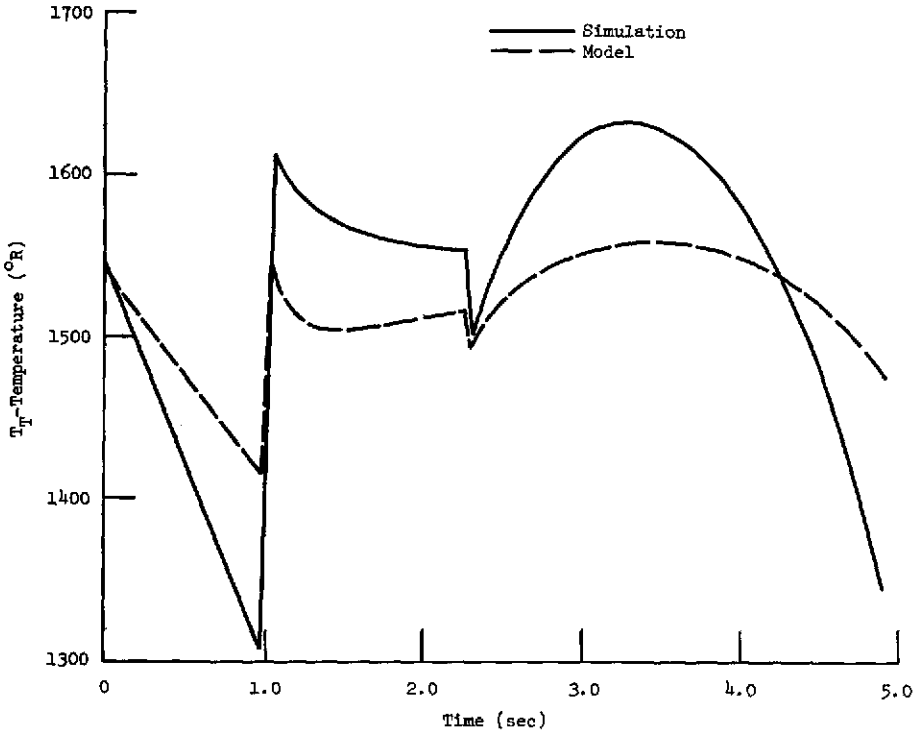

(f) Turbine inlet temperature.

Figure 3.10. - Simulation and composite model trajectories.

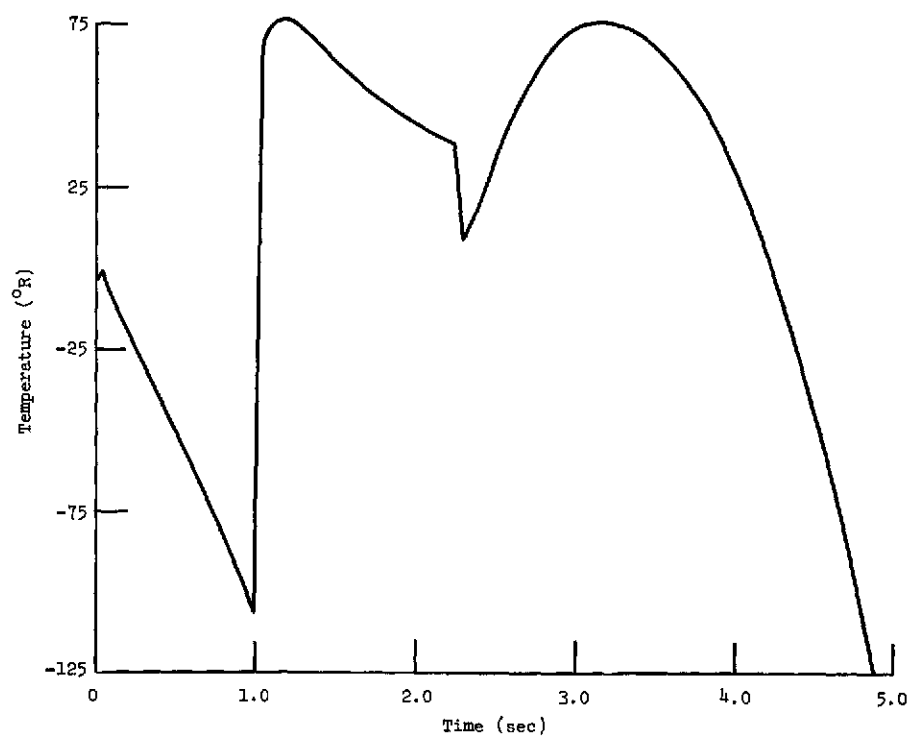

(ff) Turbine inlet temperature error.

Figure 3.10. - Simulation and composite model trajectories.

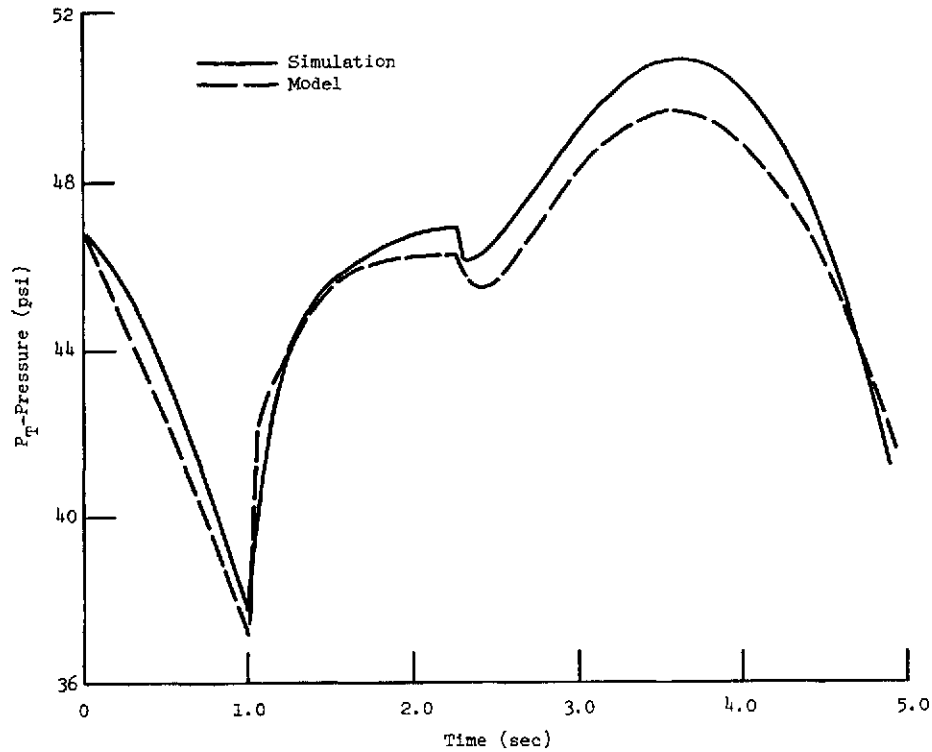

(g) Turbine inlet pressure.

Figure 3.10. - Simulation and composite model trajectories.

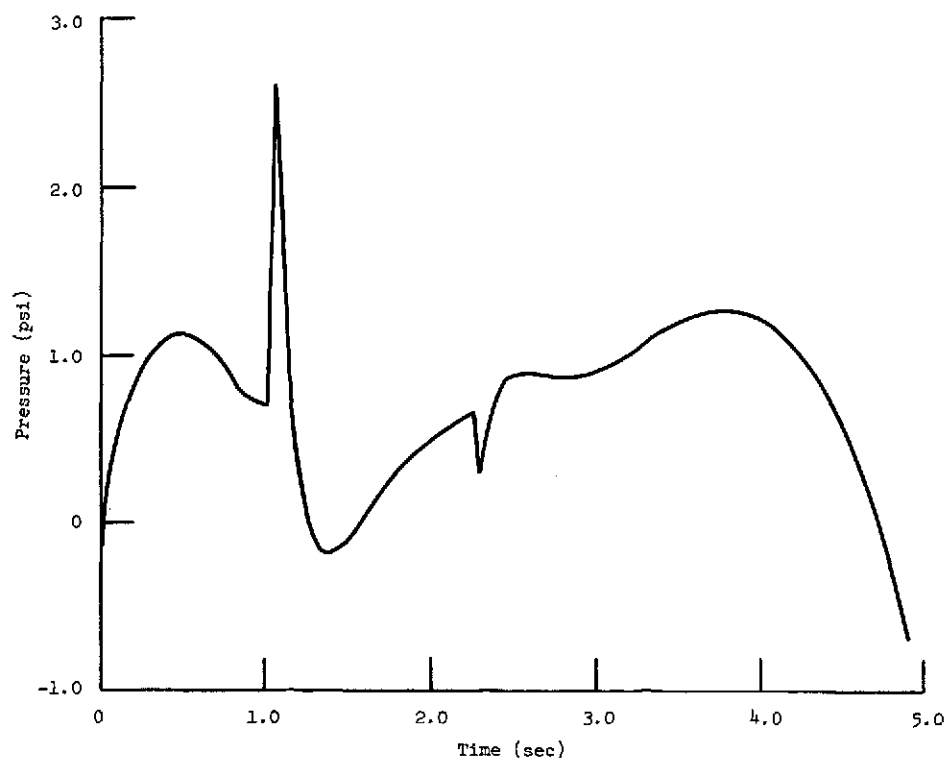

(gg) Turbine inlet pressure error.

Figure 3.10. - Simulation and composite model trajectories.

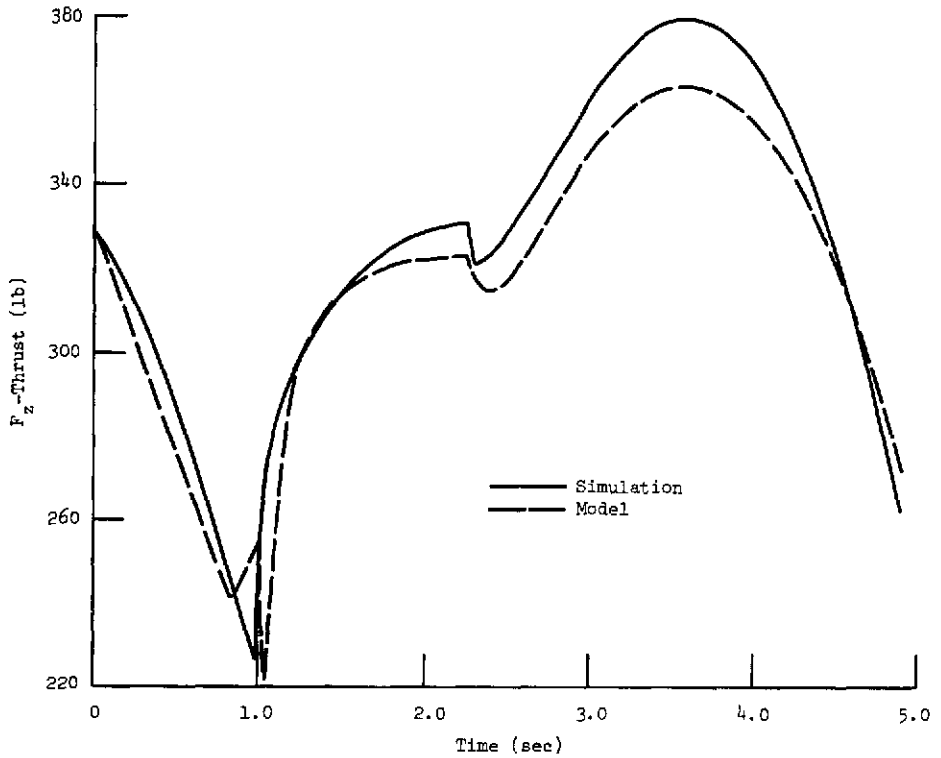

(h) Engine thrust.

Figure 3.10. - Simulation and composite model trajectories.

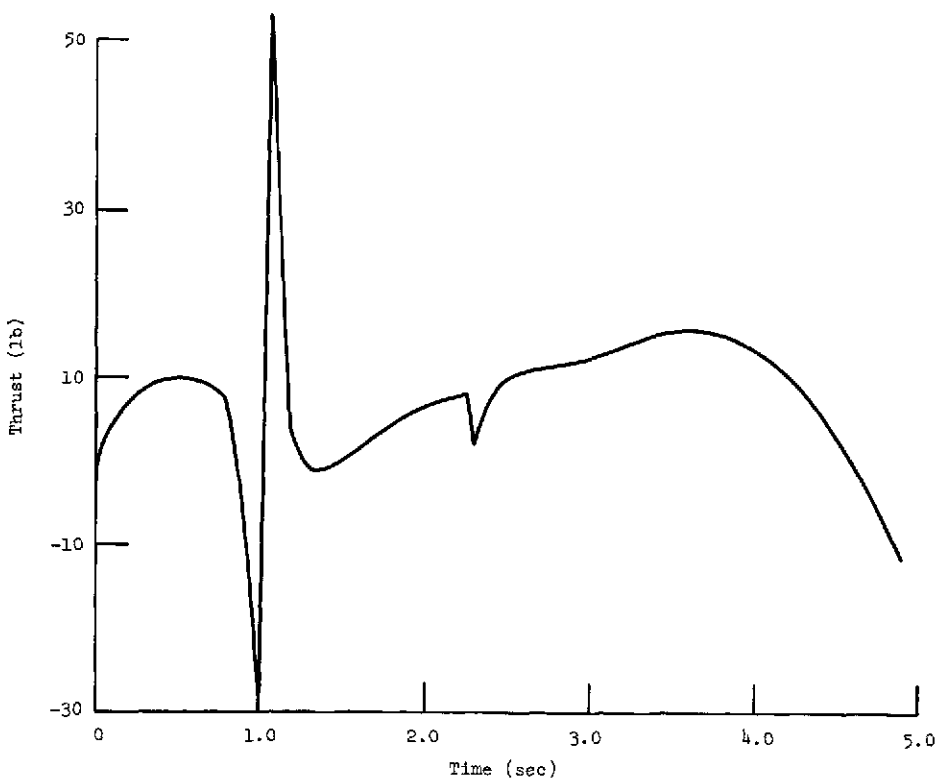

(hh) Engine thrust error.

Figure 3.10. - Simulation and composite model trajectories.

Output	Average error	Variance	Normalizing value	Normalized average error	Normalized variance
S	268.960	138860	35000	.0077	.0106
T_c	4.396	14.06	810	.0054	.00463
P_c	.8092	.3057	51.53	.0157	.0107
T_z	10.47	2484	1283	.0082	.0389
P_z	.1279	.01484	20	.0064	.0061
T_T	15.47	3345	1544	.0100	.0375
P_T	.7351	.2497	46.51	.0158	.0107
F_z	7.615	86.05	327.19	.0233	.0284

$$\text{Normal average error} = \frac{\text{Average error}}{\text{Normal value}}$$

$$\text{Normal variance} = \frac{\text{Variance}}{(\text{Normal value})^2}$$

Figure 3.11. - Average error values and variances for output error trajectories.

than 3 percent. This error is considered insignificant for control purposes and thus the model passes the verification test. Figures 3.12 and 3.13 are plots of w_{fNOM} and δw_f as determined by the composite model.

It is remarked that a more accurate model, if required, could be attained by three methods. First, the estimates obtained by the Tse and Weinert method could be enhanced by using more data in the identification procedure. More data implies either longer time history intervals or several shorter time history intervals with the resulting parameter estimates averaged together. Second, a more accurate identification technique that requires good a priori information could be applied. Using the structure and the parameters determined by the Tse and Weinert method as the assumed model structure and initial parameter conditions, the more accurate identification method would have adequate a priori information for a fast and accurate convergence of parameter estimates. Such methods include quasilinearization, invariant imbedding, and sequential identification (Sage and Melsa, 1971). Third, the data sampling period could be reduced to include higher frequency components in the identification data. Consequently, the model would be accurate over a larger frequency range and reduce the error caused by high frequency elements.

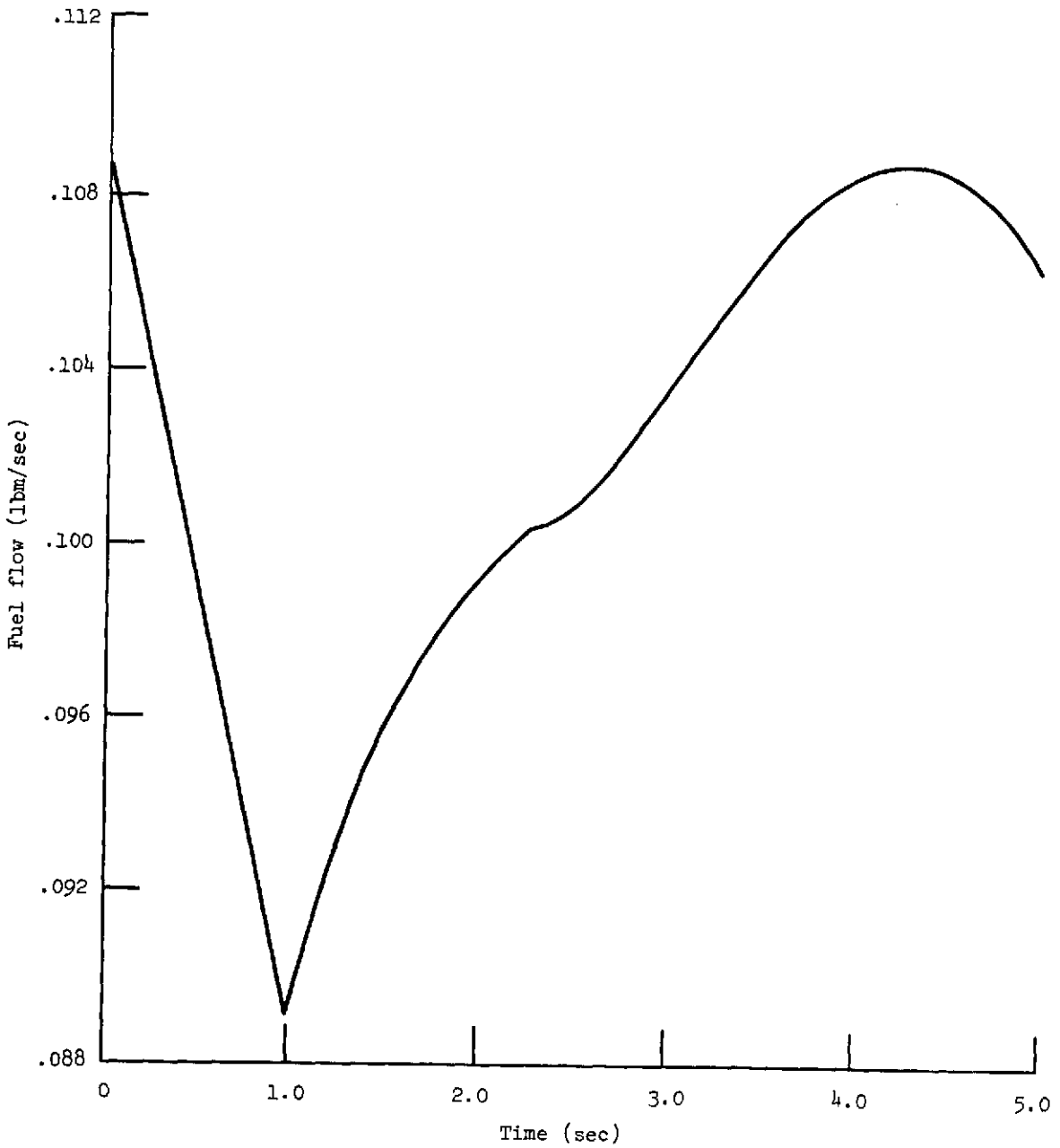

Figure 3.12. - Plot of ω_{fNOM} vs time.

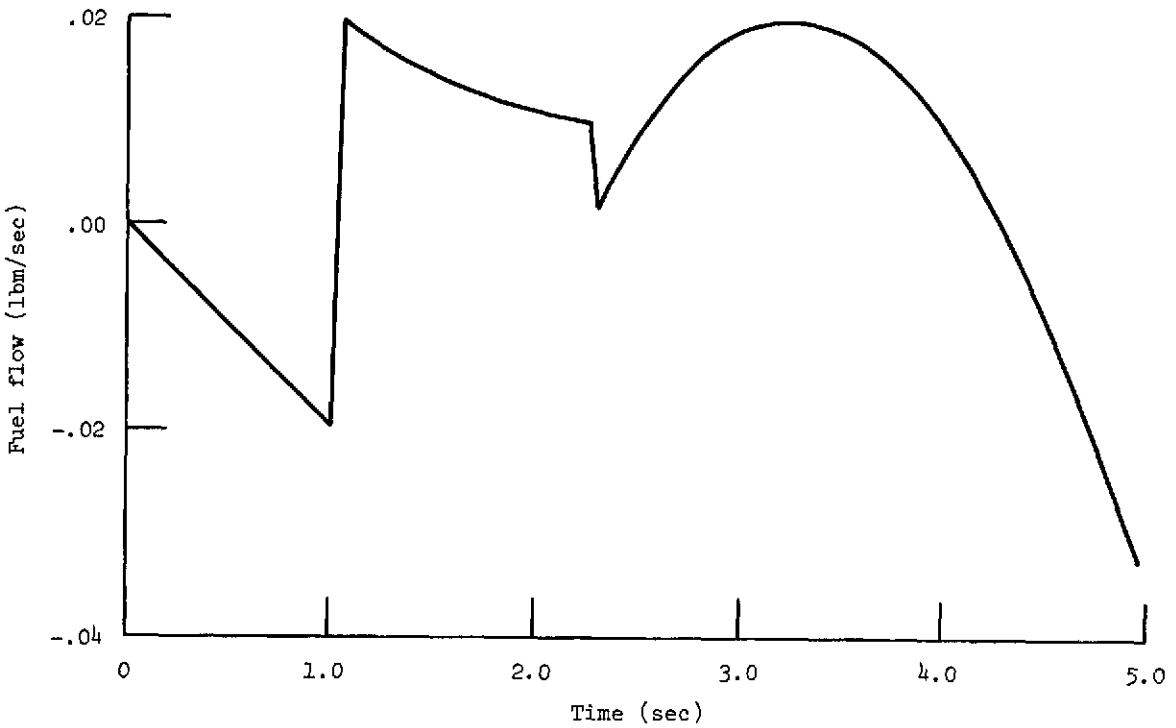

Figure 3.13. - Plot of $\delta\omega_f = \omega_f - \omega_{fNOM}$ vs time.

CHAPTER IV

ADAPTIVE DIGITAL CONTROL

This chapter discusses the development of an adaptive digital control scheme to be used for jet engine control. This adaptive digital control scheme must jointly satisfy the first and second research objectives stated in Chapter I. These objectives are to (1) develop a discrete engine control algorithm that incorporates adaptive sampling and (2) design a practical adaptive engine control using an output regulator formulation.

In a digital control system there exists a sample and hold operation that quantizes the continuous analog signal of the continuous controlled process into a discrete digital signal capable of being processed by a digital computer. One of the major engineering considerations in the design of digital control systems is the sampling frequency. If this frequency is too small, system instabilities will occur. If the sampling frequency is too large the computer will be required to process more information than is really required for adequate control. An alternative to choosing a fixed sampling frequency for the digital controller is adaptive sampling. Adaptive sampling increases sampling efficiency by varying the sampling frequency as a function of system parameter. Sampling efficiency is defined as the ratio of some quantitative measure of a system performance to the number of sampling instants required to achieve that performance.

Adaptive sampling was first developed by Dorf, et al. (1962). Later other authors such as Gupta (1963), Tomovic and Bekey (1966), Mitchell and McDaniel (1969), and Bekey and Tomovic (1966) developed alternate adaptive sampling schemes. Hsia (1974) has shown that the design of adaptive sampling laws could be unified under one analytical approach.

Since adaptive sampling increases sampling efficiency, the same level of system performance can be achieved with adaptive sampling as with fixed frequency sampling but with fewer sampling instants. Also, computer usage for control purposes is directly proportional to the number of sampling instants. Thus adaptive sampling applied to jet engine control can make efficient use of on-board computers, one of the objectives of this research.

The second objective of the research reported in this chapter is the design of a jet engine control that is simple, practical, and maintains good engine response. A simple, practical, and effective way of regulating the outputs of many systems is through constant, proportional feedback. To insure good system response, constant proportional feedback laws can be designed via optimal regulator theory, (Kwakernaak and Sivan, 1972). Michael and Farrar (1973) have shown that the continuous optimal state regulator theory can be applied to the design of controls for a jet engine. One of the assumptions necessary for the work of Michael and Farrar was the availability of all state variables. This is not always practical in jet engine control. Another solution is to reconstruct the states from the engine outputs using a Kalman filter (Kalman and Bucy, 1961) or a Luenberger observer (Luenberger, 1966). However, this would probably result in

an overly complex control. An alternate approach is to use a time-invariant optimal output regulator. Such a control would be both simple and practical since the feedback gains are constant and only output measurements are required. Levine and Athans (1970) state that the output regulator will perform well for many well-behaved systems. To facilitate the use of an on-board digital controller the optimal output regulator solution is required in discrete form. Thus the second objective will be met by an optimal discrete output regulator.

This chapter is divided into three sections. In the first section, the discrete output regulator problem for time-invariant linear systems is stated and necessary conditions for its solution are derived. Also, an algorithm for computer solution of the necessary conditions is given. The second section describes adaptive sampling and the derivation of adaptive sampling control schemes. Also computer simulation results of the application of this control scheme to a linearized fifth order jet engine model are presented.

4.1 The Optimal Discrete Output Regulator

The optimal linear state regulator is a well known and well studied problem. The fundamental results are by Kalman (1960). Several texts that extend the basic results in both discrete and continuous time formulations are also available, see for example that of Anderson and Moore (1971) and Kwakernaak and Sivan (1972).

The optimal linear state regulator requires the full state of the system to determine the feedback control. Often the order of the output vector of practical systems is less than the order of the system state vector. Thus to apply the optimal linear state regulator, either a Kalman filter (Kalman and Bucy, 1961) or a Luenberger

observer (Luenberger, 1966) is often used to generate an estimate of the state vector.

An alternate approach is to design a regulator that uses only available outputs. Results on this specific problem have been obtained for systems with a scalar control by Rekasius (1967) and for multivariable systems by Levine, et al. (1970 and 1971). Mendel (1974) has also obtained similar results.

For the discrete time case Mullis (1973) has developed weak sufficient conditions for the existence of a finite sequence of output feedback gains for which every initial state can be driven to the origin. Ermer and VandeLinde (1972) have developed the discrete output regulator for the time-varying case using dynamic programming.

In this section a sampled-data constraint is imposed on a continuous system with a quadratic cost function. The resultant discrete or sampled-data system will have cross weighting between the state and the control in the cost function. For full state feedback a quadratic cost function with cross weighting can be converted easily to one without cross weighting by a transformation involving the state and control variables. In the output feedback formulation such a transformation is not physically realizable since the full state vector is not available. This section, therefore, develops the discrete output regulator equations when the process dynamics are linear and time-invariant for a cost function with cross weighting between the state and control vectors. An iterative algorithm is developed that solves the equations of the time-invariant case, and an example problem is solved using this algorithm.

By analogy to the time-invariant state feedback regulator problem, one might expect that the optimal output feedback matrix would become time-invariant as the interval of control becomes semi-infinite. However, for many well behaved systems this is not the case. Brockett and Lee (1967) have cited an example of a second order system with one output that is both observable and controllable. The system, however, cannot be stabilized by a constant feedback gain. Yet the system can be stabilized by a time-varying gain. To avoid this difficulty, the formulation to be described constrains the feedback matrix to be a constant and assumes that a constant stabilizing output feedback matrix does exist.

Problem Formulation. Given the time-invariant linear system

$$x(k+1) = Ax(k) + Bu(k) \tag{4.1.1}$$

$$y(k) = Cx(k)$$

where $x \in R^n$, $y \in R^q$, $u \in R^m$. Consider also the quadratic cost function

$$J = \frac{1}{2} \sum_{i=0}^{\infty} x'(i)\hat{Q}x(i) + u'(k)\hat{R}u(i) + 2x'(i)Mu(i) \tag{4.1.2}$$

where it is assumed that

A is an n x n real constant matrix

B is an n x m real constant matrix

C is a q x n real constant matrix

$\hat{Q}$ is an n x n symmetric positive semi-definate real constant matrix

M is an n x m real constant matrix

$\hat{R}$ is an m x m symmetric positive definate real constant matrix

$\hat{Q} - M\hat{R}^{-1}M'$ is positive semi-definate

Now introducing the constraint

$$u(k) = -Sy(k) = -SCx(k) \tag{4.1.3}$$

the cost function becomes

$$J = \frac{1}{2} \sum_{k=0}^{\infty} x'(k)[\hat{Q} + C'S'\hat{R}SC - MSC - C'S'M']x(k) \tag{4.1.4}$$

Using a theorem from Kwakernaak and Sivan (1972), the constrained dynamic optimization problem can be converted to a constrained static problem.

Theorem 1 (Kwakernaak and Sivan, 1972). Let $x(k)$ be the solution of

$$x(k + 1) = Tx(k) \tag{4.1.5}$$

$$x(0) = x_0$$

If T and the symmetric positive semi-definate matrix V are constant and the moduli of the characteristic values of T are strictly less than one, then

$$E\left\{\sum_{k=0}^{\infty} [x'(k)Vx(k)]\right\} = Tr\left[PE\left(x_0x_0'\right)\right] \tag{4.1.6}$$

where

$$P = T'PT + V \tag{4.1.7}$$

Taking the expected value and applying Theorem 1, the cost function becomes

$$\hat{J} = E(J) = \frac{1}{2} \mathrm{Tr}\{PX_0\} \tag{4.1.8}$$

with

$$P = A_0'PA_0 + V \tag{4.1.9}$$

and

$$V = \hat{Q} + C'S'\hat{R}SC - MSC - C'S'M' \tag{4.1.10}$$

$$A_0 = A - BSC \tag{4.1.11}$$

$$X_0 = E\langle x_0 x_0' \rangle \tag{4.1.12}$$

The optimization problem now is to find a matrix S^* that minimizes the performance index of equation (4.1.8) while satisfying the constraint of equation (4.1.9).

The problem is solved by defining the Lagrangian

$$\mathcal{L} = \frac{1}{2} \mathrm{Tr}\left\{PX_0 + \left(-P + A_0'PA_0 + V\right)L'\right\} \tag{4.1.13}$$

where L is a matrix of Lagrange multipliers. The necessary conditions for optimization are

$$\left.\frac{\partial \mathcal{L}}{\partial S}\right|_* = 0, \qquad \left.\frac{\partial \mathcal{L}}{\partial P}\right|_* = 0, \qquad \text{and} \quad \left.\frac{\partial \mathcal{L}}{\partial L}\right|_* = 0 \tag{4.1.14}$$

Using the following formulas

$$\frac{\partial}{\partial x}\{\mathrm{Tr}[AXB]\} = A'B' \tag{4.1.15}$$

$$\frac{\partial}{\partial x}\{\mathrm{Tr}[AXBX]\} = A'XB' + AXB \tag{4.1.16}$$

The necessary conditions become

$$S^* = (R + B'P^*B)^{-1}(B'P^*A + M')L^*C'(CL^*C')^{-1} \tag{4.1.17}$$

$$L^* = A_0^* L^* A_0'^* + X_0 \tag{4.1.18}$$

$$P^* = A_0^{*\prime} P A_0^* + V^* \tag{4.1.19}$$

where

$$A_0^* = A - BS^*C \tag{4.1.20}$$

and

$$V^* = \hat{Q} + C'S'^*\hat{R}S^*C - MS^*C - (MS^*C)' \tag{4.1.21}$$

These equations represent necessary conditions for the optimal discrete output regulator. Both equations (4.1.18) and (4.1.19) are in the form of discrete Lyapunov equations. However, if S^* were eliminated in equations (4.1.18) and (4.1.19) via (4.1.17), then equations (4.1.18) and (4.1.19) would become a pair of coupled discrete Ricatti equations. Also, note that if C is square and invertible then these necessary conditions reduce to the steady-state equations for the discrete optimal state regulator.

Computer Algorithm. A computer program was written that solves equations (4.1.17) to (4.1.21). The algorithm that was programmed is as follows. Given the equations

(1) $S_i = \left(\hat{R} + B'P_iB\right)^{-1}\left(B'P_iA + M'\right)L_iC'\left[CL_iC'\right]^{-1}$

(2) $A_i'P_{i+1}A_i - P_{i+1} = -\hat{Q} - C'S_i'\hat{R}S_iC + MS_iC + (MS_iC)'$

(3) $A_iL_iA_i' - L_i = -I$

(4) $A_i = A - BS_iC$

where now

$X_0 = I$

(a) Set $i = 1$, $P_i = 0$

(b) Select an initial stabilizing gain matrix, S_i

(c) Calculate P_{i+1} using (2) and (4) and S_i

(d) Stop the iterative procedure if $||P_i - P_{i+1}|| < \varepsilon$

(e) Set $i = i + 1$

(f) Calculate simultaneously L_i and S_i using (1), (3), (4), and P_i

(g) Return to step (c)

The subroutines used in this algorithm are entitled CLSDLP, MULT, DISLYP, DITORF, and RICATT. They were written in Fortran IV for the IBM 7094 digital computer. A listing for each subroutine is given in Appendix C.

The subroutine MULT determines the product of two compatible matrices. The subroutine CLSDLP solves for the closed loop system matrix and its transpose given A, B, S, and C. Subroutine DISLYP solves the matrix equation

$$VPV' - P = -W \tag{4.1.22}$$

by successive approximation given a stable matrix V and a positive definate matrix W. The subroutine DITORF solves equation (4.1.17). The subroutine RICATT is the controlling subroutine that accomplishes the iterative portion of the algorithm. Convergence criteria used in RICATT and DISLYP require a matrix norm. If A_d is an $n \times n$ matrix with elements a_{ij}, then the norm of this matrix as used in RICATT and DISLYP is defined as

$$||A_d|| = \sum_{i=1}^{n} \sum_{j=1}^{n} |a_{ij}| \tag{4.1.23}$$

It is remarked that an initial gain matrix, for the full order case ($n = m$), can be obtained from an algorithm by Kleinman (1974). For the reduced order ($n > m$) output feedback case, a possible choice would be to select corresponding elements from a full order solution as elements of an initial stabilizing reduced order gain matrix. Also,

the successive approximation technique used in DISLYP is similar to the one suggested by Kleinman (1974). The algorithm of this section is comparable to Hewer's (1971) algorithm for solving the optimal discrete state regulator and is a discrete analog to the continuous algorithm developed by Levine and Athans (1970).

4.2 Adaptive Sampling

This section discusses adaptive sampling and gives a derivation for certain adapative sampling laws. As previously stated the purpose of adaptive sampling is to increase the sampling efficiency of a digital control system by varying the sampling rate with respect to a system parameter. In this regard the following definition is helpful.

Definition. If J_A is the value of a cost function associated with system A, and N_A is the number of sampling instants used in generating that cost, then the sampling efficiency of system A, η_A, is

$$\eta_A = \frac{1}{J_A N_A} \tag{4.2.1}$$

Now the following design problem is stated.

Problem Statement. Determine an algorithm that automatically adjusts the sampling period (T_i) based on some function of a scalar sampled signal $y(t)$ or other system variables. That is, let

$$T_i = f_1(e(t)) \tag{4.2.2}$$

where

$$e(t) = y(t) - y(t_i) \tag{4.2.3}$$

and

$$T_i = t_{i+1} - t_i \tag{4.2.4}$$

with the following constraint.

$$T_{min} \leq T_i \leq T_{max} \tag{4.2.5}$$

This constraint limits the variable sampling period, T_i, to an allowable range defined by the maximum processing rate of the digital controller (T_{min}) and system stability requirements (T_{max}).

Problem Solution. The solution of this problem essentially follows the approach of Hsia (1974). Consider the cost functional

$$J = J_1 + J_2 \tag{4.2.6}$$

where

$$J_1 = \frac{1}{(T_i)^a} \int_{t_i}^{t_{i+1}} [|e(t)|]^b \, dt \tag{4.2.7}$$

and

$$J_2 = f_2(T_i) \tag{4.2.8}$$

The cost J_1 is interpreted as the cost of incurring errors due to sampling, while J_2 is interpreted as the cost of taking samples. If the function $f_2(T_i)$ is the cost per sample per unit time, then for the region of constraint defined by equation (4.2.5), $f_2(T_i)$ should be non-negative and monotonically decreasing. That is for

$$T_{min} \leq T_i \leq T_{max} \tag{4.2.5}$$

then

$$f_2(T_i) \geq 0 \tag{4.2.9}$$

and

$$f_2(T_1) \geq f_2(T_2), \qquad \text{for } T_1 < T_2 \tag{4.2.10}$$

Also, to ensure a meaningful cost function a and b are restricted to the following sets of values.

$$a = \{-1, 0, 1\} \tag{4.2.11}$$

$$b = \{1, 2\} \tag{4.2.12}$$

Now an adaptive sampling law can be obtained by finding the T_i that minimizes equation (4.2.6).

To perform this minimization expand $y(t)$ in a Taylor series about t_i.

$$y(t) = y(t_i) + \dot{y}(t_i)(t - t_i) + \ldots \tag{4.2.13}$$

Since

$$T_{max} \geq t - t_i$$

and T_{max} is chosen for stability of the system producing $y(t)$, it is assumed that higher order terms in the Taylor's expansion can be neglected. Then by (4.2.3)

$$e(t) = \dot{y}(t_i)(t - t_i) \tag{4.2.14}$$

Substituting (4.2.14) into (4.2.7) and integrating gives

$$J = \frac{|\dot{y}(t_i)|^b}{b + 1} (T_i)^{b+1-a} + f_2(T_i) \tag{4.2.15}$$

Differentiating this expression with respect to T_i yields

$$\frac{\partial J}{\partial T_i} = |y(t_i)|^b \left(\frac{b + 1 - a}{b + 1}\right)(T_i)^{b-a} + \frac{df_2(T_i)}{dT_i} \tag{4.2.16}$$

To determine a necessary condition for the minimization of (4.2.6) let

$$\frac{\partial J}{\partial T_i} = 0 \tag{4.2.17}$$

From this necessary condition different adaptive sampling laws can be derived by choosing different functions for $f_2(T_i)$.

For the adaptive sampling law used in this dissertation the following choices were made

$$a = 1$$

$$b = 2$$

and

$$f_2(T_i) = A\left(1 - BT_i + \frac{B^2T_i^2}{2}\right) \tag{4.2.19}$$

Now $f_2(T_i)$ can be made non-negative and monotonically decreasing by choosing A and B such that

$$A\left(1 - BT_i + \frac{B^2T_i^2}{2}\right) \geq 0 \tag{4.2.20}$$

and

$$AB(BT_i - 1) \leq 0 \tag{4.2.21}$$

for

$$T_{min} \leq T_i \leq T_{max} \tag{4.2.5}$$

The sampling period, T_i, is constrained to be positive. Then from (4.2.20) A is positive. From (4.2.21) B is positive and

$$B \leq \frac{1}{T_i} \tag{4.2.22}$$

Since the maximum value for T_i is T_{max},

$$B = \frac{1}{T_{max}} \tag{4.2.23}$$

satisfies (4.2.22) and consequently $f_2(T_i)$ satisfies the conditions of (4.2.5), (4.2.9), and (4.2.10).

Now from (4.2.16), (4.2.17), (4.2.18), and (4.2.23)

$$0 = |\dot{y}(t_i)|^2 \frac{2}{3} T_i + \frac{A}{T_{max}}\left(\frac{T_i}{T_{max}} - 1\right) \tag{4.2.24}$$

and

$$T_i = \frac{T_{max}}{\alpha[\dot{y}(t_i)]^2 + 1} \tag{4.2.25}$$

where

$$\alpha = \frac{2}{3}\frac{1}{AB^2} > 0 \tag{4.2.26}$$

The adaptive sampling law is

$$T_i = \begin{cases} \dfrac{T_{max}}{\alpha[\dot{y}(t_i)]^2 + 1}, & T_i > T_{min} \\ T_{min}, & T_i \leq T_{min} \end{cases} \tag{4.2.27}$$

The choice of α reflects a relative weighting between the cost of sampling and the cost of errors incurred due to sampling. As α decreases the relative cost of sampling increases. Thus the number of sampling instants increases.

As an example of a calculation for α let $\dot{y}(t)$ be approximated and normalized as

$$\dot{y}(t_i) = \frac{y(t_i) - y(t_{i-1})}{T_{i-1}y(t_i)} \tag{4.2.28}$$

Assume that if $y(t_{i-1})$ and $y(t_i)$ differ by at least 10% the sampling law should predict a minimum sampling period. From equation (4.2.25)

$$T_{min} \geq \frac{T_{max}}{\alpha \dfrac{0.01}{T_i^2} + 1} \tag{4.2.29}$$

Then

$$\alpha \geq (T_r - 1)T_i^2\ 100 \tag{4.2.30}$$

for all possible T_i, where

$$T_r = \frac{T_{max}}{T_{min}} >> 1 \tag{4.2.31}$$

Since the inequality of equation (4.2.30) must hold for all T_i, then

$$\alpha \gtrsim 100\ \frac{T_{max}^2}{T_{min}}$$

It is remarked at this time that Smith (1971) has shown that the improvement in sampling efficiency may be highly dependent on the continuous process generating $y(t)$, the presence of noise in the sampled signal, and the criterion defining performance. However, the adaptive control scheme described in the next section combines adaptive sampling with a control that is parametrically dependent on the sampling period. This minor sophistication over the systems studied by Smith gives improvements in sampling efficiency that are not highly system or noise dependent.

The selection of the system parameter used in the adaptive sampling scheme is highly system dependent. One possible choice is to use an output variable as the system sampling parameter that corresponds to the slowest mode of the controlled system. Another possible choice would be the average sampling error for all available system outputs. The large number of possible choices for system sampling parameters combined with the different adaptive sampling laws allow a great deal of design flexibility.

4.3 Adaptive Digital Control

In the previous two sections both adaptive sampling and the discrete output regulator have been discussed. This section will combine these two control techniques into a simple adaptive digital control scheme. The objectives of design simplicity and practicality strongly influence the simplifications used to generate this control scheme.

Essentially the control scheme incorporates adaptive sampling and a proportional feedback gain matrix that is parametrically dependent on the sampling period. This is shown in block diagram form in Figure 4.1. The problem is to determine the functional relationship between the sample period, T, and the feedback gain matrix.

Assume for the moment that the sample period is a constant. It is shown in Appendix D that if the continuous process is time-invariant the equivalent sampled-data system will be time-invariant. Assume also for the moment that full state feedback is available. Now the constant feedback matrix could be found by application of the steady-state discrete state regulator equations to the system in question.

Now let the sampling rate vary with time. The sampled-data system is parametrically dependent on the sampling period and will be time-varying even though the continuous process is time-invariant. If the sequence of sampling periods is known over the interval of control, the time evolution of the discrete system will be known. Therefore the feedback gain matrix could be generated by the time-varying discrete state regulator over the interval of control.

Now (still assuming full state feedback) introduce adaptive sampling into the control picture. The sequence of sampling periods is now a function of a continuous system parameter. As such, the

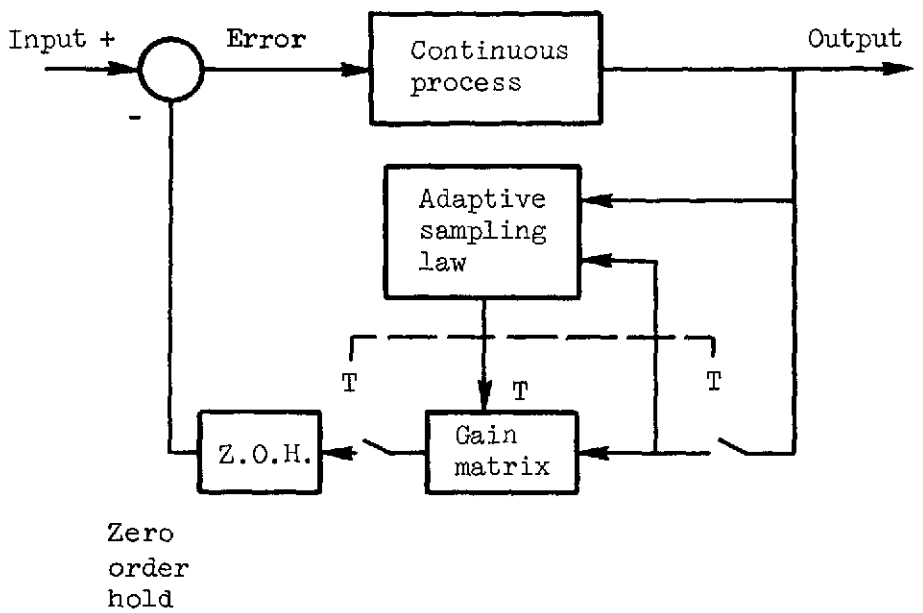

Figure 4.1. - Adaptive control scheme.

sequence will be unpredictable due to unknown system disturbances, changing environment, and noise. The most probable values of the sampling period will be the limit values T_{min} and T_{max}. However, even the possible duration of a sequence of T_{min} samples for instance, could not be determined. Thus the feedback matrix cannot realistically be determined by the time-varying regulator equations. The time-varying regulator solutions is parametrically dependent on the sample period and is computed backward in time. Thus sample periods that have not yet been predicted by the adaptive sampling law would be required for the solution of the time-varying regulator.

To overcome this problem the following simplification will be made. For each sampling period predicted by the adaptive sampling law, the feedback matrix will be determined by the steady-state solution of the discrete regulator. Note that with this simplification either the full state regulator or the output regulator of the previous section can be used to determine the feedback gain, depending on the available outputs. Also, for a given linear, time-invariant continuous process, the simplification implies that there is a unique feedback matrix for each sampling period. Thus the feedback gains for the given process can be computed off-line for a sufficient number of sampling periods to establish a functional relationship between gains and sampling period. This relationship could easily be stored by a digital controller and used on-line to generate the control input to the continuous process. This procedure would eliminate the prohibitive computation time needed to solve the discrete regulator problem on-line.

4.4 Example Problem

This adaptive control scheme was applied to a linearized model of the Pratt and Whitney Aircraft F401 advanced technology two-spool turbofan engine. This model was identified by Michael and Farrar (1973). The F401 engine is being studied for use in a V/STOL (Vertical and short takeoff and landings) application and has variable exhaust, fan, and compressor geometries. The model selected for study here has a normalized fifth-order state vector and a normalized scalar control. The model represents the dynamical engine operation for small variations about a 73° power-lever angle setting.

The fifth-order state represents turbine inlet temperature, combustor pressure, fan angular velocity, high pressure compressor angular velocity, and afterburner pressure, respectively. In this study the control represents jet exhaust nozzle area.

In state-space form the model is

$$\dot{x}(t) = Fx(t) + Gu(t)$$

where

The F matrix is

$$\begin{bmatrix} -34.0130 & -9.3030 & 12.0370 & -2.3980 & -1.2540 \\ 4.3890 & -38.7620 & -4.2210 & 28.4800 & 14.7290 \\ -4.7550 & 2.2870 & -0.4000 & -1.5460 & -2.2000 \\ 2.0460 & 1.0620 & -0.7290 & -2.1500 & -0.6240 \\ 4.1510 & -8.8140 & -0.1670 & 7.4770 & 1.0990 \end{bmatrix}$$

and

The G matrix is

$$\begin{matrix} 0.7660 \\ 0.0560 \\ 0.1560 \\ -0.1370 \\ -4.7290 \end{matrix}$$

The output vector is given as

$$y(t) = Cx(t)$$

where $y(t) \in R^m$. In this example each output element is one of the states so that each row of C has only one nonzero element and it is unity.

The control objectives are assumed to be adequately described by the performance index

$$J = \frac{1}{2} \int_0^5 [x'(t)Qx(t) + u'(t)Ru(t)]dt$$

where $Q = I$ and $R = 1$. To study the effect of adaptive sampling on the system's performance the adaptive sampling law

$$T_i = \begin{cases} \dfrac{T_{max}}{\alpha \dot{e}(t_i)^2 + 1}, & T_i \geq T_{min} \\ T_{min}, & T_i < T_{min} \end{cases}$$

was implemented. The system parameter used to vary the sampling period was a combination of the engine outputs such that

$$e(t) = \sum_{k=1}^{m} |y_k(t) - y_k(t_{i-1})|$$

where $y_k(t_i)$ is the k^{th} element of $y(t)$ sampled at time t_i. Now the error derivative can be approximated as

$$\dot{e}(t_i) = e(t_i)/T_{i-1}$$

The limits on the sampling period were selected as

$$T_{min} = 0.01$$

and

$$T_{max} = 0.5$$

The T_{min} limit was selected as three times smaller than the real part of the smallest eigenvalue. The T_{max} limit was selected to insure system stability.

The engine model and the adaptive digital control scheme were simulated on an IBM 7094 digital computer. System performance was studied for the reduction of the initial condition disturbance

$$x(0) = \begin{pmatrix} 1 \\ 2 \\ 0 \\ -1 \\ -2 \end{pmatrix}$$

to zero with different output configurations. In each experiment the performance index, J, the number of sampling instants, N_f, and the sampling efficiency

$$\eta = \frac{1}{N_f J}$$

were calculated. The results are summarized in Figure 4.2.

From these results it can be seen that sampling efficiency can be improved by a factor of 20 by the introduction of adaptive sampling with only a small increase in the system performance index. Note also that afterburner pressure is the most important of the states for control purposes.

State available as output	Adaptive sampling parameter, α	Number of sampling instants, N_f	Performance index, J	Sampling efficiency, η
1,2,3,4,5	∞	500	.6711	.00298
1,2,3,4	.0667	19	1.0415	.05053
1,2, 4,5	.0667	24	.6727	.06194
2,3,4,5	.0667	23	.6733	.06457
1	.0667	14	.9200	.07764
2	.0667	17	.9148	.06430
3	.0667	12	.9304	.08957
4	.0667	13	.8847	.08695
5	.0667	13	.6913	.11127
3, 5	.0667	15	.6760	.09862

State	Description
1	Turbine inlet temperature
2	Combustor pressure
3	Fan angular velocity
4	High pressure compressor angular velocity
5	Afterburner pressure

Figure 4.2. - Adaptive digital control results for F401 engine model.

CHAPTER V

APPLICATION OF ADAPTIVE DIGITAL CONTROL TO A JET ENGINE

The purpose of this section is to describe the application of the previous results on identification and adaptive control to a jet engine. The second-order state-space operating point models given in Chapter III are used by the adaptive control scheme of Chapter IV to determine a piecewise constant control input for the digital simulation of a single spool turbojet engine. Thus, the adaptive nature of this engine control is twofold. First, the output feedback will vary when the engine model information reflects a change in the engine operating point. Second, the output feedback will change when the adaptive sampling law varies the sampling rate.

The overall objective of this control is to provide rapid engine response to changes in the demanded steady-state operating condition while maintaining certain engine constraints. This engine regulation must be accomplished using only available engine outputs and with a minimum of computer control complexity and processing time. It has already been shown that the adaptive control scheme described in Chapter IV can satisfy the practicality constraints of the overall control objective. It remains to be shown that rapid response and engine constraint criteria can be satisfied by appropriate selection of the performance index and the output feedback variables.

5.1 The Engine Model

From Chapter III the composite engine dynamics are written as

$$\begin{aligned} \delta\dot{x} &= F(S)\delta x + G(S)\delta w_f \\ \delta y &= H(S)\delta x + E(S)\delta w_f \end{aligned} \tag{5.1.1}$$

with

$$\begin{aligned} y &= y_c + \delta y \\ w_f &= w_{fc} + \delta w_f \end{aligned} \tag{5.1.2}$$

where S is the engine rotor speed and y_c and w_{fc} are the commanded output vector and fuel flow, respectively. The commanded output, y_c, is defined as the steady-state engine output corresponding to the constant engine fuel flow input, w_{fc}.

Recall that the state-space representation selected is second-order in the state and scalar in the control. The engine simulation can supply as outputs temperatures, pressures, airflow, and thrust when given fuel flow, w_f, as input and the Mach number and altitude conditions. All results in this dissertation are given for sea-level, static conditions, i.e., the Mach number is zero and the altitude corresponds to sea-level. This condition is common among engine test studies.

For an actual engine only certain physical outputs can be measured. Thus in this chapter only rotor speed, S, compressor discharge pressure, P_c, and turbine inlet temperature, T_T, are assumed available from the engine simulation as possible feedback variables. Since the state is second-order, the output vector, y, is limited to first and second-order combinations of S, P_c, and T_T. Therefore, there exists six possible feedback combinations. Note that the elements of the commanded output vector, y_c, always correspond to the elements of the chosen output vector, y.

5.2 The Engine Control

A block diagram of the control system and the engine is given in Figure 5.1. All the elements of this diagram have been discussed except the control gains, K_i. Thus, the determination of these gains for certain cost weightings is discussed.

The Output Feedback Gains. The control objectives of the engine are assumed to be represented in the cost function

$$J = \frac{1}{2}\int_0^{t_f}\left[\delta y'(t)Q\delta y(t) + R\delta w_f^2(t)\right]dt \tag{5.2.1}$$

with $R > 0$ and $Q = Q' > 0$. This cost function and the state-space system of equation (5.1.1) can be equivalently rewritten as

$$\begin{aligned}\delta\dot{x}(t) &= F_1\delta x(t) + G_1\delta u_1(t)\\ \delta y(t) &= H_1\delta x(t) + E_1\delta u_1(t)\end{aligned} \tag{5.2.2}$$

and

$$J = \frac{1}{2}\int_0^{t_f}\left[\delta x'(t)Q_1\delta x(t) + R_1\delta u_1^2(t)\right]dt \tag{5.2.3}$$

where

$$\begin{aligned}F_1 &= F - G(E'QE + R)^{-1}E'QH\\ G_1 &= G\\ H_1 &= H - E(E'QE + R)^{-1}E'QH\\ Q_1 &= H'(Q - QE(E'QE + R)^{-1}E'Q)H\\ R_1 &= E'QE + R\end{aligned} \tag{5.2.4}$$

and

$$\delta u_1(t) = \delta w_f + (E'QE + R)^{-1}E'QH\delta x(t) \tag{5.2.5}$$

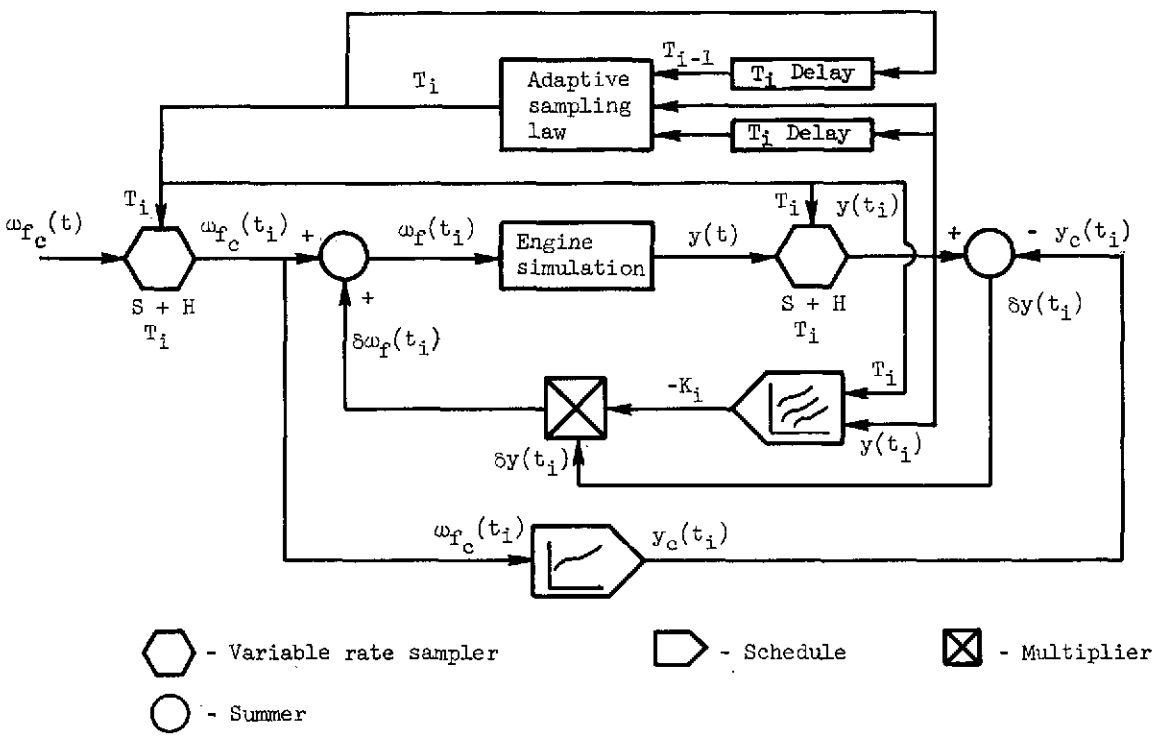

Figure 5.1. - Engine and control system block diagram.

Since F, G, H, and E are functionally related to the engine rotor angular velocity, their counterparts in the equivalent system are also.

For the equivalent system of equations (5.2.2) to (5.2.5) and the sampling period T_i, the discrete or sampled-data equivalent system is (see Appendix D)

$$\begin{aligned} \delta x(k+1) &= A\delta x(k) + B\delta u_1(k) \\ \delta y(k) &= C\delta x(k) + D\delta u_1(k) \end{aligned} \tag{5.2.6}$$

and

$$J = \frac{1}{2}\sum_{k=0}^{N_f}\left[\delta x'(k)\hat{Q}\delta x(k) + 2\delta x'(k)M\delta u_1(k) + \hat{R}\delta u_1^2\right] \tag{5.2.7}$$

Defining an auxiliary variable

$$\delta z(k) = C\delta x(k) \tag{5.2.8}$$

and using the results obtained for the infinite time optimal discrete output regulator (t_f is assumed large with respect to system time constants) in Chapter IV, the output feedback control law becomes

$$\delta u_1(k) = -K_1\delta z(k) \tag{5.2.9}$$

The piecewise constant control law over the continuous time interval $t_i < t < t_{i+1}$ becomes

$$\delta u_1(k) = -K_1\delta z(t_i) = -K_1H_1\delta x(t_i) \tag{5.2.10}$$

Substituting the control transformation of equation (5.2.5) and the original system matrices into equation (5.2.10) and simplifying, the control law becomes

$$\delta w_f(t) = -K_1\delta y(t_i) \tag{5.2.11}$$

where

$$K_i = (K_1 + R^{-1}E'Q)(I - EK_1)^{-1} \tag{5.2.12}$$

Therefore, the gain matrix, K_i, is both a function of the sampling period, T_i, and, implicitly, the engine rotor speed, S. It is remarked that the feedback matrix can be obtained by either scheduling system matrices as a function of S and computing the feedback matrix at each sampling instant on-line, or by scheduling the feedback matrix itself as a function of S and T_i. (The feedback matrix would be computed off-line for sufficiently large intervals of S and T_i and stored.) The first technique would require less storage than the second but would require more on-line computing time. The second technique would require less on-line computing time but more storage capacity than the first. Since the critical element in most digital computer control systems is on-line computing time, the second technique is preferable. Since a digital simulation rather than a real time engine is the process to be controlled in this paper, on-line computing time is not a problem. Thus, the first technique is used in this dissertation for the resultant savings in computer storage requirements.

The Cost Weighting Matrices. The cost function given in equation (5.2.1) represents a quadratic weighting of the output and control energy excursions from the steady-state operating line. The choices of Q and R, the weighting matrices, will reflect the relative importance of incurring output and control errors. Since each element of $\delta y(t)$ and $\delta w_f(t)$ vary in relative magnitudes, scaling was introduced to facilitate the choice of the weighting matrices.

To each sampled engine rotor velocity, $N = S_i$, there corresponds a steady-state operating condition of the engine. The value of the

output vector and control at this condition are y_N and w_{fN}. If a matrix Q_N is defined as

$$Q_N = \text{DIAG}[y_N] \tag{5.2.13}$$

the percentage change in the output error vector can be written as

$$\delta y_{pc}(t) = Q_N^{-1}\delta y(t) \tag{5.2.14}$$

Similarly the percentage change in the control error can be written

$$\delta w_{fpc}(t) = \delta w_f(t)/w_{fN} \tag{5.1.15}$$

In terms of the percentage changes in error the cost function of equation (5.2.1) becomes

$$J = \frac{1}{2}\int_0^{t_f} \left[\delta y'_{pc}(t)\bar{Q}\delta y_{pc}(t) + \bar{R}\delta w_{fpc}^2\right]dt \tag{5.2.16}$$

Now the choice of $\bar{Q}$ and $\bar{R}$ reflect relative weightings for the percentage changes in output and control errors. The original weighting matrices, Q and R, are determined by

$$\begin{aligned} Q &= Q_N^{-1}\bar{Q}Q_N^{-1} \\ R &= R_N^{-1}\bar{R}R_N^{-1} \end{aligned} \tag{5.2.17}$$

5.3 The Adaptive Sampling Law

From the previous chapter the adaptive sampling law was defined as

$$T_i = \begin{cases} \dfrac{T_{max}}{\alpha \dot{e}(t_i)^2 + 1}, & T_i > T_{min} \\ T_{min}, & T_i \le T_{min} \end{cases} \tag{5.3.1}$$

where $e(t_i)$ is the difference between the past and present sampled values of some system parameter.

For the application of this adaptive sampling law to the engine controller, engine rotor velocity was selected as the system parameter from which the sampling period is predicted. This choice was made for two reasons. First, engine rotor velocity is already required by the feedback gain schedule and is therefore already available. Second, S, as the slowest and smoothest responding engine variable, gives the best indication of the "dynamic position" of the engine relative to steady-state.

It is remarked at this point that if a system is in the steady-state for a long period and a sudden disturbance occurs, the slowest system output might not decrease the sampling period fast enough to handle the disturbance. This problem can be handled by conservatively choosing the T_{max} limit or by using both the slow and fast system outputs in some weighted combination to predict T_i. Such problems are not considered here.

Approximating the scaled or percentage error derivative as

$$\dot{e}_{pc}(t_i) = \frac{S(t_i) - S(t_{i-1})}{T_{i-1}S(t_{i-1})} \tag{5.3.2}$$

the adaptive sampling law is

$$T_i = \begin{cases} \dfrac{T_{max}}{\alpha(\dot{e}_{pc}(t_i))^2 + 1}, & T_i > T_{min} \\ T_{min}, & T_i \leq T_{min} \end{cases} \tag{5.3.3}$$

Preliminary engine simulations established the sampling limits as

$$\begin{aligned} T_{min} &= 0.001 \\ T_{max} &= 0.025 \end{aligned} \tag{5.3.5}$$

and the weighting term as

$$\alpha = 4x10^4 \tag{5.3.6}$$

5.4 The Simulation Results

The first simulation results were obtained for the case of rotor velocity as the only variable for feedback. In this case $y = S$. The control task was to accelerate the engine from steady-state at 90% to steady-state at 104.5% design speed (100% is 36 960 rev/min). The commanded fuel flow which represents this change in the steady-state engine condition is

$$w_{fc} = \begin{cases} 0.09244 \text{ lbm/sec} & 0 \leq t < 0.1 \\ 0.15 \text{ lbm/sec} & 0.1 < t \leq 2 \end{cases} \tag{5.4.1}$$

As a means of comparison, baseline results with a constant sampling period of $T = 0.001$ seconds were simulated with $t_f = 2$ sec. The scaled weighting matrices were selected as

$$\begin{aligned} \bar{Q} &= 10 \\ \bar{R} &= 1 \end{aligned} \tag{5.4.2}$$

The respective trajectories for rotor speed, S, compressor discharge pressure, P_c, turbine inlet temperature, T_T, engine thrust, F_z, and fuel flow, w_f, are given in Figures 5.2 to 5.6 for the commanded fuel flow w_{fc}. For future reference label this simulation test "Case 1."

For the baseline (Case 1) and subsequent simulations the weighted cost function

$$J_w = \frac{1}{2}\int_0^{t_f} \left[\delta y'(t) Q \delta y(t) + R\delta w_f^2(t)\right] dt \tag{5.2.1}$$

and the unweighted cost function

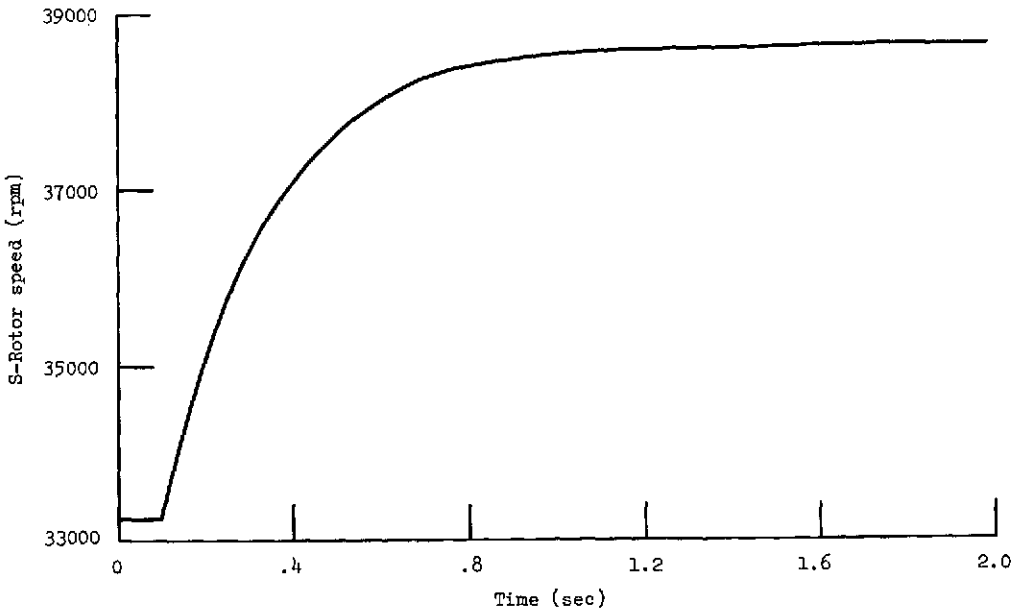

Figure 5.2. - Case 1 (baseline) engine acceleration.

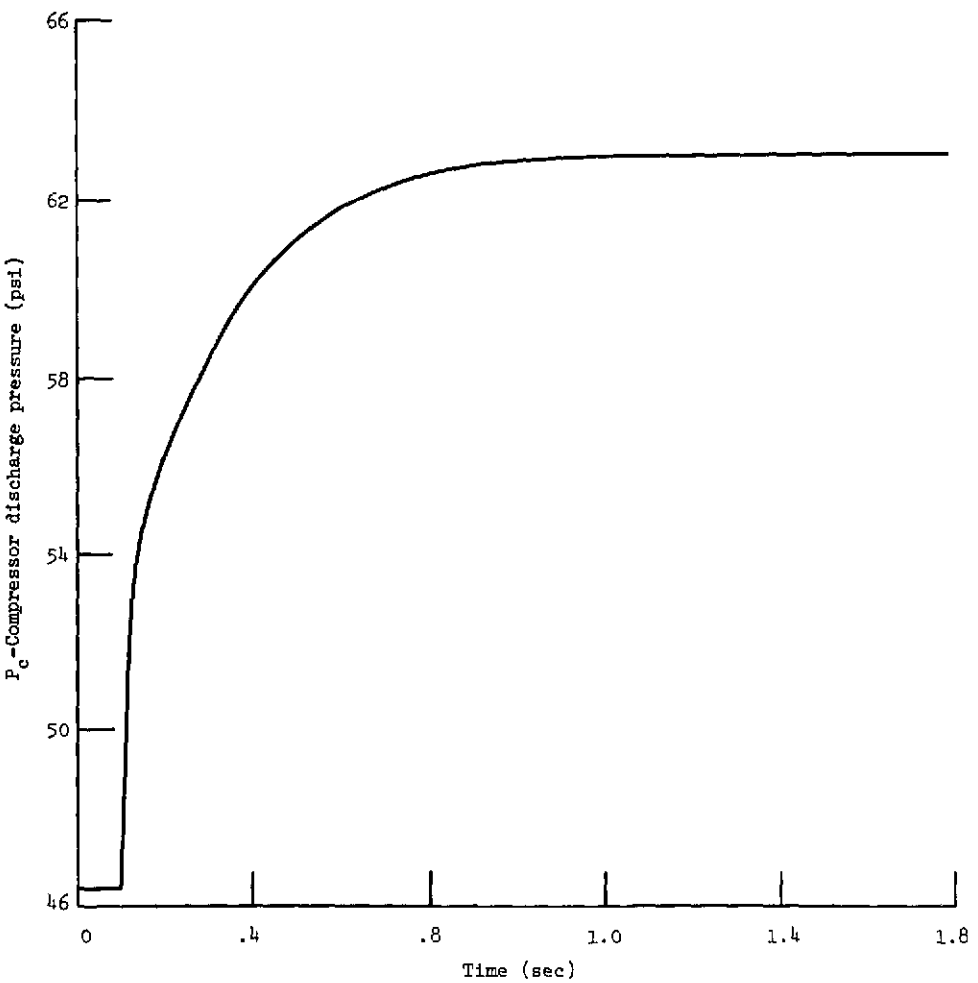

Figure 5.3. - Case 1 (baseline) engine acceleration.

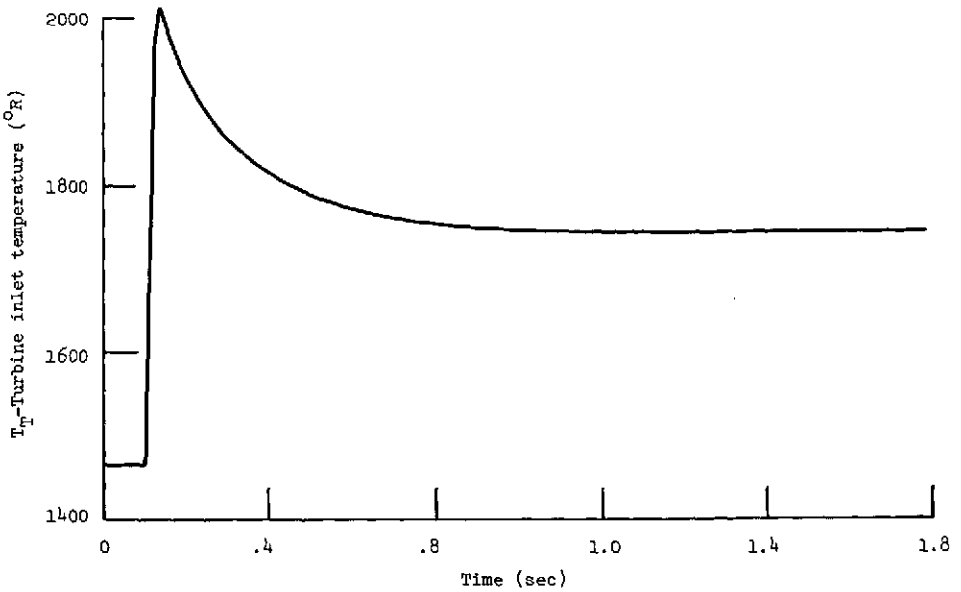

Figure 5.4. - Case 1 (baseline) engine acceleration.

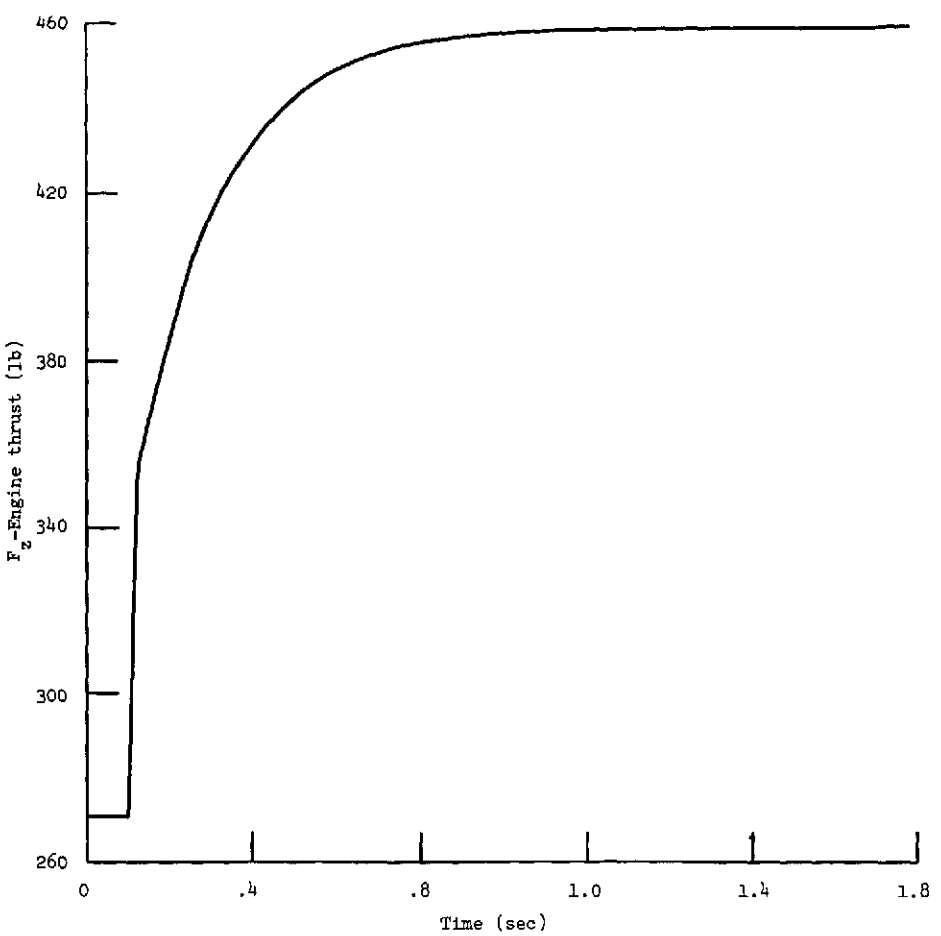

Figure 5.5. - Case 1 (baseline)engine acceleration.

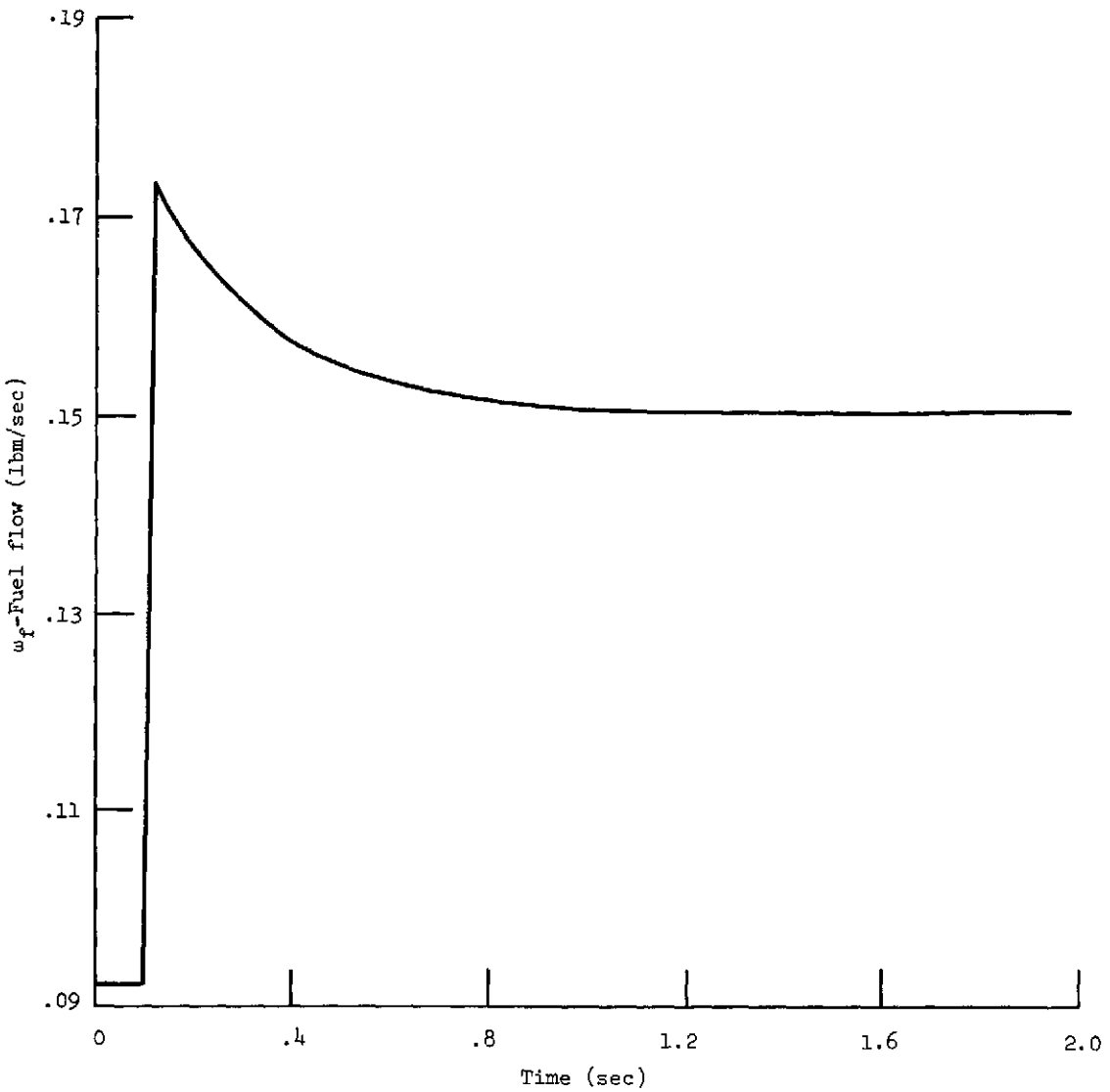

Figure 5.6. - Case 1 (baseline) engine acceleration.

$$J_u = \frac{1}{2}\int_0^{t_f} \left[\delta S^2 + \delta P_c^2 + \delta T_T^2 + \delta F_z^2 + \delta w_f^2\right]dt \qquad (5.4.3)$$

are calculated. Using the definition of sampling efficiency from Chapter IV, the weighted and unweighted sampling efficiencies

$$\eta_w = \frac{1}{J_w N_f} \qquad (5.4.4)$$

$$\eta_u = \frac{1}{J_u N_f} \qquad (5.4.5)$$

where N_f is the number of sampling instants are calculated for each simulation. These indices are summarized for each simulation at the end of this chapter in Figure 5.27.

Next, adaptive sampling was added and the simulation repeated for the commanded fuel flow of equation (5.4.1). Call this "Case 2." Again,

$$\begin{aligned} \bar{Q} &= 10 \\ \bar{R} &= 1 \end{aligned} \qquad (5.4.6)$$

The resultant trajectories are plotted with the previous baseline results to show the effect of including adaptive sampling in Figures 5.7 to 5.11. The results show no visible differences except in the turbine inlet temperature plot. A comparison of the cost and efficiency indices shows approximately a 10% increase in the cost and a 100% improvement in sampling efficiency.

To examine the effect of a change in the cost function, the cost function weighting was changed to

$$\begin{aligned} \bar{Q} &= 50 \\ \bar{R} &= 1 \end{aligned} \qquad (5.4.7)$$

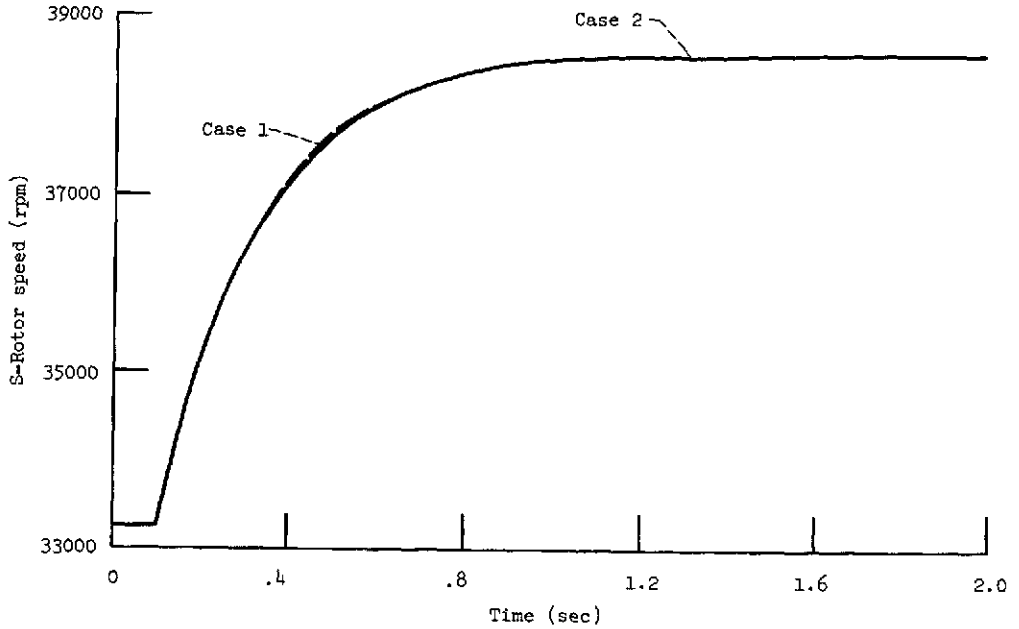

Figure 5.7. - Case 2 and Case 1 engine accelerations.

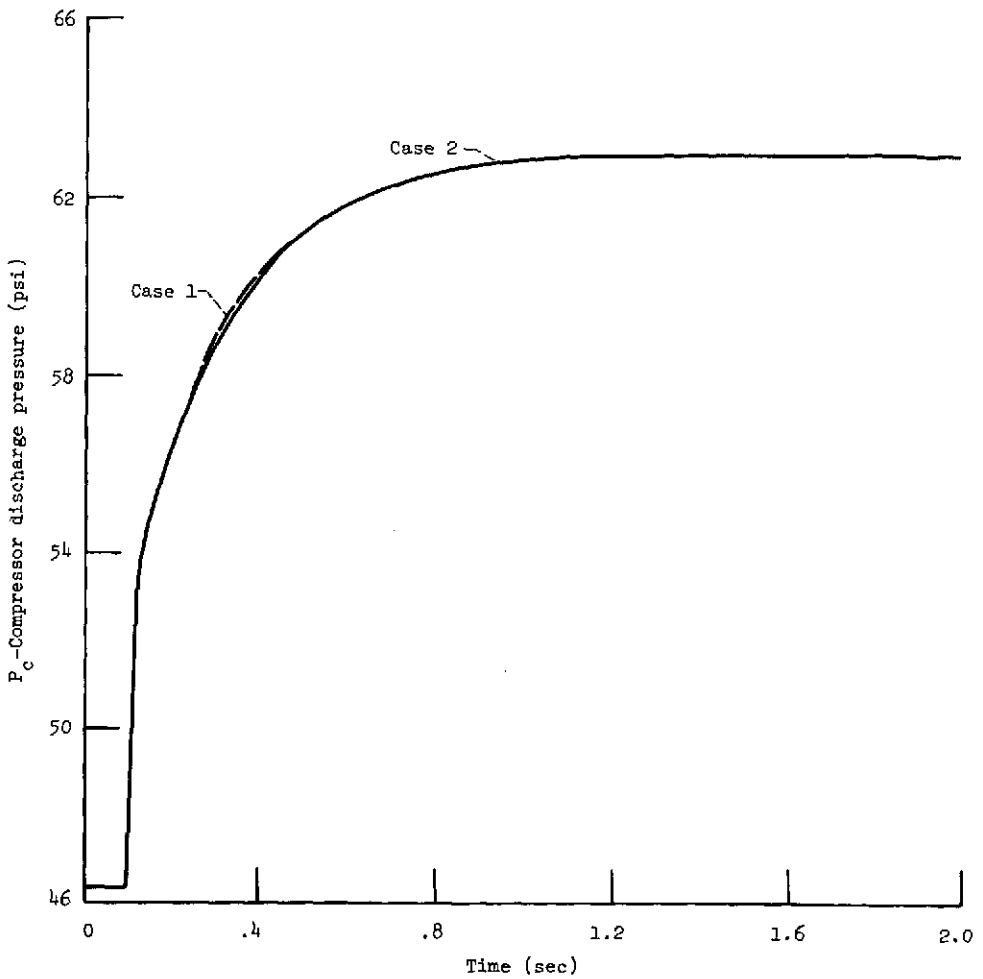

Figure 5.8. - Case 2 and Case 1 engine accelerations.

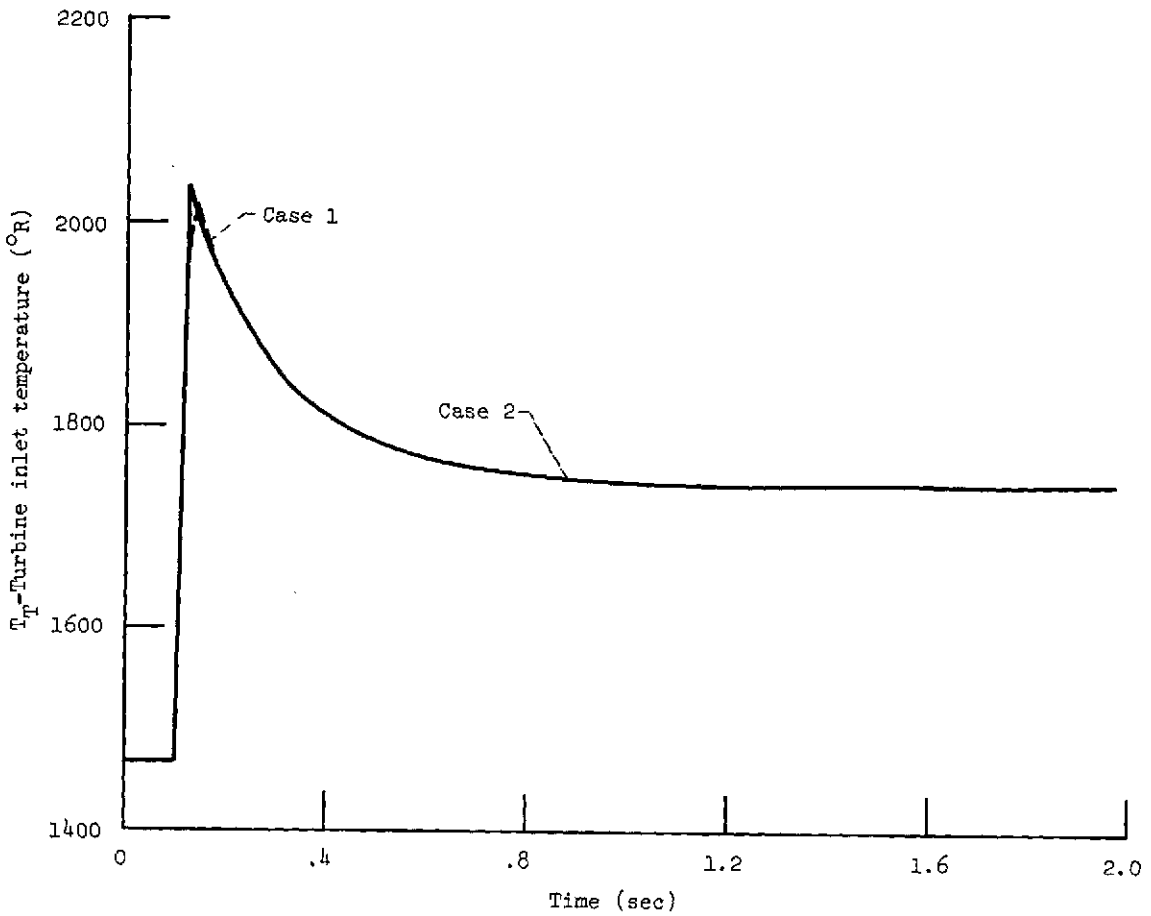

Figure 5.9. - Case 2 and Case 1 engine accelerations.

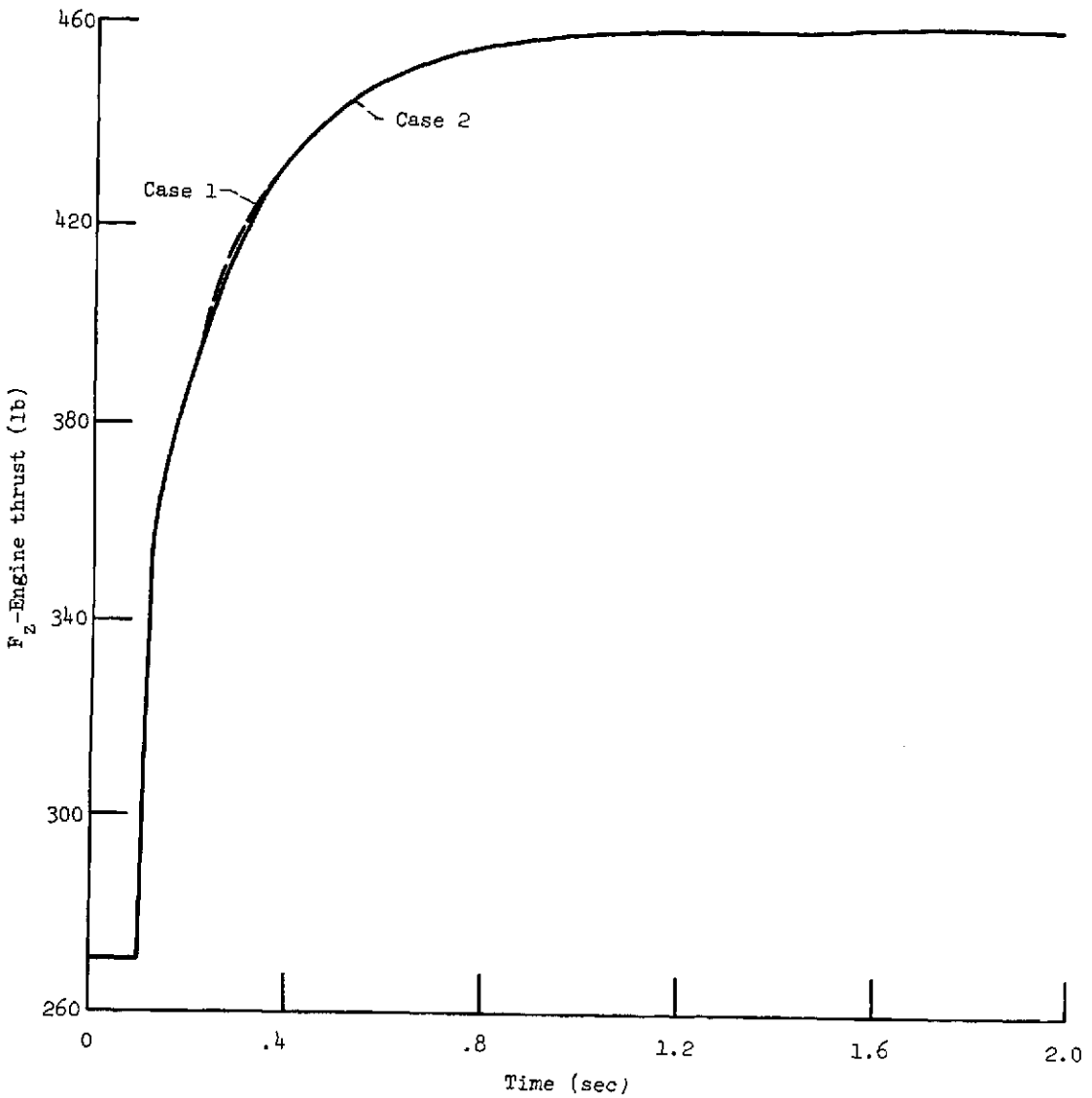

Figure 5.10. - Case 2 and Case 1 engine accelerations.

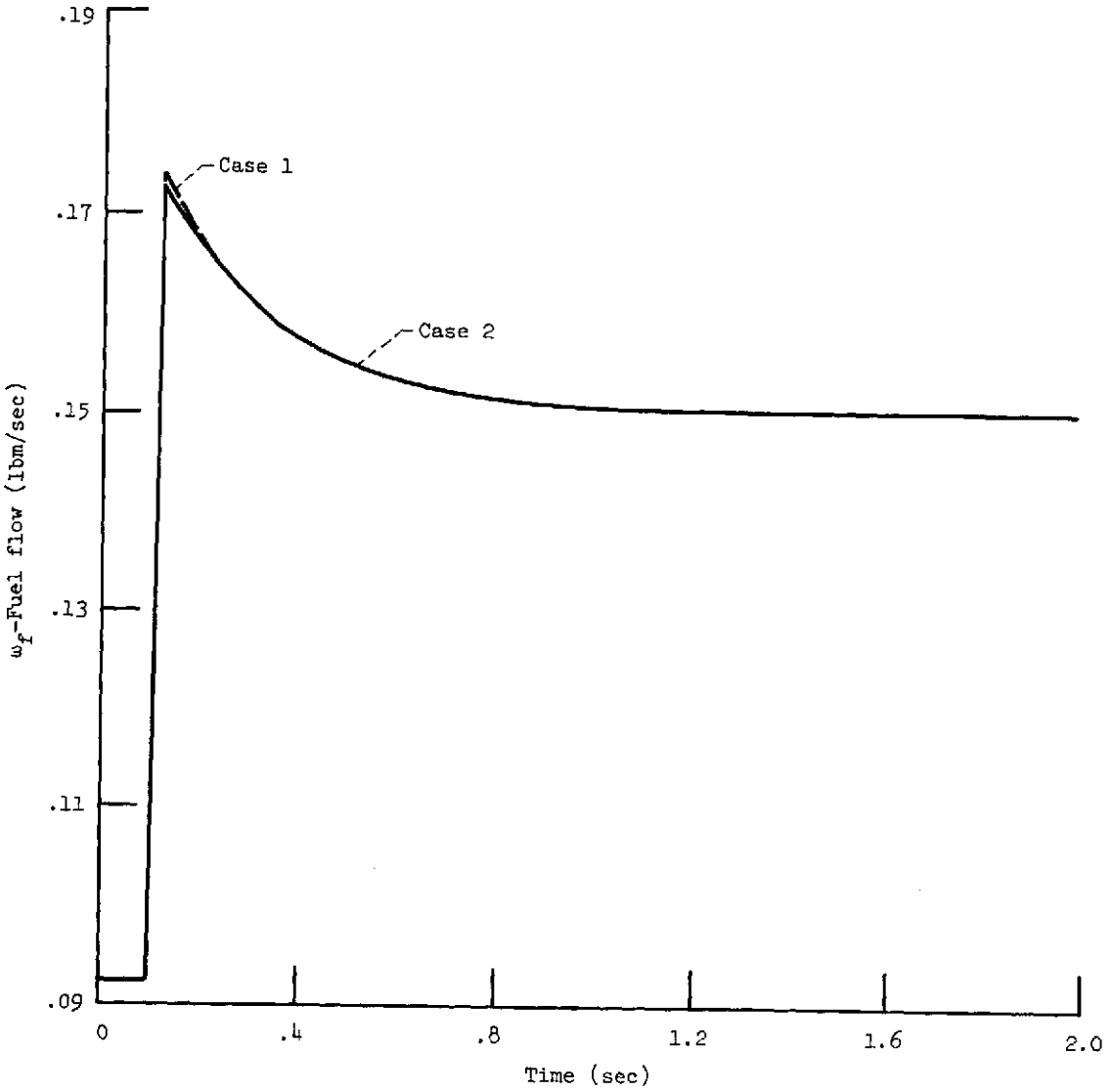

Figure 5.11. - Case 2 and Case 1 engine accelerations.

and the simulation repeated with adaptive sampling and the commanded fuel flow of equation (5.4.1). Label this simulation "Case 3." These results are plotted with those of Case 2 and are given in Figures 5.12 to 5.16. From the figures it is clear that the Case 3 control, as expected, accelerates the engine faster than the Case 2 control. For example, rotor speed is within 1% of its final steady-state value in 0.6 sec for case 3 while in Case 2 it required 1.1 sec. For engine thrust a similar analysis gives acceleration rise times of 0.4 sec for Case 3 and 1.2 sec for Case 2. The penalty for this improved acceleration of Case 3 is higher turbine inlet temperatures and additional fuel flow requirements. A comparison of the cost and efficiency indices shows that the weighted and unweighted costs are higher and the sampling efficiencies lower for Case 3 than for Case 2.

From the trajectories already presented, it is seen that the adaptive control described in this paper can rapidly accelerate the engine from one operating point to another. However, in realistic engines the temperature history of the turbine blades is also of utmost importance. High turbine inlet temperatures, T_T, can cause short lifetimes or even outright failures of the turbine blades. Thus another important control consideration is the limiting of turbine inlet temperature. To evaluate the ability of the adaptive digital control scheme to limit turbine temperature and still effectively accelerate the engine, a simulation test, called "Case 4," is devised as follows.

Suppose that the temperature limit for the single spool turbojet engine is 1900° R. The control configuration must now accelerate the engine from 90% to 104.5% design speed without violating the 1900° R temperature constraint. The commanded fuel flow is again as in

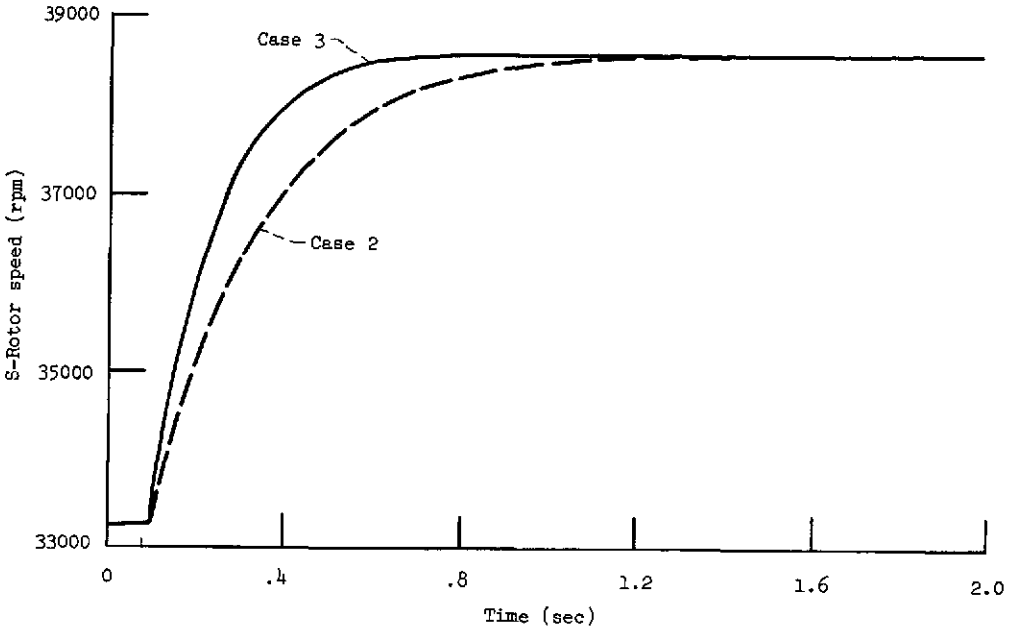

Figure 5.12. - Case 3 and Case 2 engine accelerations.

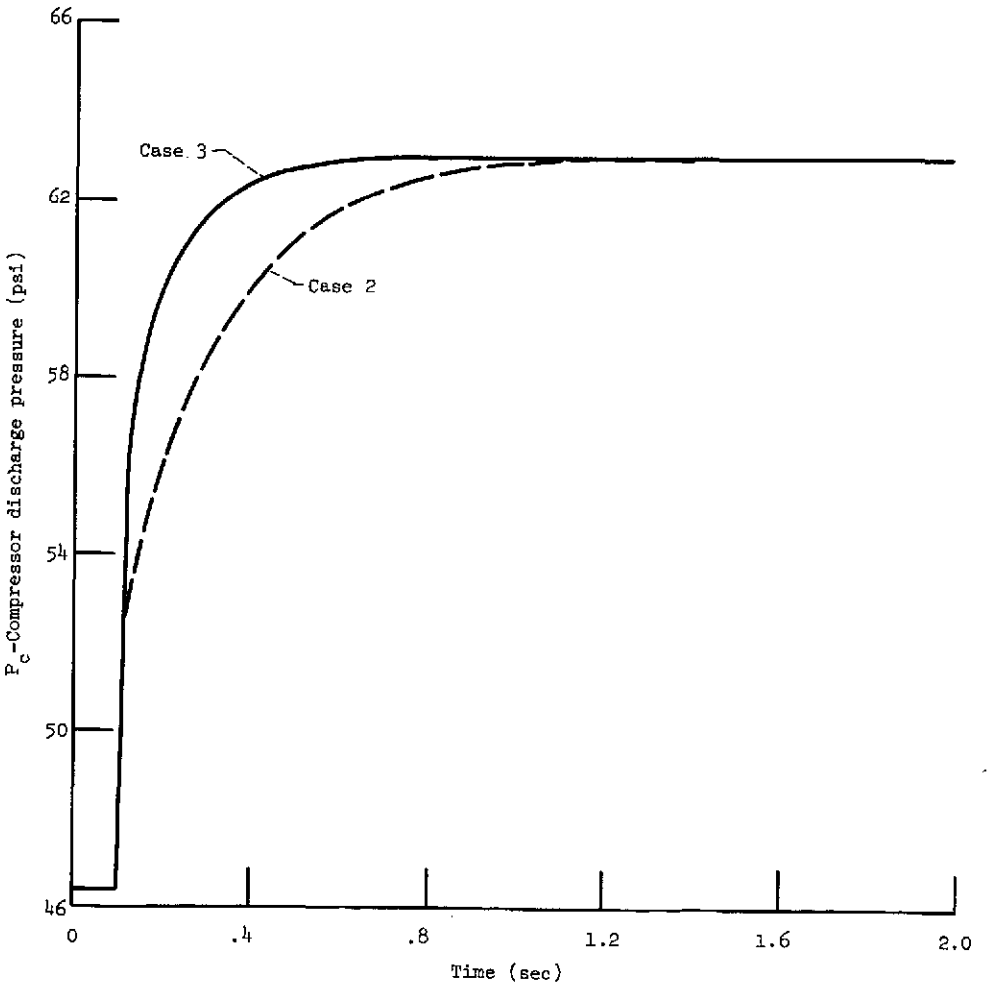

Figure 5.13. - Case 3 and Case 2 engine accelerations.

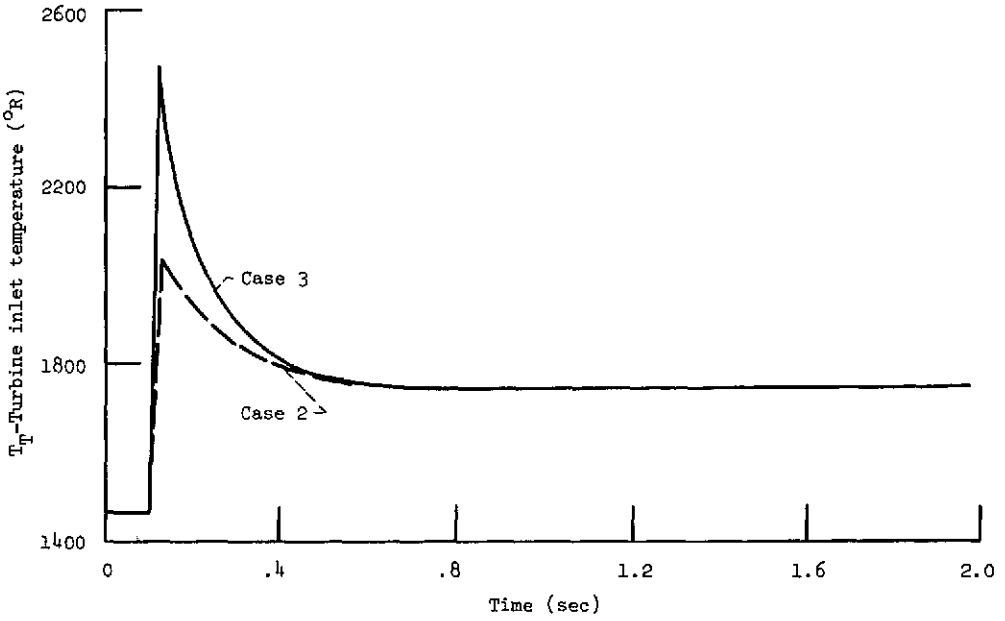

Figure 5.14. - Case 3 and Case 2 engine accelerations.

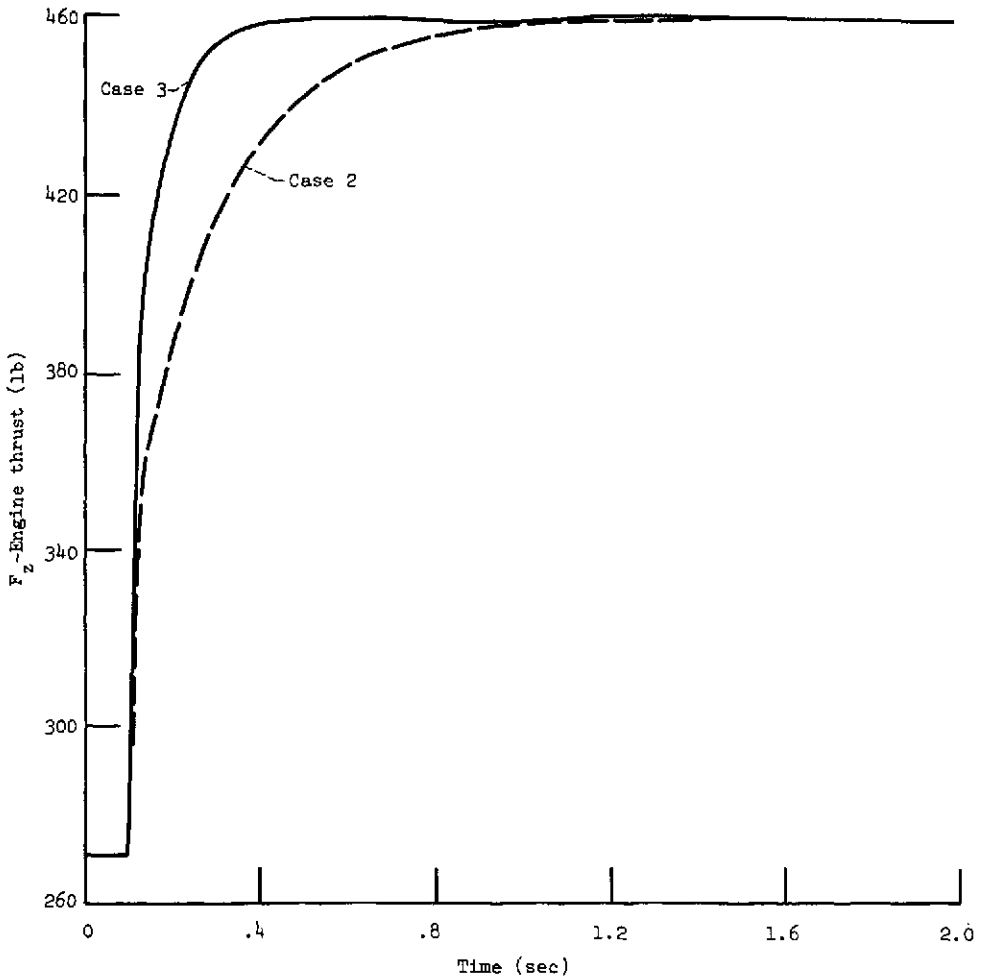

Figure 5.15. - Case 3 and case 2 engine accelerations.

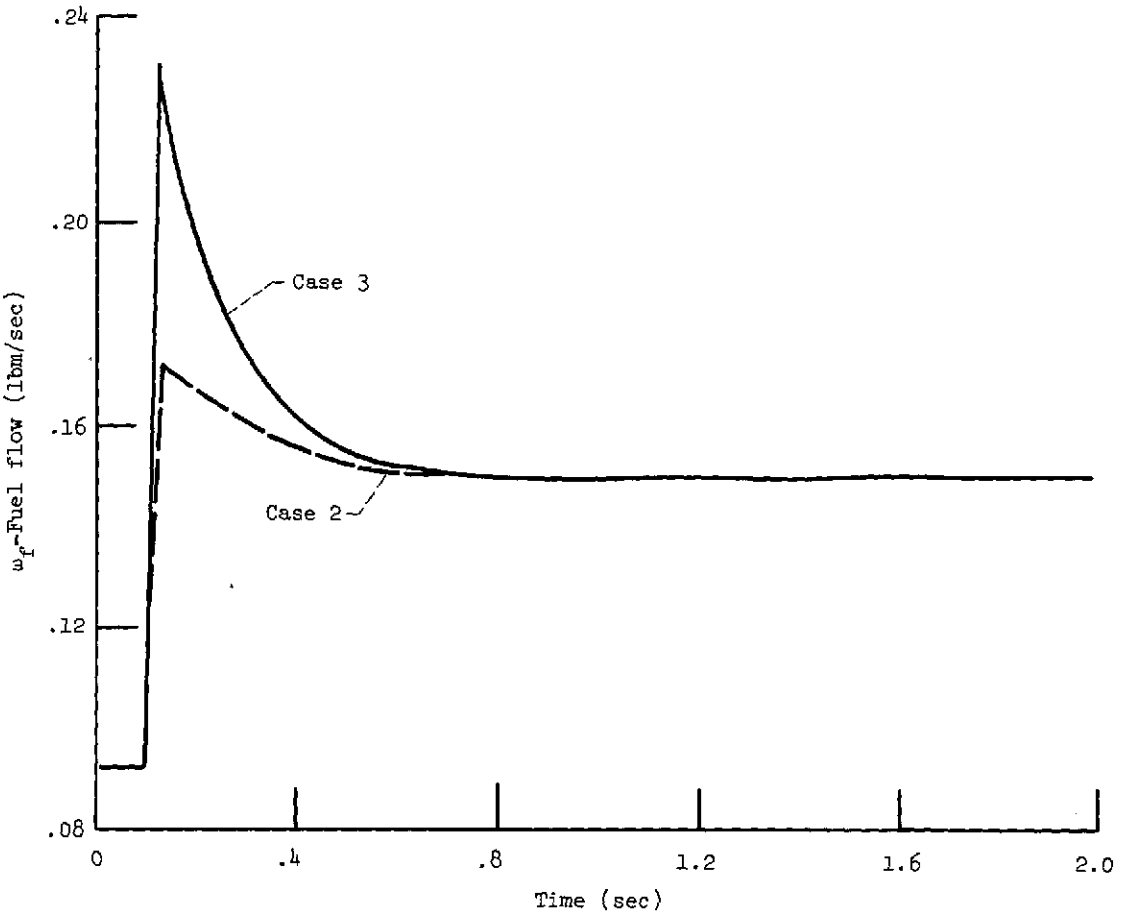

Figure 5.16. - Case 3 and Case 2 engine accelerations.

equation (5.4.1). This temperature constrained acceleration is accomplished by initially controlling the engine as in Case 2 with engine rotor speed feedback, i.e.,

$$y = S \tag{5.4.8}$$

and

$$\begin{aligned} \bar{Q} &= 10 \\ \bar{R} &= 1 \end{aligned} \tag{5.4.9}$$

until the 1900° R level is exceeded. Then the control configuration is changed to include both rotor speed, S, and turbine temperature, T_T, feedback. The output vector is now

$$y = \begin{pmatrix} S \\ T_T \end{pmatrix} \tag{5.4.10}$$

and the cost weighting matrices are chosen as

$$\begin{aligned} \bar{Q} &= \begin{pmatrix} 0.1 & 0 \\ 0 & 0.0001 \end{pmatrix} \\ \bar{R} &= 1 \end{aligned} \tag{5.4.11}$$

As before this weighting still penalizes the rotor velocity error, but now it also penalizes large temperature errors. In addition it reflects a greater importance on the conservation of control energy. Once the temperature constraint is satisfied, the control configuration reverts to the original (Case 2) feedback arrangement. The results for Case 4 are plotted along with those of Case 2 in Figures 5.17 to 5.21. From these figures it is seen that the turbine temperature is limited to 1900° R with only a small penalty in acceleration when compared to the Case 2 acceleration. A comparison of cost and

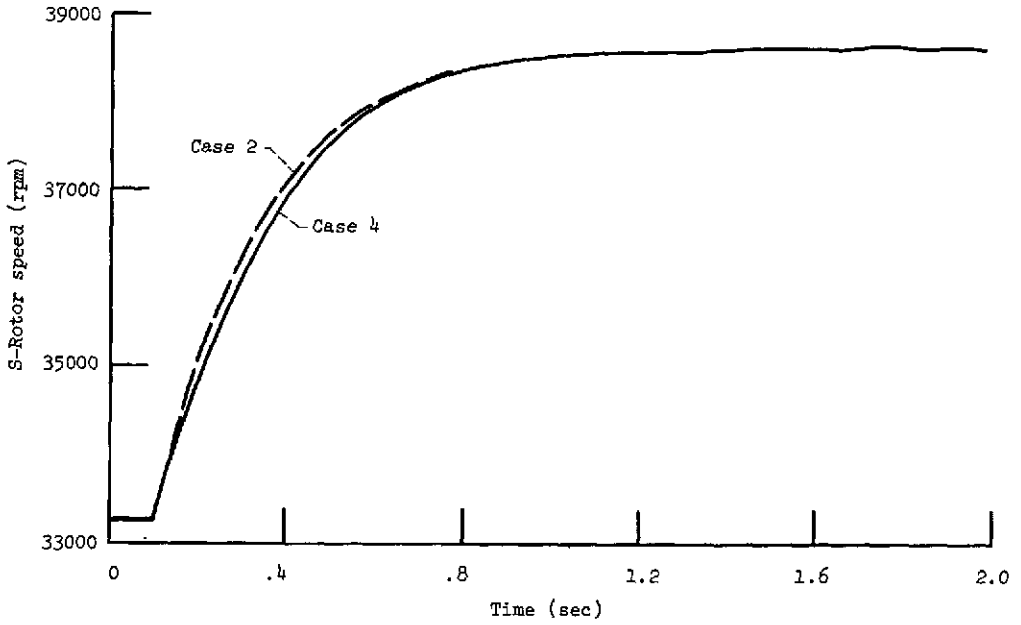

Figure 5.17. - Case 4 and Case 2 engine acceleration.

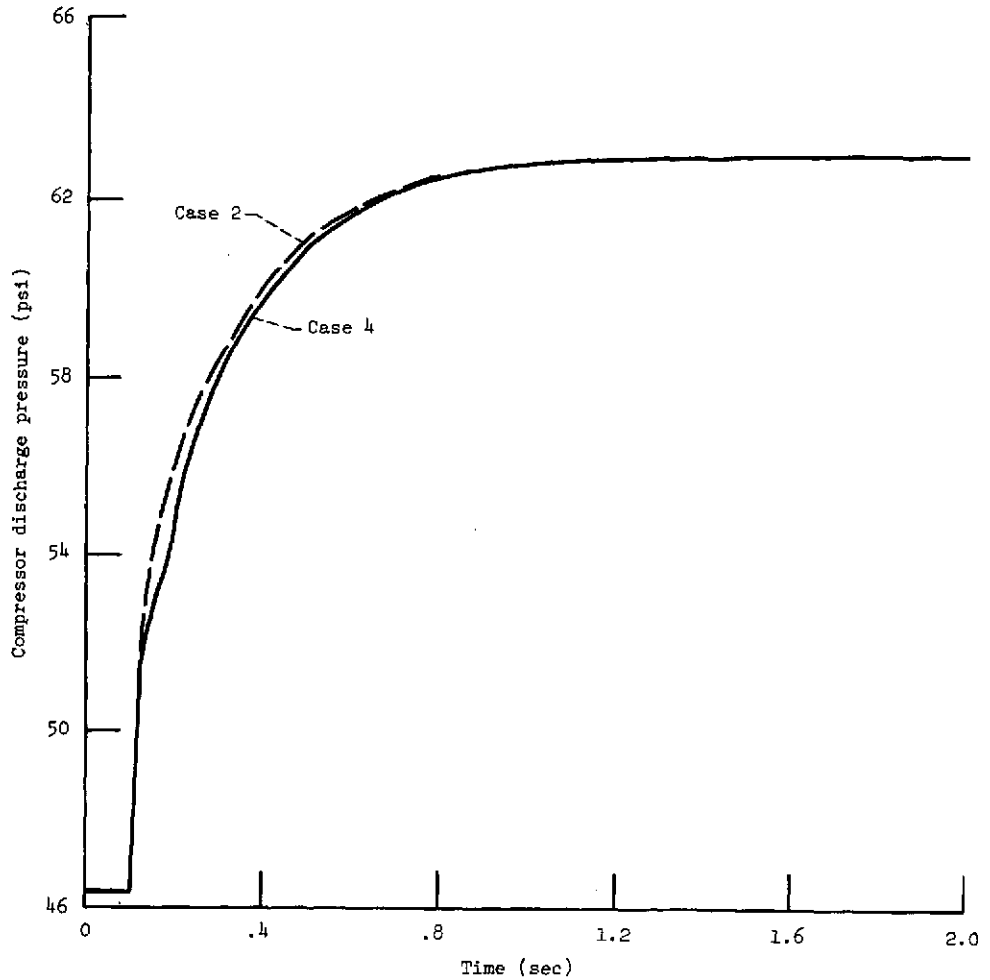

Figure 5.18. - Case 4 and Case 2 engine accelerations.

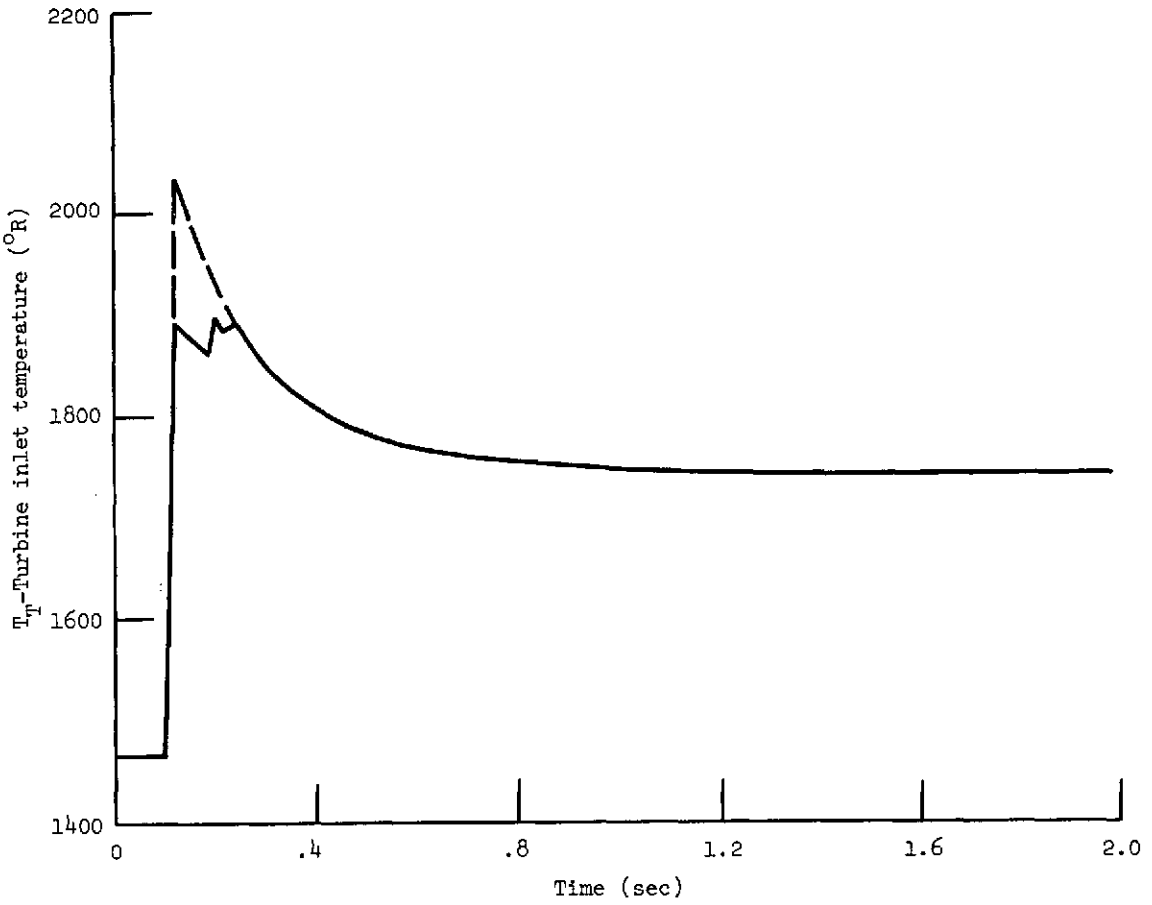

Figure 5.19. - Case 4 and Case 2 engine accelerations.

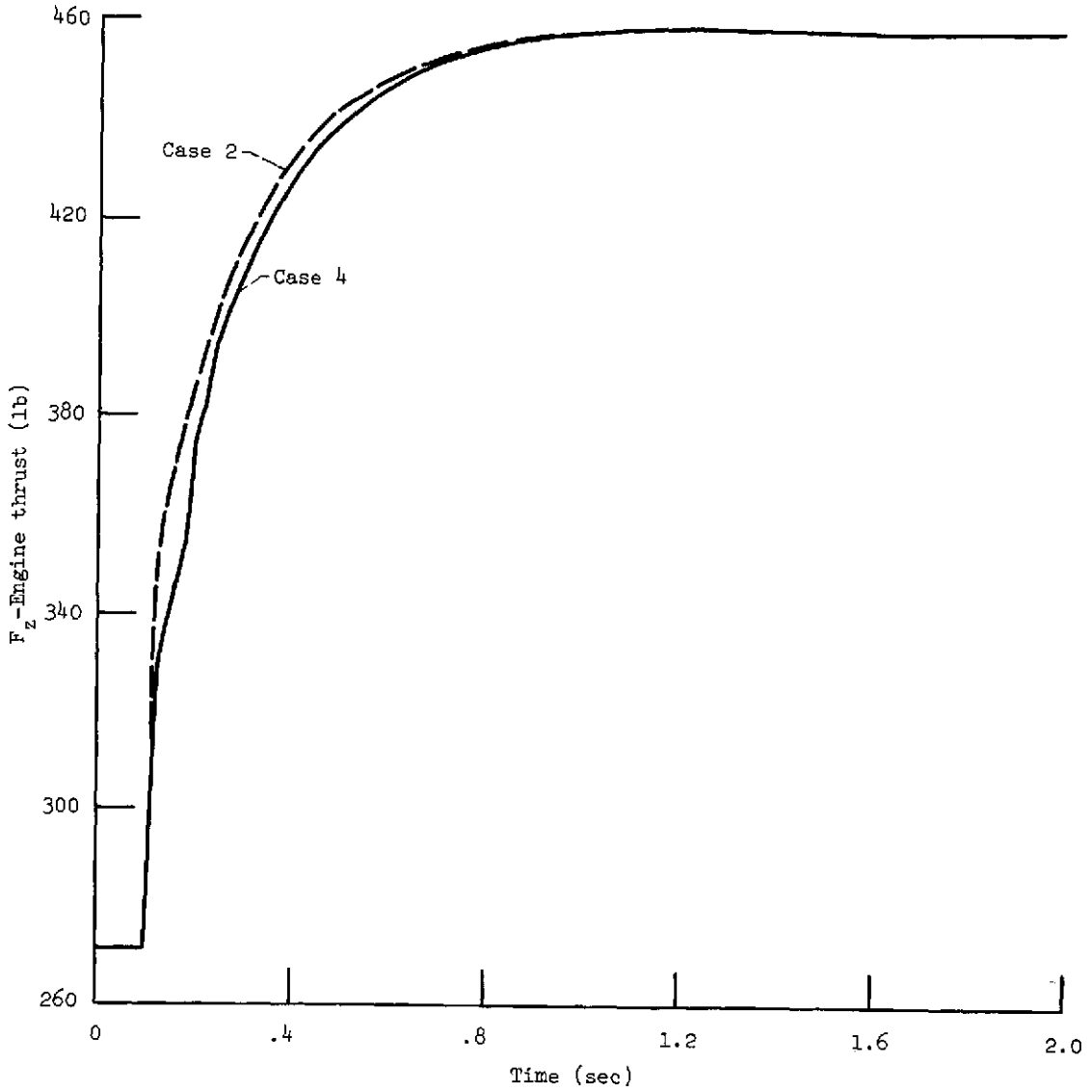

Figure 5.20. - Case 4 and Case 2 engine accelerations.

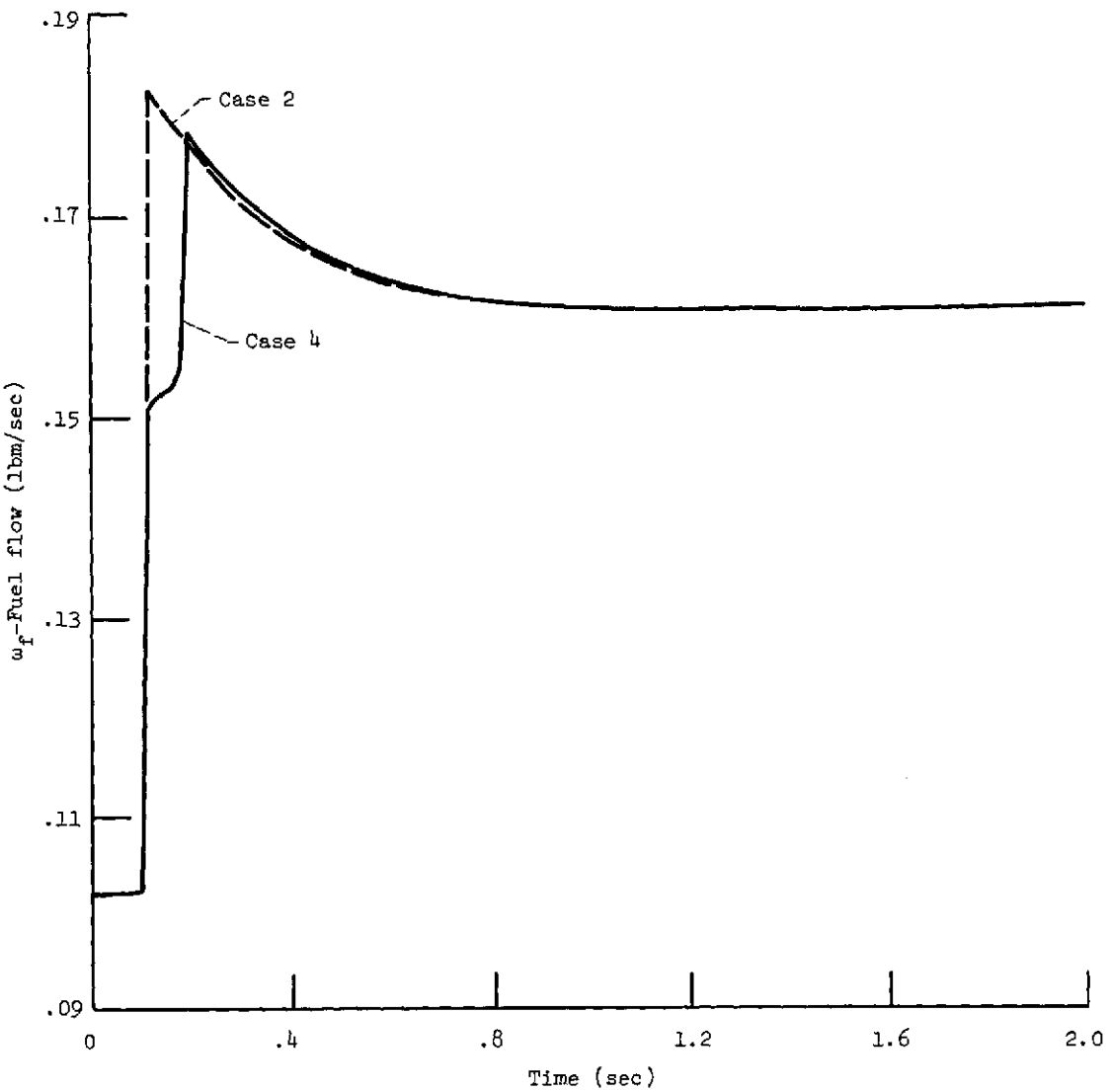

Figure 5.21. - Case 4 and Case 2 engine accelerations.

efficiency indices for Case 2 and Case 4 shows only minor variations in these values.

A final simulation test, Case 5, is now developed to determine if the addition of a second feedback variable, P_c, can improve engine acceleration. Again the commanded fuel flow input is given by equation (5.4.1). The feedback variables are

$$y = \begin{pmatrix} S \\ P_c \end{pmatrix} \tag{5.4.12}$$

and the weighting matrices are selected as

$$\bar{Q} = \begin{pmatrix} 0.2 & 0 \\ 0 & 2 \end{pmatrix} \tag{5.4.13}$$

$$\bar{R} = 1$$

The result of Case 5 are plotted along with the trajectories of Case 2 in Figures 5.22 to 5.26.

These figures show that no appreciable improvement in acceleration is obtained by the addition of the feedback variable P_c. Turbine inlet temperature is lowered somewhat, but fuel flow is increased in Case 5 when compared to Case 2. In addition, a comparison of the cost indices shows a sizeable increase in the cost from Case 5 to Case 2 while the sampling efficiency went down. However, it should be noted that the weighting selected does not emphasize the elimination of speed error as heavily as previous test simulations. In this regard it should be mentioned that the weighting matrices selected in each case were probably not the best possible. If required, more time could be devoted to achieving better results by additional test simulations.

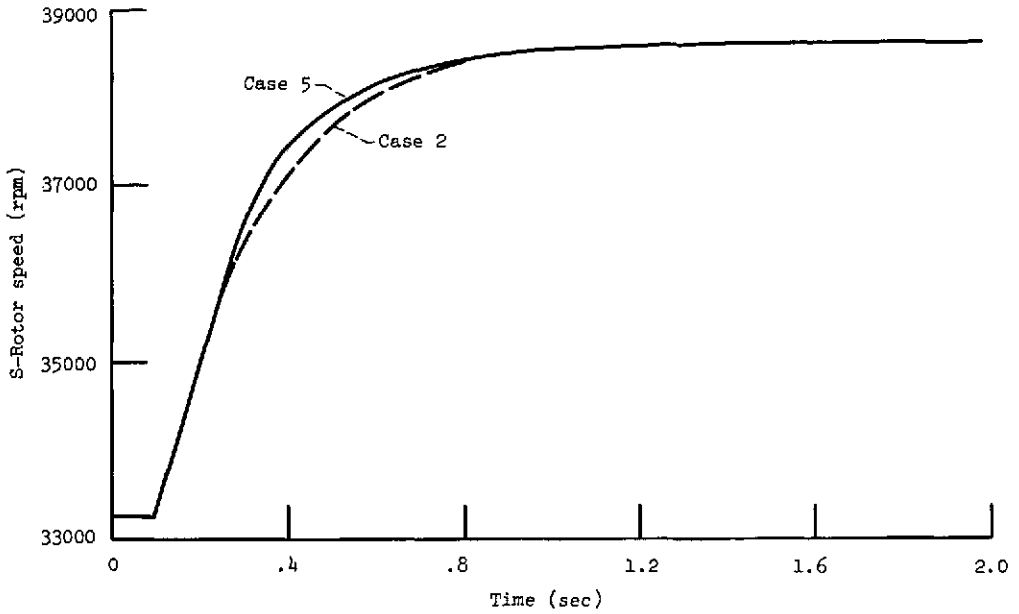

Figure 5.22. - Case 5 and Case 2 engine accelerations.

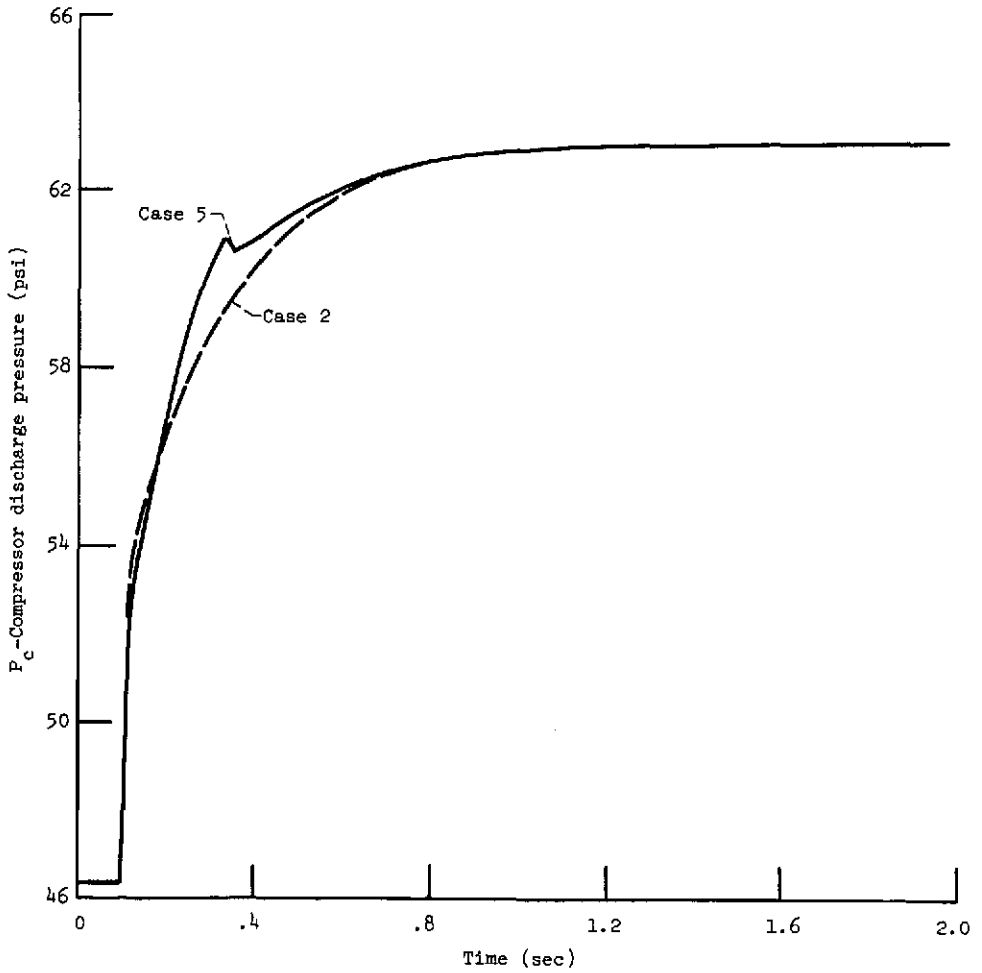

Figure 5.23. - Case 5 and Case 2 engine accelerations.

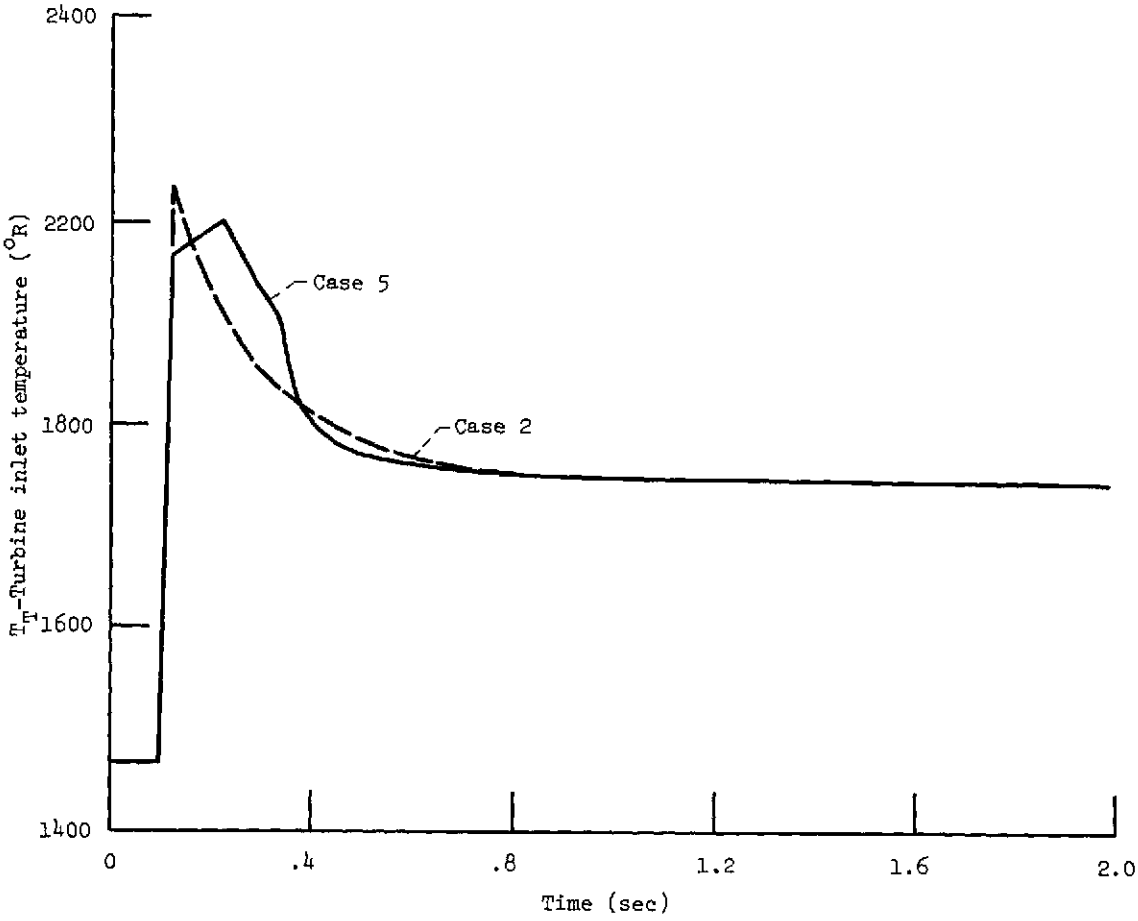

Figure 5.24. - Case 5 and Case 2 engine accelerations.

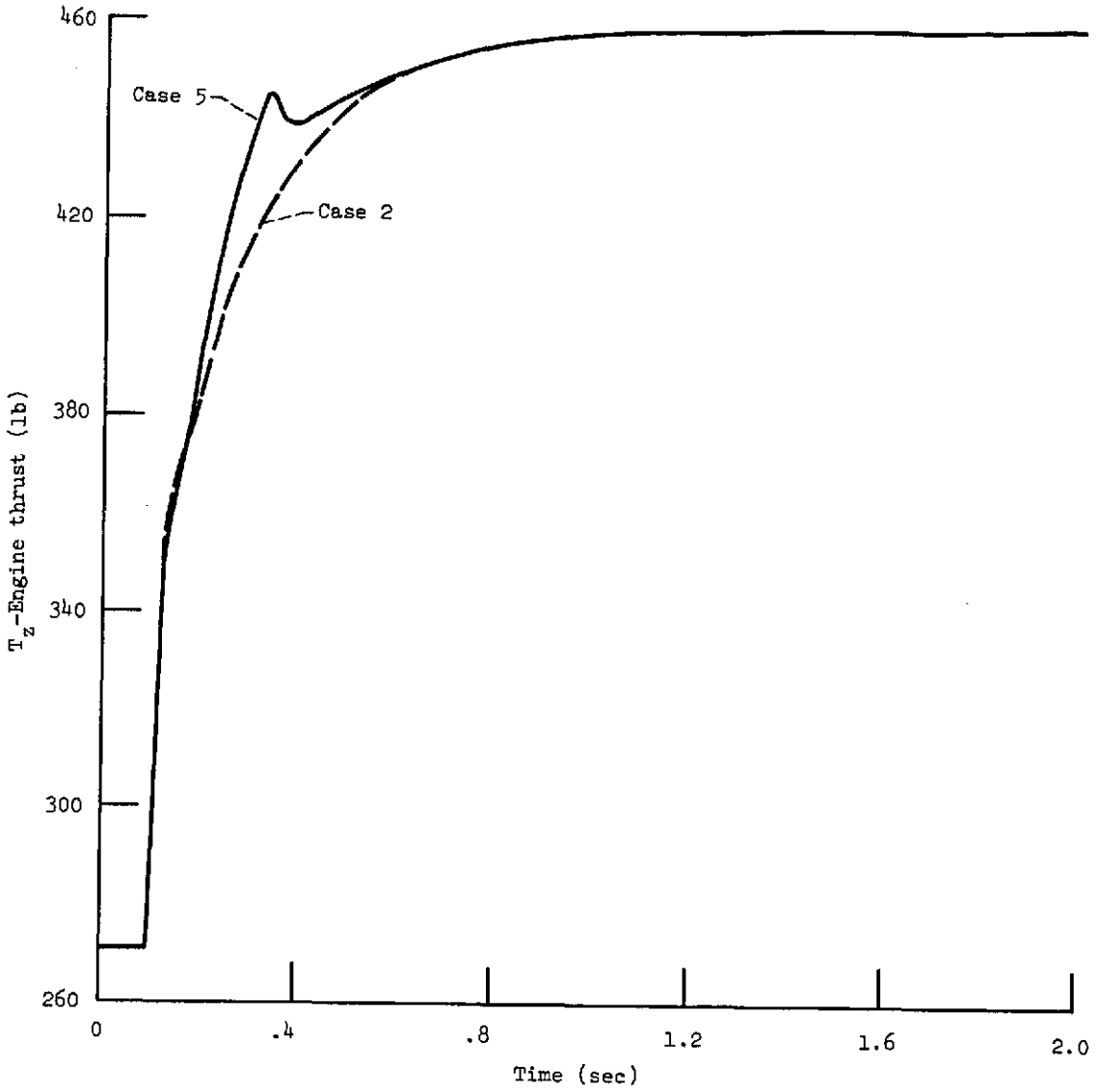

Figure 5.25. - Case 5 and Case 2 engine accelerations.

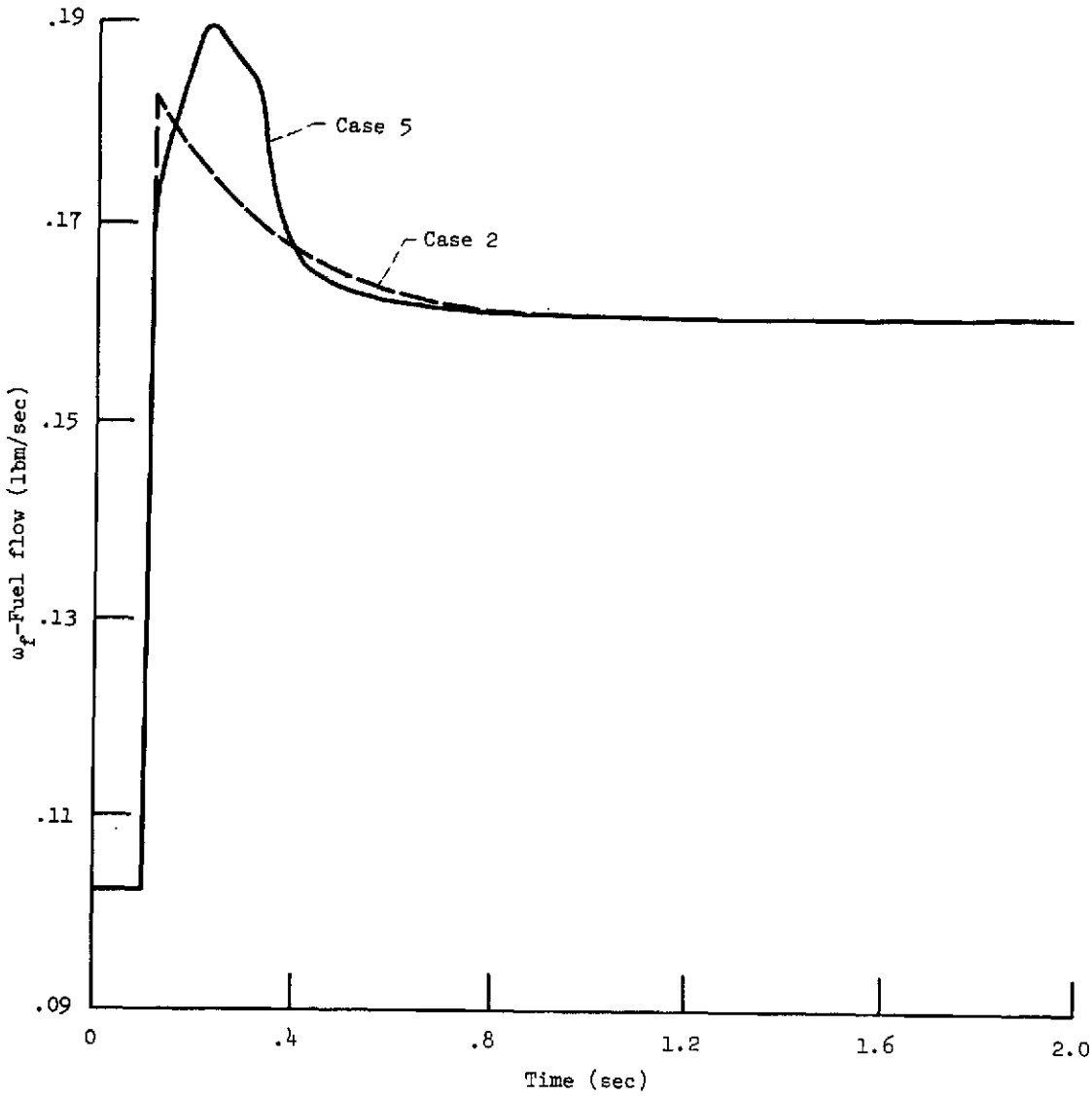

Figure 5.26. - Case 5 and Case 2 engine accelerations.

Simulation test	Output feedback variables, y	Weighting matrices, $\bar{Q},\bar{R}$	Number of sampling instants, N_f	Unweighted cost, J_u	Weighted cost, J_w	Unweighted sampling efficiency, η_u	Weighted sampling efficiency, η_w
Case 1	S	$\bar{Q}=10,\bar{R}=1$	1928	.246E-1	.315E-2	.211E-1	.165
Case 2	S	$\bar{Q}=10,\bar{R}=1$	878	.278E-1	.337E-2	.409E-1	.338
Case 3	S	$\bar{Q}=50,\bar{R}=1$	621	.591E-1	.256E-1	.273E-1	.628E-1
Case 4	S	$\bar{Q}=10.\bar{R}=1$					
	or	or					
	$\begin{pmatrix} S \\ T_T \end{pmatrix}$	$\bar{Q}=\begin{pmatrix} .1 & 0 \\ 0 & .0001 \end{pmatrix},\bar{R}=1$	900	.297E-1	.279E-2	.374E-1	.398
Case 5	$\begin{pmatrix} S \\ P_c \end{pmatrix}$	$\bar{Q}=\begin{pmatrix} .2 & 0 \\ 0 & 2 \end{pmatrix},\bar{R}=1$	842	.313E-1	.658E-2	.380E-1	.180

Figure 5.27. - Summary of simulation results.

5.5 The General Control Procedure

If this control procedure were to be applied to a different engine, the following steps would be required. First, identify operating point models from data generated by the new engine at enough points to adequately describe the engine dynamics. Second, select the appropriate outputs and schedule the commanded output against the commanded input. Third, apply the adaptive control scheme of Chapter IV to the identified model dynamics for appropriately selected cost functions, sampling periods, and operating points. Fourth, schedule the resultant feedback gains as a function of operating point and sampling period and store this function in the control computer. Finally, select a system parameter to be used by the adaptive sampling law to predict the sampling period. The total control system is now as shown in Figure 5.1.

CHAPTER VI

SUMMARY OF RESULTS AND CONCLUSIONS

In Chapter I the need for new concepts in the control of jet engines was discussed. It was pointed out that modern control theory had significant advantages in the development of these concepts. Specifically these advantages were the ability of modern control theory to design multivariable control systems that take advantage of loop interactions and the systematic way in which the control systems were designed. Specific research objectives were the identification of dynamic engine models from realistic engine data with a minimum of a priori assumptions, and the development of computer control algorithms that were both efficient and practical.

In Chapter II a brief description of the physical characteristics of air-breathing gas turbine engines was given. A summary of the basic concepts of engine control was also presented.

In Chapter III the identification of a low-order dynamic state-space model for the single spool turbojet engine was described. It was shown that a technique developed by Tse and Weinert could identify steady-state linearized operating point models with a minimum of a priori assumptions. For this technique both the model order and model parameters were determined in a noniterative fashion from realistic data generated by a digital computer dynamic simulation. Gradient techniques were used to complete the identification of the model and a comparison of the composite model and the engine

simulation was performed.

In Chapter IV discrete time algorithms were developed for efficient and practical computer control of linear systems. The optimal discrete output regulator problem on a semi-infinite interval was proposed and the necessary conditions for optimality derived by Lagrangian techniques. An algorithm for the solution of these necessary conditions was presented along with the computer listings of the required programs. Also, adaptive sampling and its ability to improve sampling efficiency were discussed. Next, adaptive sampling and the optimal discrete output regulator were combined to form an adaptive digital control scheme that was applied to a fifth-order linearized engine model. Both the sampling efficiency and control degradation under different output feedback configurations were studied.

In Chapter V the adaptive digital control scheme was applied to the operating point models of Chapter III and the resultant adaptive configuration used to control the single spool turbojet engine simulation. The twofold adaptive nature of the feedback matrix as a function of rotor angular velocity and sampling period was described. The results of the simulations showed that rapid engine acceleration from one operating point to another could be achieved with this adaptive control scheme using only rotor velocity feedback. The effect of a change in the weighting matrices on the acceleration time was studied along with the improvement in sampling efficiency. It was also shown that the addition of temperature feedback could be used to limit the maximum turbine inlet temperature. Finally, the control configuration of rotor velocity and compressor discharge pressure was simulated to study the effect of an additional feedback

variable on acceleration time and the regulation of the pressure variable. The weighted and unweighted costs and sampling efficiencies for each simulation were summarized in Figure 5.27.

From this study it can be concluded that modern control theory can be successfully applied to jet engine control. In particular using linearized operating point models to describe engine dynamics, the adaptive digital control scheme of Chapter IV can successfully control a jet engine using available outputs in a computationally efficient manner.

Specific achievements of this dissertation include

1. The identification and verification of a second-order state-space model for a turbojet engine using an identification method by Tse and Weinert and realistic engine data.

2. The derivation of the necessary conditions of optimality for the optimal discrete output regulator with crossweighting in the performance index on the semi-infinite time interval.

3. The development of a computer algorithm to solve the necessary conditions in (2).

4. The combination of adaptive sampling and the optimal discrete output regulator into an adaptive control scheme.

5. The application of the adaptive control scheme of (4) and the model of (1) to the control of a jet engine.

There are several worthwhile extensions to this research. One is the development of an on-line technique that identifies engine dynamics. Such a technique would minimize the time required for the initial control system design of a number of engines with the same configuration. In this regard the Tse and Weinert identification

technique may be used to initialize an on-line technique. A second extension is to increase the number of control variables (to include exhaust nozzle area, e.g.) and the flight conditions for which the control is designed. Since an engine operates over a range of flight conditions, a realistic control must be designed for all these conditions. Third, different adaptive sampling laws could be applied to the adaptive digital engine control scheme to determine if better sampling efficiencies can be obtained. Finally, the benefits of using additional sensed outputs as feedback variables could be compared to the cost of additional sensors by the output regulator formulation of Chapter IV. Similarly, the effect of sensor failures on engine performance could be evaluated by the output regulator formulation.

APPENDIX A

TIME SERIES ANALYSIS

Time series analysis is used to determine the parameter set $\{P_i, \beta_{ijk}\}$ described in the section on the Tse and Weinert identification method. The following derivation from Tse and Weinert (1973) shows how this is accomplished. Let

$$R(\sigma) = E\{y(k + \sigma)y'(k)\}, \qquad \sigma = 0, 1, 2, \ldots \tag{A.1}$$

$$\Sigma = E\{z(k)z'(k)\} \tag{A.2}$$

Given the system

$$\begin{aligned} z(k + 1) &= Az(k) + Bv(k) \\ y(k) &= Cz(k) + v(k) \end{aligned} \tag{A.3}$$

where $z(k) \ \epsilon R^n$, $y(k) \ \epsilon R^m$, and $v(k)$ is a zero mean Gaussian noise process with covariance

$$E\{v(k)v'(j)\} = Q\delta_{kj} \tag{A.4}$$

The following equations can be derived

$$\Sigma = A\Sigma A' + BQB' \tag{A.5}$$

$$R(\sigma) = CE\{z(k + \sigma)z'(k)\}C' + CE\{z(k + \sigma)v'(k)\}, \qquad \sigma > 0 \tag{A.6}$$

But

$$E\{z(k + \sigma)z'(k)\} = A^{\sigma}\Sigma \tag{A.7}$$

and

$$E\{z(k + \sigma)v'(k)\} = A^{\sigma-1}BQ, \qquad \sigma > 0 \tag{A.8}$$

then

$$R(\sigma) = CA^{\sigma-1}(A\Sigma C' + BQ) = CA^{\sigma-1}S \tag{A.9}$$

where

$$S = A\Sigma C' + BQ \tag{A.10}$$

Also

$$R(0) = C\Sigma C' + Q \tag{A.11}$$

Let $r_{ij}(\sigma)$ be the i,j^{th} element of $R(\sigma)$, and s_j be the j^{th} column of S. Then

$$r_{ij}(\sigma) = c_i'A^{\sigma-1}s_j, \qquad \sigma > 0 \tag{A.12}$$

where c_i' is the i^{th} row of C.

Assuming that A and C are in the canonical forms given in the chapter on identification, the parameters $\{p_i, \beta_{ijk}\}$ are related by

$$c_i'A^{p_i} = \sum_{j=1}^{i} \sum_{k=0}^{p_j-1} \beta_{ijk}c_j'A^k, \qquad \text{if} \quad p_i > 0 \tag{A.13}$$

$$c_i' = \sum_{j=1}^{i-1} \sum_{k=0}^{p_j-1} \beta_{ijk}c_j'A^k, \qquad \text{if} \quad p_i = 0 \tag{A.14}$$

Now using equations (A.13) and (A.14)

$$r_{ij}(p_i + \tau) = \sum_{\ell=1}^{i} \sum_{k=0}^{p_\ell-1} \beta_{i\ell k}c_\ell'A^kA^{\tau-1}s_j, \qquad p_i > 0 \tag{A.15}$$

$$r_{ij}(p_i + \tau) = \sum_{\ell=1}^{i-1} \sum_{k=0}^{\ell-1} \beta_{i\ell k}c_\ell'A^kA^{\tau-1}s_j, \qquad p_i = 0 \tag{A.16}$$

where $\tau = 1, 2, \ldots,$ and

$$r_{ij}(p_i + \tau) = c_i'A^{p_i}A^{\tau-1}s_j \tag{A.17}$$

Then using (A.12)

$$r_{ij}(p_i + \tau) = \sum_{\ell=1}^{i} \sum_{k=0}^{p_\ell - 1} \beta_{i\ell k} r_{\ell j}(k + \tau), \qquad p_i > 0 \tag{A.18}$$

$$r_{ij}(p_i + \tau) = \sum_{\ell=1}^{i-1} \sum_{k=0}^{p_\ell - 1} \beta_{i\ell k} r_{\ell j}(k + \tau), \qquad p_i = 0 \tag{A.19}$$

Recall that the parameter set $\{p_i\}_1^m$, is determined from the identifiability matrix. The identifiability matrix is composed of elements of $R(\sigma)$. Once the parameter set is determined, equations (A.18) and (A.19) can be solved for $\{\beta_{ijk}\}$. Thus the parameter set $\{p_i, \beta_{ijk}\}$ is determined from the matrix $R(\sigma)$. This matrix can be estimated by time series analysis as

$$\hat{R}(\sigma) = \frac{1}{N} \sum_{k=1}^{N} y(k + \sigma) y'(k) \tag{A.20}$$

APPENDIX B

LOGARITHM OF A MATRIX

Consider the matrix equation

$$e^X = A \tag{B.1}$$

All the solutions to this equation are called logarithms of A and are denoted by $\ln A$.

The characteristic values λ_j of A and ζ_j of X satisfy

$$\lambda_j = e^{\zeta_j} \tag{B.2}$$

Assume that $\det\{A\} \neq 0$ and $\lambda_i \neq \lambda_j$, that is the eigenvalues are distinct. Let

$$A = P\bar{A}P^{-1} \tag{B.3}$$

where $\bar{A}$ is a diagonal matrix and P is a similarity transformation matrix.

$$\bar{A} = \text{DIAG}[a_{jj}] = \text{DIAG}[\lambda_j] \tag{B.4}$$

Then from Gantmacher (1959) the matrix X satisfies the equation

$$X = P \ln \bar{A} P^{-1} \tag{B.5}$$

and the logarithm of $\bar{A}$ is

$$\ln \bar{A} = \text{DIAG}[\ln(\lambda_j)] = \text{DIAG}[\zeta_j] \tag{B.6}$$

APPENDIX C

COMPUTER SIMULATION SUBPROGRAMS FOR THE SOLUTION OF THE DISCRETE OPTIMAL OUTPUT REGULATOR

CLSDLP

DISLYP

DITORF

MULT

RICATT

```
C      SUBROUTINE MULT
C
C      PURPOSE
C         TO COMPUTE PRODUCT OF TWO MATRICES
C
C      DESCRIPTION OF PARAMETERS
C         ALPHA-  N X L  REAL MATRIX
C         BETA -  L X M  REAL MATRIX
C         GAMMA-  N X M  REAL MATRIX
C         N      -  NUMBER OF ROWS IN ALPHA
C         M      -  NUMBER OF COLUMNS IN BETA
C         L      -  NUMBER OF COLUMNS IN ALPHA(ROWS IN BETA)
C
       SUBROUTINE MULT(ALPHA,BETA,GAMMA,N,M,L)
       DIMENSION ALPHA(11,11),BETA(11,11),GAMMA(11,11)
       DO 10 I=1,N
       DO 10 J=1,M
       GAMMA(I,J)=0.0
       DO 10 K=1,L
    10 GAMMA(I,J)=GAMMA(I,J)+ALPHA(I,K)*BETA(K,J)
       RETURN
       END
```

```
C      SUBROUTINE CLSDLP
C
C      PURPOSE
C          TO CALCULATE THE CLOSED LOOP MATRIX
C          AA AND ITS TRANSPOSE
C          AA =  A - B*F*C
C
       SUBROUTINE CLSDLP(A,B,F,C,AA,AAT,N,M,L,NMAX)
       DIMENSION A(NMAX,1),B(NMAX,1),F(NMAX,1),C(NMAX,1),AA(NMAX,1)
       DIMENSION AAT(NMAX,1)
       CALL MULT(F,C,AAT,M,N,L)
       CALL MULT(B,AAT,AA,N,N,M)
       DO 10  I=1,N
       DO 10  J=1,N
       AA(I,J)= A(I,J) - AA(I,J)
    10 AAT(J,I)=AA(I,J)
       RETURN
       END
```

```
C      SUBROUTINE DISLYP
C
C      PURPOSE
C          TO SOLVE THE DISCRETE LYAPUNOV EQUATION
C          P = A*P*A' + S
C
C      METHOD
C          SUCCESSIVE SUBSTITUTION
C
       SUBROUTINE DISLYP(P,A,S,ERROR,N,NMAX)
       DIMENSION P(NMAX,1),A(NMAX,1),S(NMAX,1),F(11,11),AT(11,11)
       DIMENSION A1(11,11),S1(11,11)
       DO 1 I=1,N
       DO 1 J=1,N
       A1(I,J)=A(I,J)
     1 S1(I,J)=S(I,J)
       I=0
     5 SUM=0.
       I=I+1
       DO 10 I=1,N
       DO 10 J=1,N
       P(I,J) = S1(I,J)
    10 AT(J,I) = A1(I,J)
       CALL MULT(A1,P,S1,N,N,N)
       CALL MULT(S1,AT,F,N,N,N)
       DO 20 I=1,N
       DO 20 J=1,N
    20 S1(I,J) = P(I,J) + F(I,J)
C      CHECK FOR CONVERGENCE
       DO 30 I=1,N
       DO 30 J=1,N
       F(I,J) = A1(I,J)
    30 SUM = ABS(S1(I,J) - P(I,J)) + SUM
       IF(SUM.LT.ERROR) RETURN
       CALL MULT(F,F,A1,N,N,N)
       IF(I.LT.25) GO TO 5
       RETURN
       END
```

```
C      SUBROUTINE DITORF
C
C      PURPOSE
C          TO SOLVE THE FOLLOWING EQUATION
C          F = INV(R + B'*P*B)*(B'*P*A+M')*EL*C'*INV(C*EL*C')
C          FOR THE DISCRETE, INFINITE TIME, OUTPUT FEEDBACK
C          REGULATOR MATRIX F
C
       SUBROUTINE DITORF(R,B,P,A,EL,C,AM,F,N,M,L,NMAX)
       DIMENSION R(NMAX,1),B(NMAX,1),P(NMAX,1),A(NMAX,1)
       DIMENSION EL(NMAX,1),C(NMAX,1),AM(NMAX,1)
       DIMENSION BTK(11,11),ELCT(11,11),DUM1(11,11),BT(11,11),CT(11,11)
       DIMENSION LWORK(11),MWORK(11)
       KMAX=11
       DO 10 I=1,N
       DO 20 J=1,M
    20 BT(J,I)=B(I,J)
       DO 30 K=1,L
    30 CT(I,K)=C(K,I)
    10 CONTINUE
       CALL MULT(EL,CT,ELCT,N,L,N)
       CALL MULT(BT,P,BTK,M,N,N)
       CALL MULT(C,ELCT,DUM1,L,L,N)
C      INVERT THE MATRIX  DUM1= C * EL * C'
       CALL ARRAY(2,L,L,KMAX,KMAX,DUM1,DUM1)
       CALL MINV(DUM1,L,DETC,LWORK,MWORK)
       CALL ARRAY(1,L,L,KMAX,KMAX,DUM1,DUM1)
       CALL MULT(ELCT,DUM1,CT,N,L,L)
       CALL MULT(BTK,A,DUM1,M,N,N)
       DO 50 I=1,M
       DO 50 J=1,N
    50 DUM1(I,J) = DUM1(I,J) + AM(J,I)
       CALL MULT(DUM1,CT,ELCT,M,L,N)
       CALL MULT(BTK,B,DUM1,M,M,N)
       DO 40 I=1,M
       DO 40 J=1,M
    40 BT(I,J)=R(I,J)+DUM1(I,J)
C      INVERT THE MATRIX  BT = R + B'*K*B
       CALL ARRAY(2,M,M,KMAX,KMAX,BT,BT)
       CALL MINV(BT,M,DETBT,LWORK,MWORK)
       CALL ARRAY(1,M,M,KMAX,KMAX,BT,BT)
       CALL MULT(BT,ELCT,F,M,L,M)
       RETURN
       END
```

```
C      SUBROUTINE RICATT
C
C      PURPOSE
C          TO SOLVE THE OUTPUT FEEDBACK REGULATOR
C          PROBLEM FOR THE STEADY STATE DISCRETE PROBLEM USING
C          THE DISCRETE ANALOGUE OF ATHANS AND LEVINE'S METHOD
C
       SUBROUTINE RICATT(A,B,C,Q,AM,R,F,N,M,L,NMAX)
       DIMENSION A(NMAX,1),B(NMAX,1),C(NMAX,1),Q(NMAX,1),R(NMAX,1)
       DIMENSION AM(NMAX,1),F(NMAX,1)
       DIMENSION P(11,11),DD(11,11),AA(11,11),AAT(11,11),QIDENT(11,11)
       DIMENSION EL(11,11),DE(11,11),DF(11,11),DG(11,11)
       DATA NMAA,NMF,NML,NMP /2HAA,1HF,1HL,1HP /
       ERROR = FLOAT(N)**2*1.E-5
       ERR = FLOAT(M)*FLOAT(L)*1.E-5
       DO 5  I=1,N
     5 QIDENT(I,I)=1.0
   100 CONTINUE
C
C      CALCULATE THE CLOSED LOOP SYSTEM MATRIX AA= A - B*F*C
C
       CALL CLSDLP(A,B,F,C,AA,AAT,N,M,L,NMAX)
C
C      GIVEN A VALUE FOR F CALCULATE THE P MATRIX
C
       CALL MULT(F,C,DD,M,N,L)
       DO 30 I=1,M
       DO 30 J=1,N
    30 P(J,I)=DD(I,J)
       CALL MULT(R,DD,DF,M,N,M)
       CALL MULT(P,DF,DG,N,N,M)
       CALL MULT(AM,DD,P,N,N,M)
       DO 40 I=1,N
       DO 40 J=1,N
    40 DD(I,J)=DG(I,J)+Q(I,J)-P(I,J)-P(J,I)
       CALL DISLYP(P,AAT,DD,ERROR,N,NMAX)
C
C      COMPARE PAST AND PRESENT ALGORITHM SOLUTIONS
C
       SUM = 0.
       DO 10 I=1,N
       DO 10 J=1,N
       HOLD = DE(I,J) - P(I,J)
       IF(P(I,J).NE.0.) HOLD = HOLD/P(I,J)
       SUM = ABS(HOLD) + SUM
    10 DE(I,J)=P(I,J)
       IF(SUM.LT.10.*ERROR) GO TO 200
    50 CONTINUE
```

```
C
C       CALCULATE THE L MATRIX
C
        CALL CLSDLP(A,B,F,C,AA,AAT,N,M,L,NMAX)
        CALL DISLYP(EL,AA,QIDENT,ERROR,N,NMAX)
C
C       CALCULATE A NEW F MATRIX CALLED DD
C
        CALL DITORF(R,B,P,A,EL,C,AM,DD,N,M,L,NMAX)
C
C       COMPARE PAST AND PRESENT GAIN MATRICES
C
        SUM= 0.0
        DO 20  I=1,M
        DO 20  J=1,L
        IF(F(I,J).NE.0.) HOLD = HOLD/F(I,J)
        HOLD = DD(I,J) - F(I,J)
        SUM = ABS(HOLD) + SUM
   20   F(I,J)=DD(I,J)
        IF(SUM.GT.ERR)  GO TO 50
        GO TO 100
  200   CONTINUE
        RETURN
        END
```

APPENDIX D

SAMPLED-DATA SYSTEMS

Many processes are naturally modeled as continuous time processes. However, the introduction of a computer as the principal control element requires that time be quantized to match computer processing time. This combination of continuous process, digital controller, and sampling operation between process output and controller input is denoted as a sampled-data system (Levis, et al., 1971). A sampled-data system is given in Figure D.1.

To represent a sampled-data system mathematically let the continuous process be described as a time-invariant linear vector differential system of equations

$$\begin{aligned} \dot{x} &= Fx + Gu \\ y &= Hx \end{aligned} \tag{D.1}$$

where $x \in R^n$, $y \in R^m$, and $u \in R^q$. Since $u(t)$ is the output of a digital controller, a sample and hold constraint is imposed on $u(t)$. Therefore, the control is assumed piecewise-constant with changes in its value only at sampling instants t_i. Thus

$$u(t) = u(t_i) = u_i, \qquad \text{for} \quad t_i \leq t \leq t_{i+1} \tag{D.2}$$

The continuous system of (D.1) is now discretized as follows. First the trajectory $x(t)$ for the system of equations (D.1) is given by

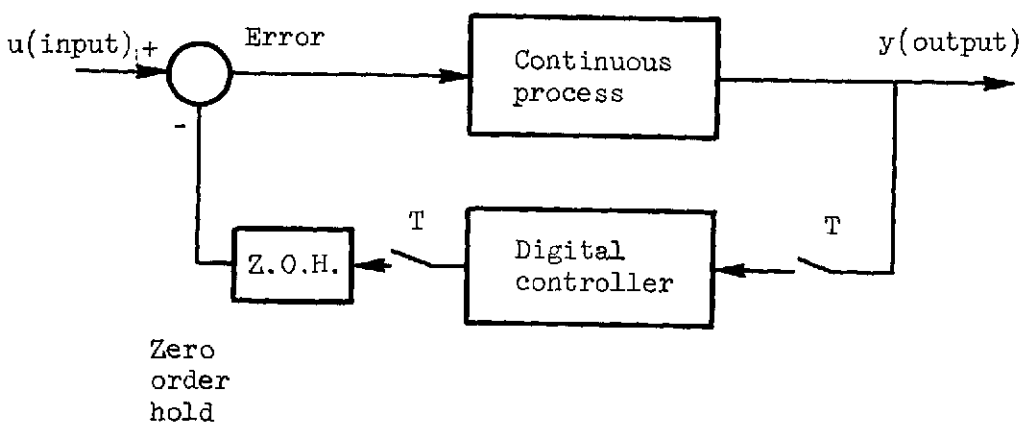

Figure D-1. - Sampled-data system.

$$x(t) = e^{F(t-t_i)}x(t_i) + \int_{t_i}^{t} e^{F(t-\tau)}Gu_i \, d\tau \tag{D.3}$$

Define

$$T = t_{i+1} - t_i \tag{D.4}$$

$$A = A(T) = e^{FT} \tag{D.5}$$

$$B = B(T) = \int_0^T e^{Ft}G \, dt \tag{D.6}$$

$$H = C \tag{D.7}$$

$$x(t_{i+1}) = x(i+1), \qquad x(t_i) = x(i), \qquad y(t_i) = y(i) \tag{D.8}$$

Then the discrete equivalent of (D.1) is

$$\begin{aligned} x(i+1) &= A(i)x(i) + B(i)u(i) \\ y(i) &= Cx(i) \end{aligned} \tag{D.9}$$

If the sample rate, T, is constant for all i, then the system (D.9) becomes time-invariant.

Given a quadratic cost function in terms of the continuous vectors y(t) and u(t)

$$J = \frac{1}{2}\int_{t_0}^{t_f} [y'(t)Qy(t) + u'(t)Ru(t)]dt + \frac{1}{2}\, y'(t_f)Q_f y(t_f) \tag{D.10}$$

where

$$Q_f \geq 0, \qquad Q \geq 0, \qquad \text{and} \quad R > 0 \tag{D.11}$$

Also,

$$Q_f' = Q_f, \qquad Q' = Q, \qquad \text{and} \quad R' = R \tag{D.12}$$

Finally,

$$Q_f + Q \neq 0 \tag{D.13}$$

The discrete equivalent is

$$J = \frac{1}{2} x'(N)Q_N x(N) + \frac{1}{2} \sum_{k=0}^{N-1} \{x'(k) \quad \hat{Q}x(k) \quad + 2x'(k)Mu(k) + u'(k)\hat{R}u(k)\} \tag{D.14}$$

where $i = 0, 1, \ldots, N-1$, when

$$T = t_{i+1} - t_i \tag{D.4}$$

$$y(k) = Cx(k) \tag{D.9}$$

$$Q_N = CQ_fC' \tag{D.15}$$

$$\hat{Q}(T) = \int_0^T A'(t)CQC'A(t)dt \tag{D.16}$$

$$M(T) = \int_0^T A'(t)CQC'B(t)dt \tag{D.17}$$

and finally

$$\hat{R}(t) = TR + \int_0^T B'(t)CQC'B(t)dt \tag{D.18}$$

The weighting matrices Q_N, $\hat{Q}$, $\hat{R}$, and M are parametrically dependent on the sampling period. Thus if the sampling period varies, the discrete system would be time-varying even though the continuous system is time-invariant.

The matrix $A(T)$, being a fundamental matrix, is nonsingular. Since $Q(R)$ is symmetric and positive semi-definite (definite), it is easily shown that $\hat{Q}(\hat{R})$ is also symmetric and positive semi-definite (definite).

BIBLIOGRAPHY

Ahlbeck, D. (1966): Simulation, Vol. 7.

Anderson, B. and Moore, J. (1971): Linear Optimal Control. Prentice Hall, N. J.

Arpasi, D. J., Cwynar, D. S., and Wallhagen, R. E. (1972): Sea Level Evaluation of Digitally Implemented Turbojet Control Functions. NASA TN D-6936.

Bekey, G. and Tomovic, R. (1966): Sensitivity of Discrete Systems to Variation of Sampling Interval. IEEE Transactions on Automatic Control. Vol. AC-11.

Bentz, C. (1974): The Role of Computers in Future Propulsion Controls. NATO Advisory Group for Aerospace Research and Development (AGARD) Conference Pre-print (CPP), no. 151, Article 11.

Brockett, R. and Lee, H. (1967): Frequency-Domain Instability Criteria for Time-Varying and Nonlinear Systems. Proceedings of the IEEE. Vol. 55, No. 5.

Chen, C. (1972): Model Reduction of Multivariable Control Systems by Means of Matrix Continued Fractions. Preprints of the Fifth World Conference of the IFAC.

Crooks, P. and Willshire, D. (1956): The Theoretical Estimation of Engine Speed Response Data for a Turbojet Engine. NGTE Report No. M268.

Cwynar, D. S. and Batterton, P. G. (1975): Digital Implementation of the TF30-P-3 Turbofan Engine Control. NASA TM X-3105.

Dorf, B., Farren, M., and Phillips, C. (1962): Adaptive Sampling Frequency for Sample-Data Control Systems. IRE Transactions on Automatic Control. Vol. AC-7.

Eccles, E. and Shutler, A. (1970): Digital Computer Control of Gas Turbine Engines. ASME Paper 70-GT-40.

Ermer, C. and VandeLinde, V. (1972): Output Feedback Gains for a Linear Discrete Stochastic Control Problem. IEEE 1972 Conference on Decision and Control, New Orleans, Louisiana.

Eykhoff, P. (1974): System Identification. Wiley & Sons, N. Y.

Frazzini, R. M. (1970): A Prototype Digital Control Concept for Aircraft Propulsion Systems. AIAA Sixth Propulsion Joint Specialist Conference Paper No. 70-693.

Gantmacher, R. (1959): The Theory of Matrices. Vol. 1, Chelsea Publishing, N. Y.

Griffiths, D. M. and Powell, R. D.: The Use of Digital Control for Complex Powerplant Management. AGARD-CCP-151. Article 26.

Gupta, S. (1963): Increasing the Sampling Efficiency for a Control System. IEEE Transactions on Automatic Control. Vol. AC-8.

Hewer, G. A. (1971): An Iterative Technique for the Computation of the Steady-State Gains for the Discrete Optimal Regulator. IEEE Transactions on Automatic Control. Vol. AC-16.

Hill, P. and Peterson, C. (1965): Mechanics and Thermodynamics of Propulsion. Addison Wesley Publishing, Reading, Mass.

Hsia, T. (1974): Analytic Design of Adaptive Sampling Control Laws in Sample-Data Systems. IEEE Transactions on Automatic Control. Vol. AC-19, No. 1.

Kailath, T. (1970): The Innovations Approach to Detection and Estimation. Proceedings of the IEEE. Vol. 58.

Kalman, R. (1960): Contributions to the Theory of Optimal Control. Bol. Soc. Mat. Mex. Vol. 5.

Kalman, R. and Bucy, R. (1961): New Resylts in Linear Filtering and Prediction Theory. ASME J. of Basic Engineering. Vol. 83.

Kleinman, D. L. (1974): Stabilizing a Discrete, Constant, Linear System with Application to Iterative Methods for Solving the Ricatti Equation. IEEE Transactions on Automatic Control. Vol. AC-19.

Kuo, B. C. (1970): Discrete Data Control Systems. Prentice Hall, Inc. Englewood Cliffs, N. J.

Kwakernaak, H. and Sivan, R. (1972): Linear Optimal Control Systems. Wiley-Interscience, N. Y.

Leeson, P. J. (1974): Gas Turbine Control Systems. AGARD-CCP-151. Article 10.

Levine, W. and Athans, M. (1970): On the Determination of the Optimal Constant Output Feedback Gains for Linear Multivariable Systems. IEEE Transactions on Automatic Control. Vol. AC-15.

Levine, W., Johnson, T., and Athans, M. (1971): Optimal Limited State Variable Feedback Controllers for Linear Systems. IEEE Transactions on Automatic Control. Vol. AC-16.

Levis, A. H., Athans, M., and Schlueter, R. A. (1971): On the Behavior of Optimal Linear Sampled-Data Regulators. Int. J. of Control. Vol. 13.

Lewis, W. G. and Munns, G. E. (1968): Digital Control of Aircraft Powerplants. The Aeronautical Journal of the Royal Aeronautical Society. Vol. 72.

Loft, Arne (1969): SPEEDTRONIC - Tomorrow's Analog and Digital Gas Turbine Control System. IEEE Transactions on Industry and General Applications. Vol. IGA-5, No. 4.

Luenberger, D. (1966): Observers for Multivariable Systems. IEEE Transactions on Automatic Control. Vol. AC-11.

MacFarlane, A. G. J., McMorran, P. D., Dixon, B. A., and Hodge, S. S. (1971): Applications of Multivariable Control Techniques to Aircraft Gas Turbines. Conference on Multivariable Control System Design and Applications. Manchester, England.

McMorran, P. D. (1970): Design of Gas Turbine Controller Using Inverse Nyquist Method. Proceedings of IEE. No. 117.

Mehra, R. (1971): On-Line Identification of Linear Dynamic Systems with Applications to Kalman Filtering. IEEE Transactions on Automatic Control. Vol. AC-16.

Mendel, J. (1974): A Concise Derivation of Optimal Constant Limited State Feedback Gains. IEEE Transactions on Automatic Control. Vol. AC-19.

Michael, G. and Farrar, F. (1973): Development of Optimal Control Modes for Advanced Technology Propulsion Systems. United Aircraft Research Laboratories (UARL) Report No. M9-11620-1.

Michael, G. and Farrar, F. (1975): Identification of Multivariable Gas Turbine Dynamics from Stochastic Input-Output Data. UARL Report No. R941620-3.

Mitchell, J. and McDaniel, J. (1969): Adaptive Sampling Technique. IEEE Transactions on Automatic Control. Vol. AC-14.

Mueller, G. (1971): Linear Model of 2-Shaft Turbojet and its Properties. Proceedings of IEE. Vol. 118, No. 6.

Mullis, C. (1973): On the Controllability of Discrete Linear Systems with Output Feedback. IEEE Transactions on Automatic Control. Vol. AC-18, No. 6.

Otto, E. and Taylor, B. (1951): Dynamics of a Turbojet Considered as a Quasi-Static System. NACA Report No. R1001.

Parzen, E. (1967): Time Series Analysis Papers. Holden-Day, San Francisco, Ca.

Prue, D. A. (1974): Engine Control for Harpoon Missile System. AGARD-CCP-151. Article 8.

Rekasius, Z. (1967): Optimal Linear Regulators with Incomplete State Feedback. IEEE Transactions on Automatic Control. Vol. AC-12.

Sage, A. and Melsa, J. (1971): System Identification. Academic Press, N. Y.

Saravanamuttoo, H. I. H. and Fawke, A. J. (1970): Simulation of Gas Turbine Dynamic Performance. ASME Paper No. 70-GT-23.

Seldner, K., Mihaloew, J. R., and Blaha, R. J. (1971): Generalized Simulation Technique for Turbojet Engine System Analysis. NASA TN D-6610.

Seldner, K., Geyser, L. C., Gold. H., Walker, D., and Burgner, G. (1972): Performance and Control Study of a Low-Pressure-Ratio Turbojet Engine for a Drone Aircraft. NASA TM X-2537.

Sellers, J. and Teren, F. (1974): Generalized Dynamic Engine Simulation Techniques for the Digital Computer. AGARD-CPP-151. Article 23.

Sevitch, G. J. and Beattle, E. C. (1974): Integrated Flight/ Propulsion Control Design Techniques Starting with the Engine. SAE Paper No. 740481.

Shannon, C. E. (1949): Communication in the Presence of Noise. Proceedings of IRE. Vol. 37.

Smith, M. (1971): An Evaluation of Adaptive Sampling. IEEE Transactions on Automatic Control. Vol. AC-16.

Sobey, A. and Suggs, A. (1963): Control of Aircraft and Missile Powerplants. Wiley Inc., N. Y.

Szuch, J. R. (1974): HYDES - A Generalized Hybrid Computer Program for Studying Turbojet or Turbofan Engine Dynamics. NASA TM X-3014.

Tomovic, R. and Bekey, G. (1966): Adaptive Sampling Based on Amplitude Sensitivity. IEEE Transactions on Automatic Control. Vol. AC-11.

Tse, E. and Anton, J. (1972): On the Identifiability of Parameters. IEEE Transactions on Automatic Control. Vol. AC-17.

Tse, E. and Weinert, H. (1973): Correction to "On the Identifiability of Parameters." IEEE Transactions on Automatic Control. Vol. AC-18.

Tse, E. and Weinert, H. (1973): Structure Determination and Parameter Identification for Multivariable Stochastic Linear Systems. Proceedings of the 1973 JACC. Paper No. 2-5.

Waters, J. H. (1974): A Digital Controller Applied to the Limitation of Reheat Combustion Roughness. AGARD-CPP-151. Article 15.

Weinert, H. and Anton, J. (1972): Canonical Forms for Multivariable System Identification. Proceedings of the 1972 Decision and Control Conference.

Weinert, H. (1973): Complete Sets of Invariants for Multivariable Linear Systems. Proceedings of the 1973 Princeton Conference on Information Science and Systems.